Distribution of Nucleoside Transporter Subtypes in Rat Brain

By

Christopher M. Anderson

A Thesis
Submitted to the Faculty of Graduate Studies in
Partial Fulfillment of the Requirements
For the Degree of

DOCTOR OF PHILOSOPHY

Department of Pharmacology and Therapeutics
Faculty of Medicine
University of Manitoba

THE UNIVERSITY OF MANITOBA

FACULTY OF GRADUATE STUDIES

*****

COPYRIGHT PERMISSION PAGE

DISTRIBUTION OF NUCLEOSIDE TRANSPORTER SUBTYPES IN RAT BRAIN

BY

CHRISTOPHER M. ANDERSON

A Thesis/Practicum submitted to the Faculty of Graduate Studies of The University of Manitoba in partial fulfillment of the requirements of the degree of

DOCTOR OF PHILOSOPHY

This thesis is dedicated to my parents.

For providing me with the upbringing and support that has given me the tools to be motivated, to be patient, to be thankful for what I have, and to be confident in my abilities. They are responsible for my successes.

TABLE OF CONTENTS

ACKNOWLEDGMENTS

Dr. Fiona Parkinson *I am honoured to have been her first Ph.D. student. At no time was I able to detect that she had never supervised a student. She always had time for me and gave me quick feedback even though her schedule was often hectic. Her incredible success in science at a young age has inspired me and shown me exactly what I should strive for. With her strong personal and scientific integrity, she cannot help but lead by example.*

Drs. Gary Glavin and Don Smyth *They have both been there for me at various times throughout the last five years. Whether it was Don offering to introduce me to Friday hockey when I first arrived in Winnipeg or Gary making sure to take the time to talk to me after a triumph or a disappointment, I really appreciate it and won't forget it.*

Wei Xiong, Chris Sinclair, Stephanie Borgland, Yi Wei Zhang *Thank you for the laughs, for the chats and for allowing me to "vent" at times. Wei, I will not forget the extra help you've given me. Chris, I hereby relinquish my control of "the chair", "the computer" and of course, "The Moose"; you're the Kingpin. I cannot imagine a better working environment. I mean that sincerely.*

Ron and Audrey Martin *My Aunt and Uncle. I thank them for making Manitoba a warm comfortable home for me.*

Armando and Divina Natividad and Bob and Dulce Intengan *I thank them very much for their incredible support, hospitality and generosity.*

Hope Intengan *I thank her for her very special friendship and support. I cannot imagine having been without it.*

ABSTRACT

Adenosine is recognized as an important inhibitory neuromodulator in the central nervous system. Through four distinct plasma membrane receptors, endogenous adenosine is able to inhibit the release of many neurotransmitters, including glutamate following cerebral ischemia, and also affect other non-neuronal cell types in brain such as astrocytes, microglia, platelets and endothelial cells. Nucleoside transport processes are instrumental in regulating endogenous adenosine levels and the associated effects of adenosine. There are two broad categories of nucleoside transporters: equilibrative and concentrative. Two equilibrative subtypes have been cloned and termed ENT1 and ENT2. The potent nucleoside transport inhibitor nitrobenzylthioinosine (NBMPR) can be used as a marker for ENT1 but not for ENT2. Two concentrative subtypes have also been cloned. CNT1 is pyrimidine nucleoside-selective while CNT2 is purine nucleoside-selective. There are no known selective ligands for these transporters. In the absence of selective ligands for transporters other than ENT1, the cloning of rat ENT2 (rENT2), CNT1 (rCNT1) and CNT2 (rCNT2) has provided the first opportunity to investigate the distributions of specific nucleoside transporter subtypes in rat brain. The distribution of mRNA for the four cloned transporters was investigated using *in situ* hybridization with ^{35}S-labeled cRNA probes in rat brain and using Northern blot analysis in human brain. Transporter protein distributions were also studied. [^{3}H]Nitrobenzylthioinosine ([^{3}H]NBMPR) autoradiography was employed to estimate the distribution of rENT1 in rat brain while rCNT1 and rCNT2 distributions were studied by mapping immunoreactivity of polyclonal antibodies generated in rabbits against both transporters using immunocytochemistry in rat brain. Northern analysis of human brain total RNA

indicated that both hENT1 and hENT2 have a wide distribution in human brain. Both probes detected RNA species in every region tested. In general, message for all four nucleoside transporters was seen in rat hippocampus, cerebellum, cerebral cortex, striatum and other regions with varying relative abundances among regions for each transporter. Binding of [^{3}H]NBMPR to rat brain sections to identify rENT1 transporters supported results from *in situ* hybridization in thalamus, cortex and striatum, however, in contrast to *in situ* hybridization, low signal intensity was seen in hippocampus and cerebellum indicating low protein expression. Immunocytochemistry using antibodies for rCNT1 and rCNT2 generally confirmed results seen with *in situ* hybridization. The broad and overlapping distributions of different nucleoside transporter subtypes demonstrated here indicates that the regulation of adenosine and other nucleosides important for salvage of nucleotides with signaling capabilities is achieved through multiple transport mechanisms.

LIST OF FIGURES

LIST OF TABLES

ABBREVIATIONS

2-CA	2-chloroadenosine
2meSATP	2 methylthioadenosine triphosphate
5'-IMP	5'-inosine monophosphate
5'-NH_2dAdo	5'-amino-5'-deoxyadenosine
8-CPT	8-cylcopentyltheophylline
αβmeATP	αβ-methylene adenosine triphosphate
βγmeATP	βγ-methylene adenosine triphosphate
μM	micromolar (10^{-6} Molar)
AR	adenosine receptor
A_1AR	adenosine A_1 receptor
A_2AR	adenosine A_2 receptor
A_{2A}AR	adenosine A_{2A} receptor
A_{2B}AR	adenosine A_{2B} receptor
A_3AR	adenosine A_3 receptor
AC	adenylyl cyclase
ADA	adenosine deaminase
ADP	adenosine diphosphate
AK	adenosine kinase
AMPA	α-amino-3-hydroxy-5-methyl-4-isoxazole proprionic acid
ANS	autonomic nervous system
APEC	2-[(2-aminoethylamino)-carbonylethylphenylethylamino]-5'-*N*-ethylcarboxamidoadenosine

APNEA	N^6-2-(4-aminophenyl)-ethyladenosine
ATP	adenosine triphosphate
AZT	azidothymidine
BzATP	3'-*O*-(4-benzoyl)benzoylATP
cAMP	cyclic adenosine 3',5'-monophosphate
CCPA	2-chloro-N^6-cyclopentyladenosine
cDNA	complementary deoxyribonucleic acid
CGS 21680	2-[*p*-(2-carbonyl-ethyl)-phenylethylamino]-5'-*N*-ethylcarboxamidoadenosine
CHA	N^6-cyclohexyladenosine
CHO	Chinese hamster ovary
Cl-IB-MECA	Cl-N^6-(3-iodobenzyl)-5'-(*N*-methylcarbamoyl) adenosine
CNS	central nervous system
CPA	N^6-cyclopentyladenosine
CPCA	5'-(*N*-cyclopropyl)-carboxamidoadenosine
CPT	cyclopentyltheophylline
CSC	chlorostyrylcaffeine
CSF	cerebrospinal fluid
DAG	diacylglycerol
DCF	2'-deoxycoformycin
d-ITU	5'-deoxy-5-iodotubercidin
DPCPX	1,3-dipropyl-8-cyclopentylxanthine
DPR	dipyridamole

DZP	dilazep
EEG	electroencephalogram
EHNA	erythro-9-(2-hydroxy-3-nonyl) adenine
GABA	γ-aminobutyric acid
GFAP	glial fibrillary acidic protein
GI	gastrointestinal
GTP	guanosine triphosphate
h	hours
hCNT1	human concentrative nucleoside transporter 1
hENT1	human equilibrative nucleoside transporter 1
hENT2	human equilibrative nucleoside transporter 2
HIV	human immunodeficiency virus
I-ABOPX	3-(3-iodo-4-aminobenzyl)-8-(4-oxyacetate)-phenyl-1-propylxanthine
IL-6	interleukin-6
ITU	5'-iodotubercidin
IP_3	inositol-1,4,5- trisphosphate
KDa	kilodalton (10^3 Daltons)
KF 17837	1,3-dipropyl-8-(3,4-dimethoxystyryl)-7-methylxanthine
K_M	Michaelis-Menton constant for concentration of permeant required to reach half-maximal transport velocity
LTD	long-term depression
LTP	long-term potentiation
min.	minutes

mRNA	messenger ribonucleic acid
NBMPR	nitrobenzylmercaptopurine riboside or nitrobenzylthioinosine
NGF	nerve growth factor
nM	nanomolar (10^{-9} Molar)
NMDA	*N*-methyl-D-aspartate
NECA	5'-*N*-ethyl-carboxamidoadenosine
PPF	paired-pulse facilitation
PTD	posttetanic depression
PLA_2	phospholipase A_2
PLC	phospholipase C
pM	picomolar (10^{-12} Molar)
pmol	picomoles
PPADS	pyridoxalphosphate-6-azophenyl-2',4'-disulfonic acid
rCNT1	rat concentrative nucleoside transporter 1
rCNT2	rat concentrative nucleoside transporter 2
rENT1	rat equilibrative nucleoside transporter 1
rENT2	rat equilibrative nucleoside transporter 2
R-PIA	N^6-(*R*-phenylisopropyl)-adenosine
RT-PCR	reverse transcriptase polymerase chain reaction
s	seconds
S-PIA	N^6-(*S*-phenylisopropyl)-adenosine
$t_{½}$	half-life
TNF-α	tumour necrosis factor alpha

UDP	uridine diphosphate
UTP	uridine triphosphate
UTPγS	uridine triphosphate, γ-sulphate
V_{max}	maximum velocity of permeant influx
XAC	xanthine amine congener

Chapter 1

Introduction and Review of Purines Literature

1. Historical Perspective

Considerable research into the physiology and pharmacology of purine nucleosides and nucleotides was initiated following the finding that adenosine and ATP have potent extracellular effects in mammalian heart (Drury and Szent-Györgyi, 1929). Such research is responsible for the identification of numerous central and peripheral actions of adenosine and ATP, and the subsequent discovery of plasma membrane receptors thought to mediate the majority of these actions.

In 1963, it was found that adenosine is produced in hypoxic heart. This and previous experiments showing vasodilatory actions of adenine compounds (Holton and Holton, 1954; Holton, 1959) led Berne to hypothesize that adenosine is involved in the metabolic regulation of coronary (Berne, 1963) and cerebral circulations (Rubio *et al.*, 1975; Winn *et al.*, 1979). In the late 1960s and early 1970s a number of lines of evidence emerged supporting the existence of plasma membrane receptors for adenosine. The first direct evidence for receptors in the CNS was provided by Sattin and Rall (1970) with the observation that adenosine increased cAMP in rodent brain slices, a process blocked by caffeine.

Following the report of Drury and Szent-Györgyi, much emphasis was placed on the functions of adenine nucleotides in the cardiovascular system. The next major steps were taken in the middle 1950s up to the early 1970s when ATP was shown to be released from sensory nerves (Holton and Holton, 1954), suggesting a role for ATP in neural transmission. In the early 1960s a component of the ANS which used neither

acetylcholine nor noradrenaline as a neurotransmitter was recognized in the GI tract and other organs such as lung and bladder. Such nerves were termed "purinergic" (Burnstock, 1972). The idea of ATP receptors was postulated by Burnstock in 1972 and evidence supporting this hypothesis grew until 1978 when the designations P_1, for adenosine receptors, and P_2, for ATP receptors, were proposed (Burnstock, 1978).

Therapeutic use of P_2 receptors has been a relatively untouched field until fairly recently when cloning allowed elucidation of tissue distribution and function of these transporters. However, the hypotensive effects of adenosine prompted investigation of adenosine as a therapeutic agent many decades ago. The potential therapeutic benefits of stimulating or blocking adenosine receptors are many and provide incentive for the high-volume quality research seen in the area today.

2. Receptors for Adenosine and Nucleotides

2.1 Nucleotide Receptors

ATP was proposed as a neurotransmitter substance on the heels of findings that it is stored in and released from nerve endings (Burnstock, 1972). As a classical neurotransmitter (Eccles, 1964), this required that there exist post-junctional plasma membrane receptors for ATP. Many papers over the next few years reported evidence for ATP receptors (Burnstock and Brown, 1981; Gordon, 1986), culminating in a review that proposed P_2 (ATP) receptors as a class of receptors distinct from P_1 (adenosine) receptors (Burnstock, 1978). Many different receptor-mediated responses to ATP, ADP, and uracil nucleotides have been observed in the years since then and many of these responses displayed different potency profiles to various ATP analogs or uracil

nucleotides. This led to the pharmacological dissociation of two P_2 receptor subclasses, termed P2X and P2Y (Burnstock and Kennedy, 1985) (see table 1). A third subclass, termed P2T, has been identified only in platelets. Further studies clearly showed that P2X and P2Y can be distinguished on the basis of signal transduction mechanisms (Abbrachio and Burnstock, 1994); P2X receptors are ionotropic, or ligand-gated ion channels, and P2Y receptors are metabotropic, G-protein coupled receptors.

2.1.1 P2X Receptors

The first P2X receptors were distinguished from P2Y receptors pharmacologically based on differing agonist potency profiles. αβmeATP>βγmeATP>ATP≈2meSATP≈-ADP was used for P2X and 2meSATP>ATP>>αβmeATP≈βγmeATP for P2Y. P2X receptors, with the exception of one subtype ($P2X_7$), are also susceptible to desensitization by αβmeATP and can be antagonized by suramin and PPADS. Dose-response curves determined for ATP analogs in many systems revealed alternative agonist potency profiles for P2X receptors, providing a basis for subclassification (Abbrachio and Burnstock, 1994) (see table 2). Currently there are 7 P2X receptor subtypes identified and cloned ($P2X_1$-$P2X_7$). The first cloned was the $P2X_1$ receptor from rat vas deferens where ATP causes smooth muscle contraction (Valera *et al.*, 1994). Each cloned subtype causes cellular signaling by increasing conductance of the cations Na^+, K^+ and Ca^{2+}. The $P2X_7$ receptor (Surprenant *et al.*, 1996), formerly the P2Z receptor (Nuttle *et al.*, 1993), subsequently forms a large pore through which molecules as large as 630 kDa may pass and in this way differs from the other P2X subtypes.

Table 1: Characteristics of P_2 Receptor Subclasses

	P2X	P2Y	P2T
Receptor Type	Ion channels, Non-selective pore	G-protein coupled	G-protein coupled
Effectors/Second Messengers	Na^+, K^+, Ca^{2+}	$\uparrow IP_3/Ca^{2+}/DAG$ $\downarrow cAMP$, $\uparrow PLA_2$	$\uparrow IP_3/Ca^{2+}/DAG$ $\uparrow cAMP$
Agonists		**See Table 2**	
Antagonists	Suramin, PPADS Desensitization by $\alpha\beta$meATP	Suramin (except $P2Y_{2,4,6}$)	ATP, Suramin, FPL66096
Distribution	Smooth muscle, brain, heart, spleen	Wide – many in brain, vasculature	Platelets

Adapted from Fredholm *et al.* (1994).

Table 2: Relative Agonist Potencies for P2X and P2Y Receptor Subtypes

P2X Subtype	Agonists	P2Y Subtype	Agonists
$P2X_1$	2meSATP>ATP>αβmeATP	$P2Y_1$	2meSATP>>ATP>ADP
$P2X_2$	2meSATP>ATP, αβmeATP inactive	$P2Y_2$	UTP=ATP>2meSATP
$P2X_3$	2meSATP>ATP>αβmeATP or ATP>2meSATP>αβmeATP †	$P2Y_3$	ADP>UTP<ATP=UDP
$P2X_4$	ATP>ADP>2meSATP>αβmeATP	$P2Y_4$	UTP>UTPγS>ATP, UDP inactive or UTP≈UDP>ATP*
$P2X_5$	ATP>2meSATP>ADP	$P2Y_5$	ATP>ADP>2meSATP>UTP
$P2X_6$	ATP>2meSATP>ADP	$P2Y_6$	UDP>UTP>ADP>>ATP
$P2X_7$	BzATP>ATP>2meSATP>ADP	$P2Y_7$	ATP>ADP=UTP

† Two groups have cloned a $P2X_3$ receptor from rat DRG cells. Chen *et al.* (1995) found 2meSATP to be more potent than ATP whereas Lewis *et al.* (1995) found ATP to be more potent than 2meSATP.

* Nicholas *et al.* (1996) call the $P2Y_4$ receptor a UTP receptor since UTP is much more potent than ATP and UDP is inactive. Communi *et al.* (1995) found UTP and UDP to be equipotent.

Adapted from Burnstock and King (1996).

P2X receptors are widely distributed but are particularly abundant in smooth muscle, heart, brain and spleen (Fredholm *et al.*, 1994). All subtypes except $P2X_1$ and $P2X_3$ have been found in the CNS of various species (Burnstock and King, 1996). The $P2X_7$ receptor is found mainly on immune cells such as macrophages and brain microglia and is of interest as a therapeutic target in areas of neuronal damage, where there are large numbers of activated microglia (Collo *et al.*, 1997).

As reviewed by Abbrachio and Burnstock (1994), there are several other potential therapeutic applications for either agonists or antagonists of P2X receptors. The $P2X_7$ receptor is a target on tumour cells because agonists cause cytotoxicity through apoptosis. Because of their ability to block smooth muscle contraction, P2X receptor antagonists have been suggested as useful agents in the treatment of renal failure and urinary incontinence caused by interstitial cystitis (Palea *et al.*, 1993).

2.1.2 P2Y Receptors

The review of Burnstock and Kennedy (1985) proposed that P2Y receptors differ from the P2X subtype by exhibiting a different ATP analog potency profile as follows:. P2Y receptors are G-protein linked receptors that regulate second messenger responses (Harden *et al.*, 1995). At least two signaling pathways exist for P2Y receptors. Stimulation can lead to activation of PLC through a G_q-type protein, or a decrease in AC activity, through a G_i protein. The PLC mechanism predominates in most systems tested to date (Harden *et al.*, 1995).

Subclassification of P2Y receptors, as with P2X receptors, is based on pharmacological differences (table 2). Observations of different affinities of ATP

analogs for P2Y receptors in different systems has led to the classification of P2Y receptors into seven subtypes ($P2Y_1$-$P2Y_7$) (Burnstock and King, 1996), all of which have been cloned. The first cloned was the $P2Y_1$ receptor from chick brain (Webb *et al.*, 1993). Since then others have cloned and expressed PLC-activating P2Y receptors from mouse, rat, bovine and human tissues. P2Y receptors are widely distributed with receptors $P2Y_{1-4}$ identified and cloned from brain of various species (Burnstock and King, 1996).

At least three of the cloned P2Y receptors are somewhat 'atypical' in that uracil nucleotides are more potent or equipotent to adenine nucleotides. The $P2Y_2$ receptor (formerly P_{2U}) is activated by UTP and ATP with equal potencies (Lustig *et al.*, 1993). Using receptor desensitization protocols, investigators demonstrated that cells desensitized to ATP still responded to UTP, indicating the existence of pyrimidinoceptors other than the $P2Y_2$ (Boehm *et al.*, 1995; Connolly, 1994). To date, two receptors, $P2Y_4$ and $P2Y_6$, have been cloned that are preferentially stimulated by uracil nucleotides relative to adenine nucleotides. Characterization of the human placental $P2Y_4$ in transfected 1321N1 human astrocytoma cells revealed equal stimulation of IP_3 formation by UTP and UDP while ATP was a partial agonist and ADP was inactive (Communi *et al.*, 1995). A separate study also used cloned $P2Y_4$ receptors expressed in 1321N1 cells and found that UTP was 50-fold more potent than ATP while UDP was inactive (Nicholas *et al.*, 1996). The $P2Y_6$ pyrimidinoceptor has been cloned from human placenta (Communi *et al.*, 1996) and rat aortic smooth muscle (Chang *et al.*, 1995). Characterization of the human placental clone indicated an agonist potency profile of UDP>UTP>ADP>ATP (Communi *et al.*, 1996). The identification of receptors selective

for uracil nucleotides has raised awareness that UTP and UDP may be endogenous signaling compounds (see Anderson and Parkinson, 1997 for review) and will almost certainly cause a change in the nomenclature and classification schemes for purino- and pyrimidinoceptors.

Another metabotropic P_2 receptor, found on platelets but not yet cloned, is termed P2T. The P2T receptor is activated by ADP and antagonized by ATP (table 1). Since ADP is a potent activator of platelets, an active area of research in antithrombotic drugs is the development of P2T receptor antagonists. Since it is metabotropic (Harden *et al.*, 1995) it may eventually be classified with the P2Y receptors. Ultimately, cloning and characterization of binding and signaling properties will determine how the P2T receptor is classified.

Like P2X receptors, P2Y receptors are being considered as potential therapeutic targets. Abbrachio and Burnstock (1994) have proposed that P2Y receptor agonists may be useful in the treatment of diabetes as they increase insulin production and glucose tolerance. Also, improved Cl^- conductance caused by $P2Y_2$ agonists may be beneficial in cystic fibrosis.

2.2 Adenosine Receptors

In 1978, Burnstock proposed separate receptor classes for adenosine and ATP. This was based on different relative potencies of ATP, ADP, AMP and adenosine, the ability of methylxanthines to antagonize the effects of adenosine but not ATP, changes in cAMP levels caused by adenosine but not ATP and induction of prostaglandin synthesis by ATP but not adenosine (Abbrachio and Burnstock, 1994).

By the late 1970s it was evident that more than one subtype of adenosine receptor existed and two subtypes (A_1AR and A_2AR) were proposed based on their abilities to either activate (A_2AR) or inhibit (A_1AR) AC activity (Londos *et al.*, 1980; van Calker *et al.*, 1979). A_2ARs have since been further divided into A_{2A}ARs and A_{2B}ARs since they both activate AC but display different agonist binding properties and vary in relative anatomical distributions (Olah and Stiles, 1995). In 1991, cDNA cloning using degenerate PCR primers based on other AR subtypes produced a fourth AR subtype termed the A_3AR (Meyerhof *et al.*, 1991). Little is known about the signaling mechanisms and physiological functions of the A_3AR relative to the other AR subtypes.

2.2.1 A_1 Adenosine Receptors

After van Calker *et al.* (1979) proposed the existence of two adenosine receptor subtypes based on work in cultured nerve cells, many groups focused on the purification of the A_1AR allowing its reconstitution with inhibitory G-proteins (Palmer and Stiles, 1995). Using degenerate PCR primers based on the third and sixth transmembrane domains of several G-protein linked receptors, two cDNAs were isolated from dog thyroid and termed RDC7 and RDC8 (Libert *et al.*, 1989). Subsequent expression in mammalian cells indicated that RDC7 was the canine A_1AR based on ligand binding properties. The availability of the canine A_1AR sequence allowed the cloning of A_1AR cDNAs from rat (Mahan *et al.*, 1991; Reppert *et al.*, 1991), bovine (Olah *et al.*, 1992; Tucker *et al.*, 1992), human (Libert *et al.*, 1992; Townsend-Nicholson and Shine, 1992) and rabbit (Bhattacharya *et al.*, 1993) cDNA libraries. Modeling of cloned A_1ARs predicts a 326 amino acid, 36.7 kDa protein with the seven transmembrane domains

typical of other G-protein coupled receptors (Olah and Stiles, 1995). Amino acid identity is about 90% among species homologs for cloned A_1ARs.

When expressed in mammalian cells, A_1AR clones bind AR agonists with the potency order R-PIA>NECA>S-PIA, the profile traditionally used to identify A_1ARs (Olah and Stiles, 1995). Caffeine is an antagonist at A_1ARs at concentrations greater than 20 μM, plasma levels often reached in coffee drinkers (Fredholm *et al.*, 1994). Theophylline is slightly more potent but other modified xanthines such as CPT, 8-PT and DPCPX are far more potent. DPCPX is a selective A_1AR antagonist with a K_i value less than or equal to 1 nM (Fredholm *et al.*, 1994). There are a number of compounds considered to be selective agonists for A_1ARs (table 3). CPA, CCPA and CHA stimulate A_1ARs in the range of 0.3-3 nM (Fredholm *et al.*, 1994) without effects at other known AR subtypes. Because of the rapid metabolism of adenosine *in vivo*, it has proven difficult to determine the affinity of adenosine for A_1ARs. It is estimated that the equilibrium dissociation constant for adenosine is about 14 nM for the high affinity, G-protein coupled state of the A_1AR and 7.6 μM for the low affinity state (Cohen *et al.*, 1996).

A_1ARs are linked to $G_{i\,(1\text{-}3)}$ and G_o proteins (Freissmuth *et al.*, 1991; Munshi *et al.*, 1991). Binding of an A_1AR agonist causes a number of second messenger signaling events depending on the system being studied. The most well-documented event associated with the activation of A_1ARs is inhibition of AC causing decreases in cAMP levels (Fredholm, 1995) but A_1ARs can also activate inwardly rectifying outward K^+ currents independent of changes in cAMP levels (Fredholm, 1995). N-type Ca^{2+} channels are inhibited by A_1ARs but this likely occurs secondary to changes in cAMP

(Palmer and Stiles, 1995). In some systems such as DDT_1 MF-2 cells A_1AR agonists cause activation of PLC and elevation of intracellular IP_3 and Ca^{2+} levels by a cAMP independent and pertussis toxin sensitive mechanism (Gerwins and Fredholm, 1992). In general this signaling mechanism is less well-defined and more system-dependent as A_1ARs have been shown to inhibit (Long and Stone, 1987), activate (Gerwins and Fredholm, 1992) or have no effect (Nanoff *et al.*, 1990) on IP_3 accumulation, depending on the cell type investigated. In addition, A_1ARs can activate voltage-dependent Cl^- channels and phospholipase D although these actions may be secondary to the above signaling processes (Fredholm, 1995).

Pharmacologically, A_1AR interaction with G-proteins can be manipulated by a compound called PD 81,723. PD 81,723 caused a 3-fold increase in the fraction of A_1ARs found in the high-affinity G-protein coupled conformation and a greater than 2-fold increase in the potency of R-PIA in CHO cells transfected with the human A_1AR (Bhattacharya and Linden, 1995). PD 81,723 may also potentiate constitutive activity of A_1ARs independent of A_1AR agonists (Kollias-Baker *et al.*, 1997).

Desensitization, or lessened functional response of a receptor upon prolonged exposure to an agonist, has been studied for A_1ARs. *In vivo*, multi-day infusions of rats with R-PIA or other A_1AR agonists leads to decreased ability of A_1ARs to mediate usual physiological responses caused by A_1AR agonists (Olah and Stiles, 1995). Decreases in receptor density and $G_{i\alpha\ 1,2}$ levels, as well as impaired coupling to G-proteins are seen (Olah and Stiles, 1995). Further studies in DDT_1 MF-2 cells have shown that R-PIA causes aggregation and phosphorylation of A_1ARs at the cell surface, followed by a slow

decrease in cell surface [^{3}H]R-PIA binding sites due partly to internalization and partly to the inability of cell surface A_1ARs to bind ligand (Ciruela *et al.*, 1997).

Autoradiography, mainly with [^{3}H]DPCPX, [^{3}H]CHA or [^{3}H]CPA, *in situ* hybridization and immunohistochemistry have determined that A_1ARs have a wide tissue distribution including testis, heart, lung and kidney (Fredholm *et al.*, 1994). A_1ARs are highly expressed in brain and are particularly abundant in cortex, hippocampus, cerebellum and thalamus (Olah and Stiles, 1995). In addition, they are co-localized and functionally linked with D_1 dopamine receptors on GABAergic striatonigral neurons; A_1AR antagonists can potentiate the motor effects of D_1 receptor stimulation (Popoli *et al.*, 1996). In general, A_1ARs are inhibitory in brain by attenuating the release of many neurotransmitters. Their wide brain distribution and functional coupling to important neurotransmitter systems is the reason A_1ARs have been linked functionally with many CNS processes such as ethanol intoxication, sleep and ischemic preconditioning. A_1ARs have been considered as therapeutic targets for conditions such as stroke, epilepsy and pain (Guieu *et al.*, 1997).

2.2.2 A_{2A} Adenosine Receptors

A_{2A}ARs were differentiated from A_1ARs based on the ability of the former to stimulate, rather than inhibit cAMP formation. Pharmacological differences, particularly in the potency of some 2-substituted adenosine analogs, provided evidence for two A_2AR subtypes (A_{2A}AR and A_{2B}AR) (Braun and Levitzki, 1979). The RDC8 cDNA isolated from dog thyroid was found to be an A_{2A}AR (Maenhaut *et al.*, 1990) and A_{2A}ARs have since been cloned from rat (Fink *et al.*, 1992) and human (Furlong *et al.*, 1992) cDNA

libraries, and a mouse genomic DNA library (Ledent *et al.*, 1997). A_{2A}AR clones from various species share a high degree of amino acid homology (~90%) (Ongini and Fredholm, 1997) and code for a seven transmembrane domain G-protein coupled integral membrane protein. A_{2A}ARs are larger than the other AR subtypes with 410-412 amino acids and a molecular mass of 45 kDa (Olah and Stiles, 1995). The extra 80-90 amino acids compared to other ARs correspond to the intracellular carboxyl tail. Since A_{2A}ARs can undergo more rapid desensitization than other ARs it was speculated that the carboxyl tail is important for this process, however at least one study indicates this is not the case (Palmer and Stiles, 1997).

A_{2A}AR clones expressed in mammalian cells display the traditional AR agonist potency profile for A_{2A}ARs, NECA>R-PIA>S-PIA. The compound [^{3}H]CGS 21680 is used to localize A_{2A}ARs and is a selective agonist, stimulating cAMP formation at concentrations just above 1 nM while having no effect at other ARs (Fredholm *et al.*, 1994). Like A_1ARs, caffeine and other xanthine derivatives can antagonize A_{2A}ARs. Caffeine is effective at concentrations above about 30 μM (Fredholm *et al.*, 1994), however xanthine derivatives, in general, display no selectivity for the A_{2A}AR. An exception is CSC, which is an effective antagonist of A_{2A}ARs in the 20 nM range but does not affect other AR subtypes. Another selective antagonist with similar affinity is KF 17837 (Palmer and Stiles, 1995). Adenosine itself seems to have similar affinities for both A_{2A}ARs and A_1ARs (table 3); the equilibrium binding constant for A_{2A}ARs is estimated at between 1-20 nM (Fredholm *et al.*, 1994).

Table 3: Characteristics of Adenosine Receptors

	A_1	A_{2A}	A_{2B}	A_3
G-protein	$G_{i\,(1\text{-}3)}$, G_o	G_s	G_s	unknown
Effectors	↓ cAMP ↑ IP_3/Ca^{2+} ↑ I_K	↑ cAMP	↑ cAMP	↓ cAMP ↑ IP_3/Ca^{2+}
Selective agonists	CPA, CCPA, CHA	CGS 21680	none	Cl-IB-MECA
Selective antagonists	DPCPX, XAC	CSC, KF 17837	none	none
Activation by adenosine	3-30 nM	1-20 nM	5-20 μM	>1 μM
Brain distribution	Cortex, cerebellum, hippocampus, thalamus	Striatum, nucleus accumbens, olfactory tubercle	pars tuberalis, glial cells	Species-dep. **RAT** – hippocampus, cerebellum

Adapted from Fredholm *et al.* (1994).

A_{2A}ARs cause activation of AC through the G_s-protein. A_{2A}ARs display unusually "tight" coupling to G_s-proteins as demonstrated by data showing that the addition of GTP failed to diminish agonist binding (Nanoff *et al.*, 1991). Unlike A_1ARs, no other signaling mechanisms have been observed consistently. However recent studies have shown that A_{2A}ARs can inhibit superoxide anion formation by a cAMP-independent activation of serine/threonine protein phosphatases in human neutrophils (Revan *et al.*, 1996), and can activate MAP kinase in endothelial cells (Sexl *et al.*, 1997).

Like A_1ARs, A_{2A}ARs undergo desensitization, however A_{2A}ARs appear to desensitize more rapidly. In DDT_1 MF-2 cells the $t_{½}$ for A_1AR and A_{2A}AR desensitization was 16 h and 45 min., respectively (Ramkumar *et al.*, 1991). In CHO cells, short-term treatment (30 min.) with AR agonists markedly decreased stimulation of AC accompanied by a 2-fold reduction in agonist affinity but no change receptor number (Palmer and Stiles, 1994). Agonist exposure for 30 min. also induced PKA-independent phosphorylation of A_{2A}ARs. Some evidence points to a PKC-dependent desensitization mechanism since inhibition of PKC markedly blocked the suppression of AC type VI (AC6) during A_{2A}AR desensitization (Lai *et al.*, 1997). Recent experiments showed that threonine 298 is essential for agonist-stimulated receptor phosphorylation and short-term desensitization (Palmer and Stiles, 1997). It could be a combination of phosphorylation events, both at A_{2A}ARs and specific AC isoforms that is responsible for short-term A_{2A}AR desensitization. After 24 h of AR agonist treatment, A_{2A}ARs downregulate and $G_{i\alpha\ 2,3}$ expression increases, much the same type of desensitization that A_1ARs undergo. Interestingly, threonine 298 is not important for this process (Palmer and Stiles, 1997).

Northern blotting shows expression of mRNA for A_{2A}ARs in peripheral tissues such as heart, thymus, liver and adipose tissue (Olah and Stiles, 1995). A_{2A}ARs are also abundant on neutrophils, platelets and in blood vessels. In brain, autoradiography with [^{3}H]CGS 21680 showed enriched expression of A_{2A}ARs in the caudate-putamen, nucleus accumbens, olfactory tubercle and the lateral segment of the globus pallidus (Parkinson and Fredholm, 1990). RT-PCR and functional studies have shown that A_{2A}ARs are also present in regions such as hippocampus, cortex and nucleus tractus solitarius (Ongini *et al.*, 1997). The physiological roles of A_{2A}ARs became better understood with the development of an A_{2A}AR knockout mouse. Elimination of A_{2A}ARs in mice resulted in increased anxiety, aggressiveness, blood pressure, heart rate and platelet aggregation while exploratory behaviour and response to acute pain were attenuated (Ledent *et al.*, 1997). In contrast to the inhibitory role of A_1ARs, A_{2A}ARs in the CNS are excitatory. They can stimulate the release of a number of neurotransmitters and interact with neurotransmitter receptors systems as well. Possible therapeutic uses of A_{2A}ARs include disorders involving basal ganglia dopaminergic systems (see section 3.1.7), respiratory stimulation mediated through arterial chemoreceptors and enhancing cognition or controlling dementia (e.g. Alzheimer's Disease) through stimulation of acetylcholine release (Sebastião and Ribeiro, 1996).

2.2.3 A_{2B} Adenosine Receptors

As reviewed by Olah and Stiles (1995), A_{2B}ARs were discriminated from A_{2A}ARs based on the lower affinity of A_{2B}ARs for AR agonists, as well as on the basis of different anatomical distributions. A_{2B}ARs have been cloned from both rat (Stehle *et al.*,

1992) and human (Pierce *et al.*, 1992) cDNA libraries. The size of the rat protein (332 amino acids) is similar to the A_1AR and A_3AR and is 78 residues smaller than the rat A_{2A}AR. The lack of high affinity or selective compounds for A_{2B}ARs has made characterization and even identification of clones difficult. Clones were identified as A_{2B}ARs by lack of binding of CGS 21680 and low affinity binding of NECA; NECA is at least 25-fold less potent at A_{2B}ARs compared with A_{2A}ARs (Fredholm *et al.*, 1994). Xanthine derivatives are effective A_{2B}AR antagonists, however they are not selective. DPCPX and 8-PT are antagonists beginning at about 20 nM whereas they are not effective until about 200 nM for A_{2A}ARs (Fredholm *et al.*, 1994). Similar to A_{2A}ARs, caffeine is an A_{2B}AR antagonist at concentrations above about 30 μM. A_{2B}ARs have a much lower affinity for adenosine as well when compared to the other ARs. It is estimated that adenosine stimulates cAMP formation through A_{2B}ARs starting at concentrations from 5-20 μM (Fredholm *et al.*, 1994) (table 3).

A_{2B}ARs are linked to the G_s-protein and activate AC. The ability of A_{2B}AR agonists to stimulate cAMP production is increased by agents that activate PKC in several cells (Fredholm, 1995) indicating that lower concentrations of adenosine may have greater effects when PKC activators are present; it is thought that PKC exerts this effect at the G-protein level. In addition, recombinant A_{2B}ARs can activate Ca^{2+} channels *via* PLC activation in cRNA-injected *Xenopus* oocytes (Yakel *et al.*, 1993).

Northern analysis in rat shows abundant A_{2B}AR mRNA in cecum, large intestine and urinary bladder, with lesser amounts in brain, spinal cord and lung (Stehle *et al.*, 1992). Although mRNA levels are relatively low in brain, A_{2B}ARs appear to be more widely distributed than A_{2A}ARs, with heaviest concentration in the pars tuberalis of the

pituitary (Linden, 1993). The most abundant AR subtype in astrocytes seems to be the A_{2B}AR (Altiok *et al.*, 1992) and this may account for the observed ubiquitous brain distribution of A_{2B}ARs. Since A_{2B}ARs require high concentrations of adenosine to activate AC, glial cell ARs are likely activated in pathophysiological conditions when adenosine formation is enhanced.

2.2.4 A_3 Adenosine Receptors

In 1991, using degenerate PCR primers, Meyerhof *et al.* cloned a cDNA from rat testis that resembled an adenosine receptor subtype and was termed an A_3AR. A_3ARs were subsequently cloned from sheep (Linden *et al.*, 1993) and human (Salvatore *et al.*, 1993) cDNA libraries and are 72% similar to the rat A_3AR at the amino acid level, displaying more species variation than other AR subtypes. The rat A_3AR is a similar size to the A_1AR, encoding a protein of 320 amino acids. Modeling predicted a seven transmembrane domain structure, similar to the other G-protein linked adenosine receptors.

The rat A_3AR cDNA expressed in CHO cells exhibited an agonist potency profile different from previously identified adenosine receptors (R-PIA=NECA>S-PIA) and the affinities were lower than for the A_1 or A_{2A} adenosine receptors. Strikingly, xanthine derivatives bound very poorly to this receptor (Zhou *et al.*, 1992), a characteristic not shared by any of the other AR subtypes. Sheep and human A_3ARs are somewhat more sensitive to xanthines than rat or mouse A_3ARs (Linden, 1994). Discovery of compounds selective for A_3ARs has been slow but appears to have been more successful lately. APNEA binds to and stimulates A_3ARs with a K_d of 15 nM but is not selective as it is

also a potent A_1/A_2 agonist (Zhou *et al.*, 1992). Currently, the most selective and potent agonist available for A_3ARs is Cl-IB-MECA; it is 2500- and 1400-fold more potent at A_3ARs than at A_1ARs and A_{2A}ARs, respectively (von Lubitz, 1997). Certain substituted xanthine derivatives such as I-ABOPX are able to antagonize A_3ARs, however selectivity has not been attained. Recently, pharmaceutical companies have disclosed compounds purported to be selective antagonists for A_3ARs (von Lubitz, 1997). Adenosine appears unable to activate A_3ARs until it reaches concentrations greater than 1 μM (Fredholm *et al.*, 1994). Like A_{2B}ARs, this may mean that A_3ARs are important in pathophysiological conditions when adenosine levels are high.

Like the A_1AR, more than one second messenger system has been noted upon stimulation of A_3ARs. The first observations were that A_3ARs could inhibit forskolin-stimulated increases in cAMP through a link with the G_i-protein (Zhou *et al.*, 1992). Subsequent reports have revealed that A_3ARs can stimulate IP_3 and intracellular Ca^{2+} production by activation of PLC (Ramkumar *et al.*, 1993). It is unclear under which conditions each system predominates. At least one study indicates that this may be determined by agonist concentration and length of exposure (Ceruti *et al.*, 1996).

Like other characteristics of A_3ARs, tissue distribution is species-dependent. In rat, A_3ARs are most abundant in testis, followed by kidney, lung and heart; lower levels are seen brain (Zhou *et al.*,1992). In sheep, lung, spleen and pineal gland have the highest concentration of A_3ARs while brain regions including cortex, cerebellum, striatum and hypothalamus have fewer (Linden *et al.*, 1993). Data in humans indicate that lung, liver and placenta are enriched in A_3ARs while fewer are found in brain, liver, heart and kidney (Salvatore *et al.*, 1993). While A_3ARs are expressed at relatively low

levels in rat brain, there are significant regional differences in levels of A_3AR mRNA. One report showed that hippocampus and cerebellum have the highest levels within rat brain (De *et al.*, 1993).

CNS functions of the low affinity A_3AR remain unclear; however, one study showed that A_3AR stimulation by Cl-IB-MECA desensitizes the inhibitory effect of A_1ARs in rat hippocampus (Dunwiddie *et al.*, 1997). A_3ARs have also been reported to enhance glutamate toxicity in cooperation with metabotropic glutamate receptors, cause apoptosis in astrocytes and suppress TNFα release from human macrophage and microglial cells (von Lubitz, 1997). Considering these functional observations of A_3ARs, it is tempting to speculate that manipulating the occupancy of A_3ARs may provide therapeutic benefit in some CNS disorders.

3. Potential Therapeutic Uses of Adenosine Receptors

3.1 Physiological Roles of Adenosine in the CNS: Therapeutic Implications

Adenosine has been implicated in many CNS processes including apoptosis, synaptic plasticity, sleep/alertness and antinociception. The localization of adenosine receptors in the CNS and the development of selective agonists and antagonists has allowed researchers to determine specific receptor subtypes responsible for many of these actions. This has created opportunities to explore possible therapeutic benefits of manipulating adenosine receptor occupancy for conditions such as stroke, seizure, schizophrenia, Parkinson's disease, pain and dementias.

3.1.1 Antinociception

Adenosine analogs administered intrathecally or systemically produce antinociception in tactile, pressure and heat models of the acute pain response (Sollevi, 1997). This effect is mediated through the spinal cord where A_1ARs and A_2ARs have been localized to the substantia gelatinosa (implicated in the control of nociception) of the dorsal horn (Guieu *et al.*, 1997). The antinociceptive effects are thought to be mediated by A_1ARs (Sollevi, 1997) as CPA produced more effective antinociception than CGS 21680 in a rat transcutaneous stimulation model (Reeve and Dickenson, 1995). Since methylxanthines were able to block antinociceptive effects produced by morphine and β-endorphin and opioid receptor activation caused adenosine release in spinal cord (Sweeney *et al.*, 1987), adenosine is thought to contribute to the antinociceptive effects of opioids.

Several mechanisms have been proposed to explain the antinociceptive effects of AR stimulation. Antinociceptive doses of R-PIA administered to rats intrathecally decreased cerebrospinal fluid levels of substance P (Sjolund *et al.*, 1997), a known mediator of certain pain responses. The ability of A_1ARs to decrease glutamate release has been implicated since CPA inhibited glutamate-associated electrophysiological pain responses in rat dorsal horn neurons (Reeve and Dickenson, 1995). Finally, the anti-inflammatory effects of A_1AR stimulation may produce relief from pain associated with inflammation (Guieu *et al.*, 1997). These findings of the antinociceptive effects of adenosine receptor stimulation have spurred the research and development of adenosine receptor agonists and metabolic inhibitors of endogenous adenosine (AK inhibitors) as

local anesthetics and analgesics for acute and chronic pain, including neuropathic pain (Guieu *et al.*, 1997).

3.1.2 Adenosine and Sleep/Alertness

The most widely used psychotropic drug in the world is caffeine. The effects of caffeine on maintaining alertness are well-known and studies are now showing that this is likely due, at least in part, to antagonism of adenosine receptors (discussed in following section).

Mesopontine and basal forebrain cholinergic neurons play a major role in EEG arousal associated with alertness. It has been shown that A_1ARs inhibit cholinergic transmission in these neurons along with associated EEG arousal (Rainnie *et al.*, 1994; Porkka-Heiskanen *et al.*, 1997). Microdialysis of adenosine into the cholinergic basal forebrain and mesopontine cholinergic nuclei reduced wakefulness and EEG arousal in cats (Porkka-Heiskanen *et al.*, 1997) while A_1AR antagonists reduced paradoxical sleep (Guieu *et al.*, 1997). An important question arises: Is EEG activity associated with mesopontine cholinergic neurons under tonic inhibitory control by endogenous adenosine? Studies have found that endogenous adenosine levels increase during wakefulness and decrease during delta wave sleep (Huston *et al.*, 1996; Porkka-Heiskanen *et al.*, 1997). Since neuronal metabolic activity decreases during prolonged wakefulness, it is plausible to hypothesize that increasing endogenous adenosine levels throughout wakefulness leads to decreased alertness and increased propensity for sleep. This hypothesis was supported with the use of a potentiator of endogenous adenosine (adenosine transport inhibitor), NBMPR. NBMPR, microdialyzed into the cholinergic

forebrain, was able to mimic levels of endogenous adenosine and sleep-wakefulness patterns seen in sleep-deprived cats; this effect was not observed following microdialysis of NBMPR into non-cholinergic forebrain regions (Porkka-Heiskanen *et al.*, 1997). Another study also found that an adenosine transport inhibitor, soluflazine, decreased waking and increased sleep in rats (O'Connor *et al.*, 1991).

A_{2A}ARs may also mediate sleep as Satoh and co-workers (1996) found that CGS 21680 was able to mimic the sleep-inducing activity of prostaglandin D_2 in rostral basal forebrain; caffeine would also be expected to antagonize this effect. Besides blocking adenosine receptors, caffeine may also contribute to decreased sleep by inhibiting melatonin production in the pineal gland (Wright *et al.*, 1997). Experiments such as those discussed here have provided evidence that adenosine is a physiological mediator of degree of alertness and may also explain the mechanism of caffeine's ability to suppress recovery sleep.

3.1.3 Adenosine and Apoptosis

While necrosis is a form of cell death that occurs in response to toxic signals and involves disruption of nuclear membranes, apoptosis is a form a cell death that occurs in an organized, programmed manner. Cell membrane integrity is maintained while chromatin condenses and nuclear disruption occurs. Chromatin is then cleaved to high molecular weight DNA fragments which are subsequently degraded further. Cytotoxic effects of adenosine have been observed in human thymocytes, embryonic neurons, astrocytes, microglia and endothelial cells (Chow *et al.*, 1997). In bovine pulmonary arterial endothelial cells it was proposed that adenosine causes apoptosis through an

intracellular mechanism by altering *S*-adenosylmethionine-mediated methylation reactions (Dawicki *et al.*, 1997). In other systems, adenosine-induced apoptosis appears to be receptor-mediated (Chow *et al.*, 1997).

The question of what AR subtypes are involved has not yet been answered adequately. In human thymocytes, CGS 21680 appears to be the most potent inducer of apoptosis, suggesting a role for the A_{2A}AR (Szondy, 1994), while in human neutrophils A_{2A}ARs delayed apoptosis (Walker *et al.*, 1997). In rat microglia, adenosine analogs caused apoptosis with a potency profile suggestive of no known AR subtype (Ogata and Schubert, 1996). One line of research showed that high concentrations of the A_3AR agonists I-AB-MECA and Cl-IB-MECA caused xanthine-insensitive apoptosis in HL-60 leukemia cells (Khono *et al.*, 1996) and primary rat astrocyte cultures (Abbracchio *et al.*, 1997). As reviewed by Abbracchio *et al.* (1997), A_3AR induced apoptosis could be beneficial by playing a role during brain development. It could also allow the orderly death of irreversibly damaged cells in order to spare energy for recovering cells following trauma or stroke. Alternatively, A_3AR-induced apoptosis could be a mechanism of pathological cell death in neurodegenerative events as apoptosis has been observed in ischemia, epilepsy, HIV encephalopathy and neurodegenerative diseases (Abbracchio *et al.*, 1997).

3.1.4 Adenosine and Synaptic Plasticity

The physiological basis of learning and memory likely involves changes in the efficiency of synapses between neurons integrated in a network. Adenosine is thought to be a modulator of a number of different forms of synaptic plasticity.

Paired-pulse facilitation (PPF) is the enhancement of a second stimulus when it is preceded (tenths to hundreds milliseconds) by an initial stimulus. Adenosine was shown to enhance PPF in hippocampus both in CA1 Schaffer collateral fibres (Dunwiddie and Haas, 1985) and cultured pyramidal cells (Debanne *et al.*, 1996). By inhibiting release, adenosine is thought to conserve neurotransmitter to be released in a second potentiated response following an initial stimulus. In a phenomenon termed heterosynaptic posttetanic depression (PTD), extracellular adenosine, accumulated during synaptic activity, can also inhibit neural activity in a neighbouring pathway for a short time period, likely until adenosine is taken up or metabolized (de Mendonça and Ribeiro, 1997). Two more processes, termed long-term potentiation and long-term depression, in which adenosine has been implicated have more relevance in terms of long-term learning and memory.

Long-term potentiation (LTP) is the long-term strengthening of synaptic activity in response to high-frequency stimulation of afferent pathways. LTP is most well-studied in the hippocampus and has been implicated as a mechanism of memory storage. In the 1980s it was found that adenosine and adenosine analogs such as 2-CA inhibited LTP in various hippocampal neural pathways (de Mendonça and Ribeiro, 1997), an effect blocked by the A_1AR antagonist DPCPX. DPCPX was also able to enhance LTP on its own (Arai and Lynch, 1992) and NBMPR decreased LTP (de Mendonça and Ribeiro, 1994) indicating that endogenous adenosine could play a role in the modulation of LTP in the CA1 region of the hippocampus. A_{2A}ARs may also contribute to LTP as CGS 21680 facilitated evoked potentials in the hippocampal CA1 region in response to stimulation of

Schaffer fibres (de Mendonça and Ribeiro, 1994). Acting at A_{2A}ARs, adenosine may balance the effects of A_1AR stimulation.

Long-term depression (LTD) is associated with a long-term decrease in synaptic efficiency following low-frequency stimulation. DPCPX potentiated LTD (de Mendonça and Ribeiro, 1997) and endogenous adenosine, through A_1ARs, appears to attenuate LTD. Adenosine is thought to exert its effects on both LTP and LTD through inhibition of NMDA responses, although NMDA-independent LTP in hippocampal CA3 pyramidal cells can also be decreased by adenosine (Harris and Cotman, 1986).

The effects of endogenous adenosine on LTP make it tempting to hypothesize that A_1AR agonists may depress cognition while antagonists of A_1ARs may function as cognitive and memory enhancers.

3.1.5 Adenosine and Ethanol Intoxication

Some stimulatory effects of AR antagonists such as caffeine are thought to be mediated by blockade of the tonic inhibitory effects of adenosine in the CNS. It was proposed that the CNS depressant effects of ethanol may result from enhancement of these effects (Proctor and Dunwiddie, 1984).

Adenosine and ethanol have many similar effects at the cellular level and cross-tolerance between ethanol and adenosine was observed in brain (Dar *et al.*, 1994) suggesting that the effects of ethanol may be mediated by the adenosinergic system. Further evidence for this hypothesis was provided when it was found that ethanol potentiated the effects of adenosine by inhibiting uptake (Nagy *et al.*, 1990) and enhancing release (Clark and Dar, 1989). A_1ARs are thought to mediate the effects of

ethanol on motor-incoordination (MI). Intracerebellar CHA accentuated ethanol-induced MI in mice (Dar, 1990) while DPCPX was able to antagonize the motor effects of ethanol (Dar, 1996). Furthermore, it was found that pertussis toxin and stable cAMP analogs reversed the effects of CHA (Dar, 1997). A_2ARs are thought to have a minimal role in mediating the motor effects of ethanol.

Therapeutic applications of this effect of adenosine are limited, however it seems that drinking coffee may indeed attenuate motor disabilities caused by ethanol intoxication.

3.1.6 Adenosine and Epilepsy

During convulsions, neurons use ATP at a very high rate and endogenous adenosine in brain increases to micromolar levels (Winn *et al.*, 1979). This adenosine may be protective by acting as an endogenous anticonvulsant. Enhancing endogenous adenosine in rat prepiriform cortex decreased seizure susceptibility (Zhang *et al.*, 1993) and adenosine inhibited neuronal activity by activating K^+ channels and hyperpolarizing membranes (Gerber *et al.*, 1989). The effects of adenosine are thought to be mediated by A_1ARs as A_1AR agonists inhibited seizures in mice (von Lubitz *et al.*, 1994) and suppressed status epilepticus in rats while A_2AR agonists had no effect (Young and Dragunow, 1994). Recently A_3ARs have been investigated for their role in the anticonvulsant effects of adenosine. Chronic IB-MECA administration protected mice against chemically-induced seizures (von Lubitz *et al.*, 1995); the mechanism is unclear. Based on current ideas, A_1AR agonists may be useful anticonvulsants, however, unwanted sedation associated with A_1AR stimulation is a drawback.

3.1.7 Adenosine and Affective Disorders

In the mid-1970s it was noticed that caffeine could mimic the motor effects of dopamine receptor agonists (Fredholm *et al.*, 1976). Identification and localization of A_{2A}ARs to the dopamine-rich striatum caused speculation that A_{2A}ARs may play a role in this effect of caffeine.

The most abundant type of neuron in the striatum is the GABAergic medium spiny neuron, of which there are two subtypes. The striatonigral and striatoentopeduncular neurons contain substance P and dynorphin and coexpress dopamine D_1 and A_1ARs. Dopamine D_2 receptors and A_{2A}ARs are colocalized on the striatopallidal neurons, which contain enkephalin (Ferré *et al.*, 1997). Correlating with the original data showing the ability of caffeine to potentiate dopamine D_2 receptor effects, A_{2A}ARs and D_2 receptors were shown to be functionally linked in cultured cells and in the striatum. A_{2A}AR stimulation caused a decrease in the affinity of dopamine receptor agonists for D_2 receptors (Ferré *et al.*, 1991). Also, dopamine denervation or chronic D_2 receptor blockade led to upregulation of A_{2A}ARs and increased sensitivity to the motor effects of A_{2A}AR antagonists (Ferré and Fuxe, 1992). *In vivo*, CGS 21680 administered into the caudate-putamen inhibited D_2 antagonist-induced decreases in GABA levels in the globus pallidus while theophylline potentiated the effects of D_2 agonists (Ferré *et al.*, 1993). Motor activation caused by A_{2A}AR antagonists was eliminated by reserpine (dopamine depletion) or D_2 receptor blockade while CGS 21680 inhibited the motor-activating effects of D_2 agonists, importantly indicating that observed functional coupling of the two receptors can be seen behaviourally (Ferré *et al.*, 1992).

At the molecular, cellular and behavioural levels, it is clear that A_{2A}ARs and D_2 receptors function in an antagonistic manner in the striatum. There are exciting possible therapeutic implications of this relationship. Theophylline has been reported to improve the antiparkinsonian effects of L-dopa (Mally and Stone, 1994) raising the possibility that A_{2A}AR antagonists given with D_2 agonists may be useful in Parkinson's disease. Hyperkinesia in Huntington's chorea is associated with striatopallidal damage; A_{2A}AR agonists may be beneficial in this case (Ferré *et al.*, 1997). Classical anti-psychotic drugs used in the treatment of schizophrenia are antagonists of D_2 receptors in the striatum. A_{2A}AR agonists may be good anti-psychotics by decreasing stimulation of D_2 receptors. Furthermore, the major problem with using phenothiazines and haloperidol (commonly used anti-psychotics) is tardive dyskinesia thought to be caused by chronic blockade of D_2 receptors. Some groups report that tardive dyskinesias are more prominent with D_2 blockade in the dorsal rather than the ventral striatopallidal system, the region of the more powerful A_{2A}AR-D_2 interaction (Ferré *et al.*, 1994). A_{2A}AR agonists may offer relief from symptoms of schizophrenia while causing fewer extrapyramidal side effects.

3.1.7 Adenosine and cerebral blood flow

Adenosine is a metabolic factor involved in the regulation of cerebral blood flow. Several factors have led to this conclusion. Brain levels of adenosine rise rapidly following hypoxia, ischemia or seizure (Winn *et al.*,1979a,b and 1981a). All of these conditions are associated with decreased cerebrovascular resistance (Phillis, 1989). Adenosine (A_{2A}) receptors have been localized to, and cause dilation of, isolated cerebral vessels, indicating a role for A_{2A}ARs in the vascular response to adenosine. Brain

microvessels also possess the enzymes to form and catabolize adenosine, and they can take up adenosine through transport processes. Decreased resistance caused by excess adenosine in times of metabolic challenge may be a mechanism by which blood flow is autoregulated in ischemia, hypoxia or seizure. Furthermore, adenosine may be cleared from brain parenchymal tissues by passage into the blood stream across the blood-brain barrier, allowing blood-brain barrier adenosine transporters to be targeted therapeutically in enhancing brain adenosine levels and neuroprotection in ischemic conditions.

3.2 Neuroprotective Effects of Adenosine in Cerebral Ischemia

During cerebral ischemia, ATP synthesis is severely compromised and interstitial levels of its precursor, adenosine, can rise from basal levels of about 50 to 300 nM, to low micromolar levels (Rudolphi *et al.*, 1992). Observations that adenosine analogs inhibit excessive neuronal activity associated with ischemia-induced depolarization have led to speculation that adenosine is an endogenous neuroprotective agent. In smooth muscle, neutrophils, platelets, glial cells and neurons, adenosine has effects that support this hypothesis. Almost all of these actions have been linked to the activation of specific adenosine receptor subtypes. The inhibitory A_1ARs are suspected to be the most important receptors for the neuroprotective effects of adenosine but there are also benefits derived from A_{2A}ARs, A_{2B}ARs and possibly A_3ARs as well.

3.2.1 A_1ARs and Neuroprotection

Neuronal death due to ischemia is associated with disturbed ion homeostasis and excess membrane depolarization, excitatory amino acid neurotransmitter release

(primarily glutamate), glutamate receptor stimulation, and Ca^{2+} entry into cells. Necrosis is thought to occur in response to toxic accumulation of Ca^{2+} and may be a result of events such as lipid peroxidation, radical generation, activation of proteolytic enzymes and pathological gene activation (Siesjö and Bengtsson, 1989). In brain, striatum and hippocampus are regions particularly vulnerable to ischemic damage. High affinity A_1ARs are located pre- and post-synaptically in these regions and are co-localized with NMDA-type glutamate receptors (Rudolphi *et al.*, 1992).

Pre-synaptically, adenosine inhibits the release of a number of neurotransmitters, including glutamate (Fredholm and Dunwiddie, 1988). Calcium-dependent glutamate release occurs upon pre-synaptic membrane depolarization associated with ischemia. A_1ARs can inhibit Ca^{2+} influx and enhance K^+ efflux (Fredholm and Dunwiddie, 1988), thus stabilizing the membrane and decreasing glutamate release (figure 1). It is not known how adenosine affects Ca^{2+}-independent glutamate release or glial glutamate uptake and release.

In post-synaptic neurons, A_1ARs act by a number of different mechanisms, essentially leading to reduced Ca^{2+} accumulation (figure 1). Again, A_1ARs inhibit Ca^{2+} influx directly through N-type Ca^{2+} channels. A_1ARs also hyperpolarize membranes by activating K^+ efflux and Cl^- influx (Mager *et al.*, 1990), thereby allowing less Ca^{2+} entry through other voltage-operated Ca^{2+} channels as well. Ca^{2+} accumulation through glutamate-gated ion channels of the NMDA and AMPA/kainate subtypes is attenuated by A_1ARs because of their pre-synaptic effects on glutamate release. This decrease in glutamate release also accounts for decreased Ca^{2+} mobilization from intracellular stores

Figure 1: Neuroprotective Effects of A_1 Adenosine Receptors

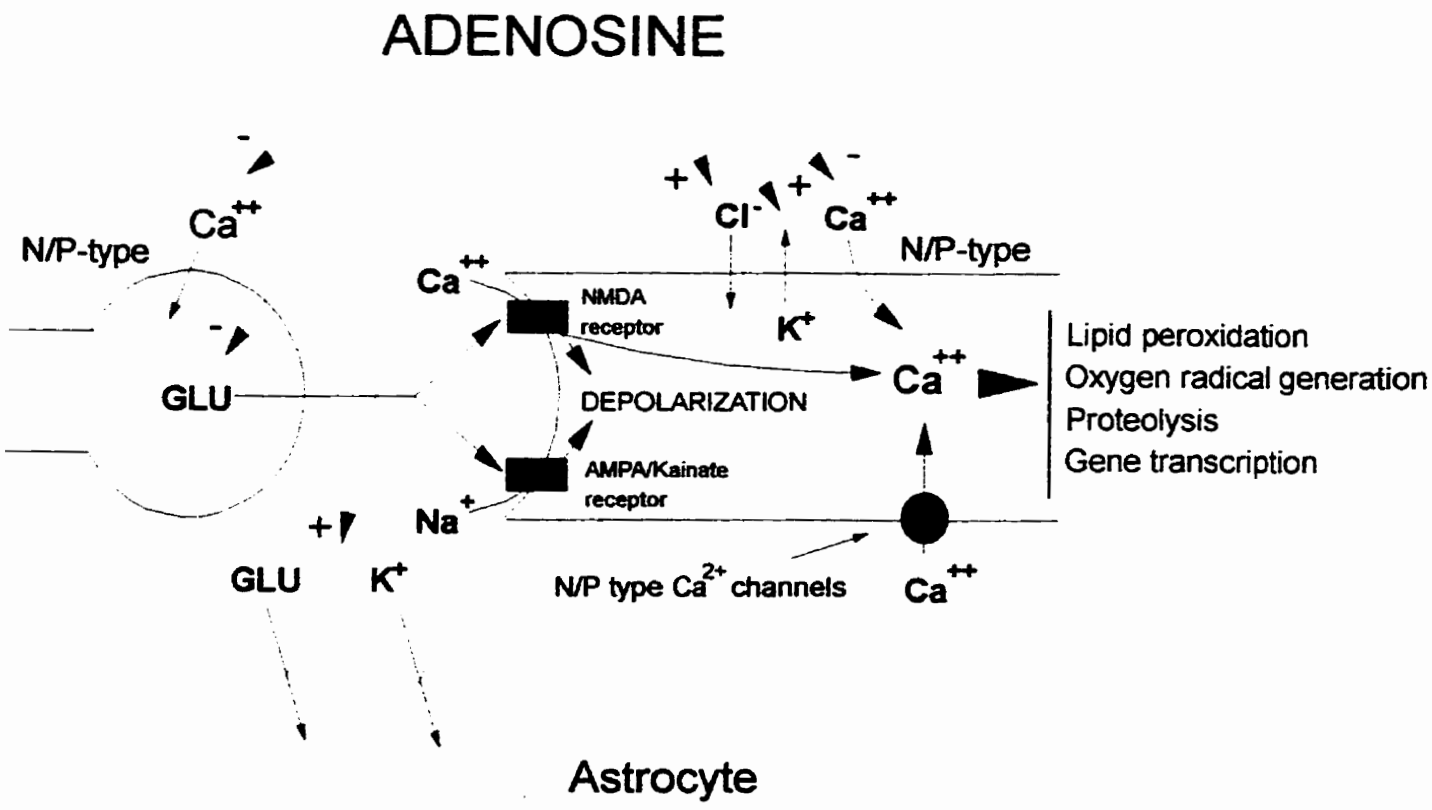

A_1AR stimulation hyperpolarizes neuronal membranes through inhibition of N/P-type Ca^{2+} channels and activation of K^+ and Cl^- currents. This causes decreased glutamate release from pre-junctional nerves and decreased toxic Ca^{2+} accumulation in post-synaptic nerves. Glial cells are also hyperpolarized and may assist neurons by taking up glutamate and K^+.

in response to stimulation of metabotropic glutamate receptors (Rudolphi *et al.*, 1992). It is evident that A_1AR stimulation leads to a decrease in Ca^{2+} accumulation and associated toxicity by a number of different mechanisms.

A_1ARs on glial cells may also aid in protecting neurons from ischemic damage. No clear role for A_1ARs on microglial cells has been described, however one study reported that both A_1AR and A_2AR activation was necessary to cause microglial activation and proliferation (Gebicke-Haerter *et al.*, 1996). A_1ARs on astrocytes cause membrane hyperpolarization and by this mechanism are thought to be protective by improving uptake of excessive glutamate and K^+ (Miller and Hsu, 1992). Observations of protective effects of A_1AR stimulation at the cellular and molecular levels have been verified *in vivo*. As summarized by Miller and Hsu (1992), the A_1AR agonists R-PIA and CHA protected hippocampal CA1 neurons from damage in both global and focal ischemia models in rat and gerbil when given up to 30 minutes post-ischemia. The importance of adenosine as an endogenous neuroprotective agent was underlined by data that showed enhanced neuronal damage in many species in response to acute treatment with A_1AR antagonists (Rudolphi *et al.*, 1992). Of interest is the observed regimen-dependence of neuroprotective effects seen with AR agonists and antagonists (table 3). Chronic treatment of gerbils with DPCPX (1 mg/kg) afforded significant protection, presumably due to A_1AR upregulation, while chronic CPA treatment led to enhanced damage and mortality compared to controls (von Lubitz *et al.*, 1994). Thus, while acute treatment with AR agonists was neuroprotective, chronic treatment exacerbated ischemic damage. The reverse was true for AR antagonists. The opposite results obtained with

chronic, compared to acute, administration likely reflect regulation of receptor densities and/or signal transduction pathways.

Table 3: Chronic Versus Acute Effect Reversal for Peripherally-Administered Adenosine Receptor Agonists and Antagonists in Cerebral Ischemia

	A_1AR		$A_{2A}AR$		A_3AR	
	Agonist CPA	*Antagonist* DPCPX	*Agonist* APEC	*Antagonist* CSC	*Agonist* IB-MECA	*Antagonist* None
Acute	++	-	0	++	-	NA
Chronic	-	++	++	+	++	NA

- Data taken from Jacobson *et al.* (1997)
- + signifies neuroprotection (number of symbols signifies relative degree of protection)
- - signifies enhanced neuronal damage
- NA, not applicable

Ischemic preconditioning occurs in heart and brain when brief periods of sublethal ischemia protect cells from a subsequent more severe ischemic insult. Adenosine is a mediator of ischemic preconditioning through A_1ARs and potentially A_3ARs in heart (Linden, 1994). In brain, adenosine levels are enhanced following an ischemic episode due to reduced ATP synthesis. A_1ARs are activated and

neuroprotection against a subsequent insult occurs *via* opening of ATP-sensitive K^+ channels (Herteaux *et al.*, 1995). A possible application of the preconditioning phenomenon may be surgically-induced ischemia, wherein short ischemic episodes in cardiac and brain tissues may protect against later unavoidable insults.

3.2.2 A_2ARs and Neuroprotection

During ischemia/hypoxia, extracellular adenosine levels can increase substantially in brain (Winn *et al.*, 1979, 1981a; Rudolphi *et al.*, 1992) and are thought to contribute to regulation of cerebral blood flow (Winn *et al.*, 1981b). Stimulation of A_2ARs is reported to have neuroprotective effects in cerebral ischemia by enhancing cerebral blood flow (Rudolphi *et al.*, 1992), however more recent discoveries of excitatory actions caused by A_2ARs have made for an unclear picture of whether adenosine and A_2AR agonists are neuroprotective.

In brain, A_{2A}ARs were first localized in striatum, blood vessels, platelets and neutrophils and this distribution is still thought to represent the major A_{2A}AR abundance in brain. Beneficial effects of A_{2A}AR stimulation during ischemia may include improvement of blood and nutrient supply by vasodilation and inhibition of platelet activity (Rudolphi *et al.*, 1992). A_{2A}AR-mediated inhibition of neutrophil activation is thought to decrease peroxide and superoxide radical formation by stimulated neutrophils, thus decreasing radical-induced neuronal death (Miller and Hsu, 1992). Decreased adherence of activated neutrophils to endothelial cells also limits capillary blocking and further ischemic damage.

In addition to the effects of A_{2A}ARs discussed above, a number of trophic effects are mediated by A_2ARs on different CNS cell types and may be important for neuroprotection. A_2AR stimulation by adenosine in pathophysiological conditions may stimulate production of neurotrophins, pleiotrophins and neuroprotective compounds by glial cells, and may enhance neurite growth and neuronal survival.

Several studies have indicated that A_2AR activation may affect the re-growth and differentiation of neurons following ischemia. For example, A_2ARs induced neurite elongation in human neuroblastoma and PC12 cells (Neary *et al.*, 1996). Furthermore, A_{2A}AR activation caused increased NGF expression in rat microglia (Heese *et al.*, 1997) and may also be responsible for the hypoxic induction of other growth factors such as vascular endothelial growth factor (Takagi *et al.*, 1996).

A characteristic event following ischemia is proliferation and hypertrophy of astrocytes around the area of neuronal damage. Astrocytes are thought to be support cells for neurons and are necessary for axonal growth and guidance. In cultured human astrocytoma cells, adenosine and ADP caused increased DNA synthesis through an A_2AR (Rathbone *et al.*, 1992) and *in vivo*, GFAP staining doubled 48 hours after cortical injection of the non-selective AR agonist CPCA; this was abolished by an A_2AR antagonist, DPMX (Hindley *et al.*, 1994). It cannot be determined which A_2AR subtype is responsible since high agonist and antagonist concentrations were used in these experiments. A_{2A}ARs can activate MAP kinase in human endothelial cells (Sexl *et al.*, 1997) and may act similarly in astrocytes to initiate a key element in the signal transduction pathways involved in cellular proliferation, providing a possible mechanism

Figure 2: Neuroprotective Effects of Adenosine A_2 Receptors

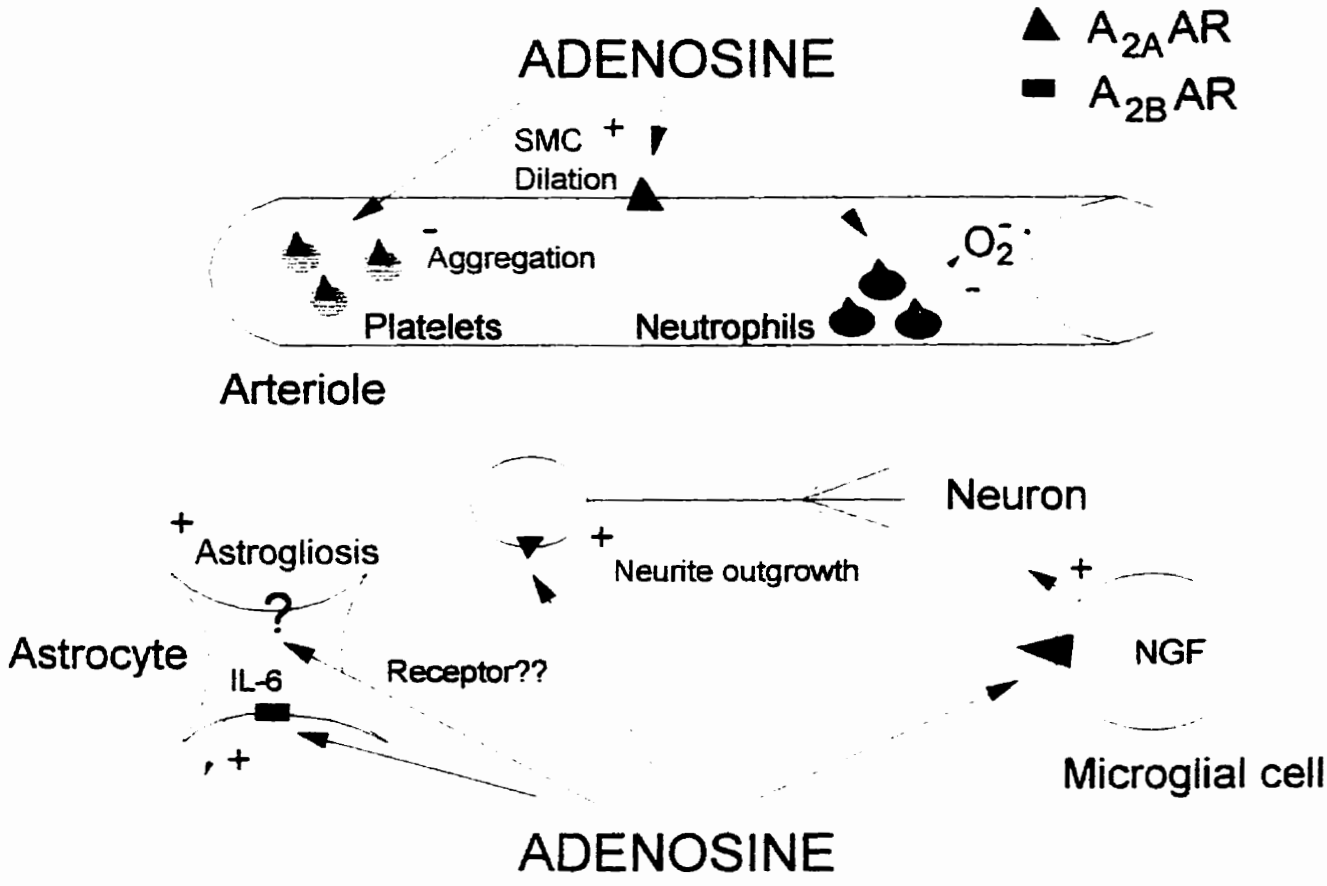

A_{2A}ARs improve blood flow by causing vasodilation and by inhibiting platelet activity and neutrophil adhesion to endothelial cells. Inhibition of neutrophil activity also reduces production of radical species. The A_{2A} receptor also stimulates NGF release from microglia and causes neurite outgrowth while A_{2B}ARs enhance IL-6 release from astrocytes. Reactive astrogliosis is caused by A_2ARs although it is not known which subtype is responsible.

for observations of astrocytic proliferation caused by stimulation of A_2ARs. A_2ARs also enhance the release of neuroprotective substances from astrocytes. In a recent study it was shown that adenosine can increase secretion of IL-6 from astrocytes 4- to 10-fold through A_{2B}ARs (Schwaninger *et al.*, 1997). IL-6 can protect neurons from glutamate toxicity and stimulate neuronal differentiation, and this may be yet another neuroprotective effect of A_2AR stimulation. While A_2ARs have not specifically been implicated, some data suggest that adenosine induces astrocytic release of other compounds such as NGF, neurotrophin-3 and pleiotrophins like bFGF (Neary *et al.*, 1996).

Besides having beneficial effects, adenosine, through stimulation of A_{2A}ARs, is an excitatory neuromodulator in some discrete neuronal pathways (Ongini *et al.*, 1997; Sebastião and Ribeiro, 1996). For example in rat cortex, CGS 21680 enhanced ischemia-evoked glutamate and aspartate release (O'Regan *et al.*, 1992). These data conflict with those previously described which suggest a protective role for A_2ARs and make prediction of *in vivo* function of A_2ARs in stroke models difficult.

Treatment of gerbils with the A_{2A}AR agonist APEC improved cerebral blood flow but did not affect neuronal survival (Jacobson *et al.*, 1996), suggesting that beneficial effects of A_{2A}AR stimulation on blood flow may not be able to overcome A_{2A}AR-induced stimulation of excitatory amino acid release. Acute A_{2A}AR antagonist (CSC) administration significantly protected hippocampal neurons (Jacobson *et al.*, 1996) supporting these results. Based on this study, one may hypothesize that a blood-borne A_{2A}AR agonist that does not cross the blood-brain barrier may be neuroprotective.

3.2.3 A_3ARs and Neuroprotection

The role of A_3ARs in cerebral ischemia is poorly understood. It is known that A_3ARs have a low affinity for adenosine and are likely activated only when adenosine levels rise many times above basal levels as in ischemia. One might hypothesize that A_3ARs have a similar function to A_1ARs in ischemia since they both inhibit cAMP synthesis when stimulated. In fact, this does not appear to be the case. In contrast to A_1AR agonists, acute treatment of gerbils with the A_3AR agonist IB-MECA resulted in a significant increase in morphological damage and enhancement of post-ischemic mortality (Jacobson *et al.*, 1996). It may be the ability of A_3ARs to constrict arterioles and limit blood flow, or alternatively, the ability of A_3AR activation to desensitize inhibitory responses to A_1ARs (Dunwiddie *et al.*, 1997) that account, in part, for enhanced damage caused by IB-MECA.

A_3ARs have been implicated in apoptosis in astrocytes. High concentrations of A_3AR agonist caused astrocytic apoptosis while lower concentrations and shorter exposure times caused reactive astrogliosis (Abbracchio *et al.*, 1997). As mentioned earlier, it is unclear whether apoptosis in select neurons, which likely occurs with pathophysiological concentrations of adenosine, protects other neurons. Large numbers of activated microglia are present following transient brain ischemia. Proliferating microglial cells acquire a number of cytotoxic properties, one of which is the ability to release TNFα (Schubert *et al.*, 1997). Stimulation of A_3ARs suppressed TNFα release from human macrophages (U937) (Sajjadi *et al.*, 1996) and cultured rat microglia (Schubert *et al.*, 1997), suggesting a possible protective role for A_3ARs. Much work

remains to bring our knowledge of the CNS functions of A_3ARs to a point where we can clearly explain the *in vivo* actions of A_3AR ligands.

3.3 Adenosine Receptor Therapeutics: Strategies and Limitations

The development of adenosinergic drug treatments has been slow. To date, the only adenosine-based therapies used clinically are adenosine itself (Adenocard™), which is useful for acute treatment of paroxysmal supraventricular tachycardia, and dipyridamole (Persantine™), a potentiator of endogenous adenosine, which is used as an anti-thrombotic agent. Neither treatment is for use in the CNS yet many possible applications have been described (see section 3.1).

Many investigations have applied A_1AR therapeutics to small animal models of cerebral ischemia. Direct A_1AR activation by non-metabolizable adenosine analogs is the most obvious strategy. Administered pre- or post-ischemia, in both focal and global ischemic models, A_1AR agonists can decrease mortality, reduce neuronal loss in selectively vulnerable regions and ameliorate behavioural neurological dysfunction in rats gerbils, mice and pigs (Bischofberger *et al.*, 1997). Progress in the clinical development of these compounds has been retarded by a number of limitations discussed below.

Efficacy of peripherally administered A_1AR agonists has been questioned because of an apparent limited ability to cross the blood-brain barrier (Brodie *et al.*, 1987). In addition, A_1AR agonist administration is associated with mild hypothermia which is neuroprotective (Miller and Hsu, 1992); it is a debatable issue whether A_1AR-induced neuroprotection is achieved through inhibition of neuronal activity (see section 3.2.1) or

indirectly through hypothermia. Some groups found that maintaining normothermia eliminated protection afforded by A_1AR agonists (Miller and Hsu, 1992) while others contend that when body and brain temperatures are controlled, hypothermia is not the principal mechanism of A_1AR-mediated neuroprotection (Bischofberger *et al.*, 1997). A third uncertainty is the discrepancy reported between neurological outcomes for acute and chronic dosing regimens for A_1AR agonists. As discussed previously, acutely administered A_1AR agonists are protective whereas chronic administration enhances neuronal damage (Jacobson *et al.* 1996). The fourth and likely most prohibitive problem with A_1AR agonists is that they cause bradycardia and hypotension, effects often undesirable in stroke patients. These difficulties must be circumvented before A_1AR agonists can be used safely and effectively in humans.

Recently, one A_1AR agonist, called ADAC, was shown to reduce mortality and protect neurons at a lower dose (75-100 μg/kg) than other A_1AR agonists without causing the usual cardiovascular side effects (von Lubitz *et al.*, 1996). Furthermore, in contrast to CHA, ADAC is not associated with "regimen-dependent effect reversal" (Bischofberger *et al.*, 1997). Since these effects and the effectiveness of ADAC up to 12 h post-ischemia conflict with previous observations of A_1AR agonist actions, it is possible that another mechanism is involved. However, ADAC and other structurally similar A_1AR agonists currently represent the most encouraging avenue of clinical development of neuroprotective agents acting at A_1ARs.

An alternative adenosinergic therapeutic strategy in ischemia involves using compounds to inhibit metabolism or cellular uptake of excess adenosine released during energy failure. This enhances adenosine receptor activation in areas of elevated

endogenous adenosine, producing neuroprotective effects. Additional discussion of potentiators of endogenous adenosine will be provided in subsequent sections.

4. Regulation of Adenosine and Adenine Nucleotide Levels in Brain

Because of the wide distribution of receptors for adenosine and nucleotides in brain, it is important to consider how extracellular adenosine and adenine nucleotide levels are regulated. Points of regulation include formation, storage, catabolism, release, extracellular metabolism and uptake into cells. It may be possible to manipulate receptor occupancy using compounds that alter these pathways.

4.1 Sources and Metabolism of Adenine Compounds

Extracellular levels of endogenous adenosine have been measured using many techniques. Methods that minimize degradation of ATP after death or trauma are considered to give the most reliable results. The cortical cup technique indicated adenosine levels of 15-50 nM (Phillis *et al.*, 1988), microdialysis has suggested levels of 70 nM in striatum (Pazzagli *et al.*, 1995) and 200 nM in hippocampus (Headrick *et al.*, 1994), and CSF sampling yielded a level around 35 nM (Walter *et al.*, 1988). Focused microwave irradiation may be the best method for sacrificing animals when adenosine levels need to be measured accurately as energy charge is maintained at 0.8 (Delaney and Geiger, 1996), indicating more healthy tissues containing high levels of ATP versus adenosine. This need for rapid fixation (denaturation) of the metabolic enzymes of cells shows the extent and speed of adenosine accumulation with a change in metabolic activity.

4.1.1 Intracellular Fates of ATP and Adenosine

Several intracellular pathways contribute to the fates of ATP and adenosine (fig. 3). ATP is synthesized in mitochondria and can be stored in vesicles in nerves or used as an energy currency. Specific vesicular ATP transporters have been identified (Gualix *et al.*, 1996) and vesicular release of ATP occurs in central and peripheral nerves, leading to stimulation of P_2 receptors (Harden *et al.*, 1995). Release of nucleotides from cells can occur by processes other than exocytosis as well. For example, hemodynamic shear stress (Hasséssian *et al.*, 1993), mechanical stimulation (Lazarowski *et al.*, 1995), and metabotropic receptor activation (Katsuragi *et al.*, 1996) have been shown to cause cellular release of ATP. Intracellular ATP can also be broken down to adenosine. The rate-limiting step in this process is catabolized by soluble 5'-nucleotidase, which cleaves the phosphate from AMP to form adenosine. This represents the major pathway of adenosine formation in cells. Therefore, ATP and adenosine levels are closely linked, explaining why adenosine levels increase substantially when ATP is used at a high rate, such as in seizure, or when ATP cannot be synthesized, such as during glucose and/or oxygen deprivation. Minor pathways of adenosine formation in brain include catabolism of *S*-adenosylhomocysteine by SAH hydrolase (Geiger *et al.*, 1997), as well as cAMP breakdown and *de novo* purine synthesis *via* 5'-IMP. Adenosine release from nerves has been reported in response to electrical stimulation (Hoen and White, 1990), increased glutamate levels (Rudolphi *et al.*, 1992) and the presence of NO donors (Fallahi *et al.*, 1996). Both Ca^{2+}-dependent and Ca^{2+}-independent adenosine release have been documented but vesicular release has not been demonstrated (Geiger *et al.*, 1997). It appears that adenosine release from cells is at least partially mediated by bidirectional

membrane protein transporters (equilibrative transporters) that allow adenosine efflux when intracellular levels exceed extracellular levels. Efflux through concentrative, energy-dependent nucleoside transporters may be induced by perturbation of the cellular energy state (Borgland and Parkinson, 1997).

Adenosine levels are tightly controlled under basal conditions. Once formed or taken up into cells intracellular adenosine is quickly catabolized by one of two enzymes. Adenosine kinase (AK) can phosphorylate adenosine to AMP to salvage nucleotides. AK is thought to be subject to substrate inhibition and this may hinder adenosine clearance when adenosine levels are high (Fisher and Newsholme, 1984). Adenosine deaminase (ADA) can deaminate adenosine to form inosine and is not subject to substrate inhibition. Inhibitors of both AK and ADA have been pursued as therapeutic targets in ischemia, seizure and pain.

4.1.2 Extracellular Fates of ATP and Adenosine

The receptor-mediated effects of ATP and adenosine are influenced by the hydrolytic activity of ecto-nucleotidases, widely distributed plasma membrane-bound enzymes with active sites oriented to the extracellular medium (fig. 4). In addition, ATP is a substrate for ecto-protein kinases (Seifert and Schultz, 1989) and adenosine can be catabolized by ecto-adenosine deaminase to form extracellular inosine (Ciruela *et al.*, 1996). Four enzymatic reactions are collectively termed nucleotidase and include ATP $\rightarrow$ ADP, ADP $\rightarrow$ AMP, AMP $\rightarrow$ adenosine and ATP $\rightarrow$ AMP. A number of enzymes have been described to account for these reactions.

Ecto-ATPase, or E-type ATPase catabolizes ATP and is unique from intracellular ion-motive or mitochondrial ATPases in that it has broad nucleotide selectivity and is not inhibited by vanadate, ouabain or oligomycin, inhibitors of the classical ATPases. Ecto-ATPase activity has a ubiquitous distribution (Plesner, 1995) and enzymes associated with this activity have been isolated from several tissues and species. Ecto-ATPase activity may be carried out by an ecto-ATPase, which hydrolyzes ATP to ADP, or by an ecto-ATP diphosphohydrolase (ecto-ATPDase or ecto-apyrase) which hydrolyzes ATP to AMP. ATPase activity not associated with ATPDase was evident in preparations including striatal cholinergic synapses (James and Richardson, 1993). In contrast, ATP hydrolysis by ATPDase was detected in rat cortical synaptosomes (Battastini *et al.*, 1991). Activity of ADPase, an enzyme that hydrolyzes ADP to AMP but does not hydrolyze ATP or AMP, was identified in rat erythrocytes (Lüthje *et al.*, 1988) and lung (Dawson *et al.*, 1986). In contrast, ATPDase appeared responsible for hydrolysis of ADP in rat cortical synaptosomes (Müller *et al.*, 1993). Ultimately, cloning of the enzymes responsible for hydrolysis of ATP and ADP, as has recently been accomplished for the CD39/ecto-ATPDase (Wang and Guidotti, 1996), and subsequent cellular localization is necessary to resolve which combinations of enzymes are responsible for hydrolysis of nucleotides in different tissues and cell types.

The extracellular enzyme responsible for the formation of nucleosides is ecto-5'-nucleotidase, an enzyme with broad substrate selectivity (James and Richardson, 1993; Zimmermann, 1992). Ecto-5'-nucleotidase is ubiquitous with respect to tissue distribution but apparently not with respect to cellular distribution. For example, it is rarely found on neurons but it is located on astrocytes and oligodendrocytes

Figure 3: Intracellular Fates of ATP and Adenosine

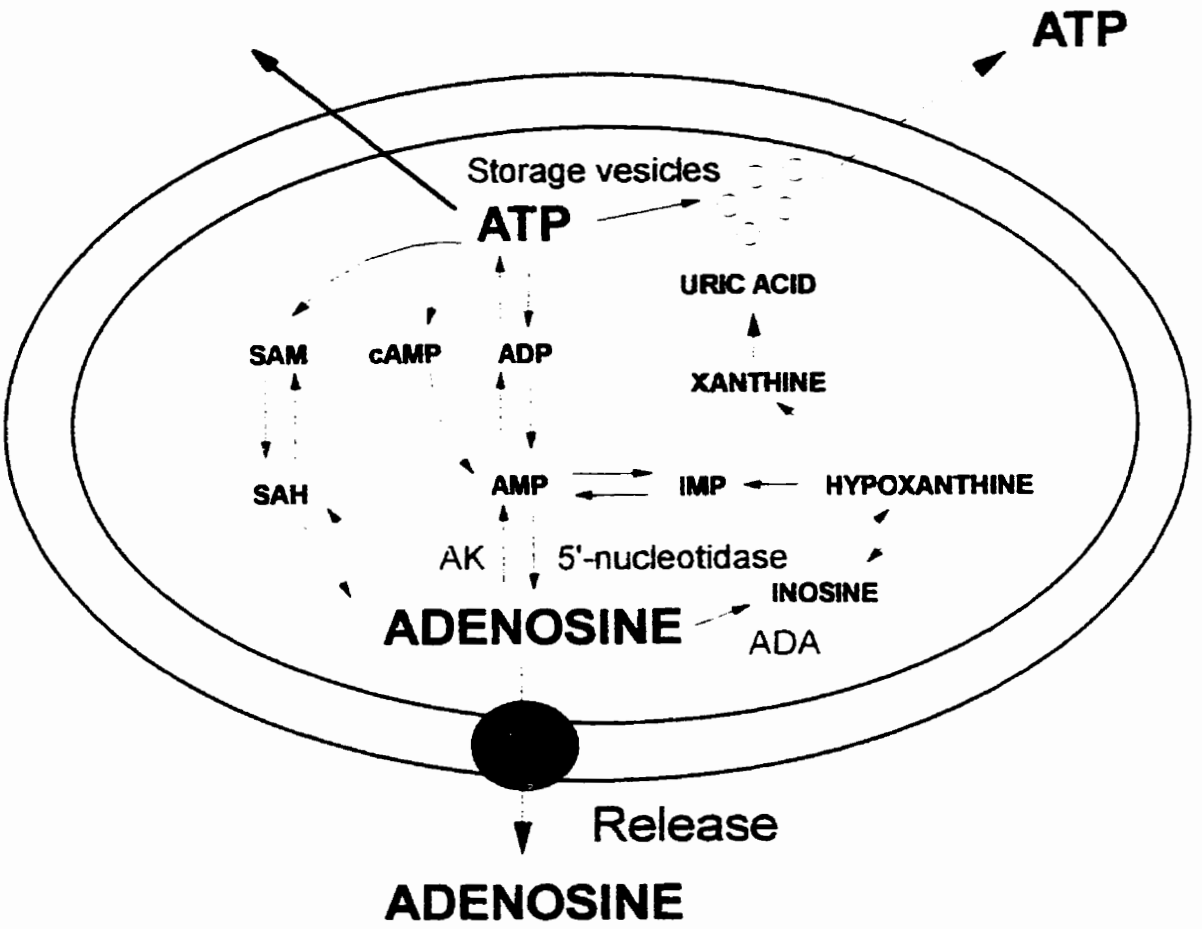

ATP is synthesized mainly in mitochondria, then is stored, released or catabolized to adenosine. Adenosine can be formed intracellularly by the breakdown of ATP by ATPases and 5'-nucleotidase or to a lesser extent, by the action of S-adenosylhomocysteine hydrolase. Intracellular adenosine can be released or metabolized to inosine or AMP by adenosine deaminase or adenosine kinase, respectively.

(Zimmermann, 1992). Ecto-5'-nucleotidase is important when considering ATP breakdown and adenosine formation because of the role of adenosine as a signaling molecule via cell surface receptors.

Extracellular catabolism of ATP and formation of adenosine is achieved by combinations of ecto-nucleotidase enzymes that work in concert with one another to produce cell-specific extracellular half-lives for ATP and adenosine. Studies in striatal cholinergic synaptosomes (James and Richardson, 1993) show a delayed production of adenosine following ATP breakdown. This may be due to feedforward inhibition of ecto-5'-nucleotidase by ADP that accumulates because of a decreased capacity of ADPase relative to ATPase. In contrast, ATP and ADP hydrolysis proceed with similar K_M and V_{max} values in smooth muscle cells and no delay in adenosine production was seen (Pearson, 1980). This picture is complicated further by the discovery that soluble nucleotidases can be released with ATP from sympathetic nerves (Todorov *et al.*, 1997). Thus, extracellular ATP and adenosine levels may be partially regulated by nucleotidases released from cells. Clearly, these types of tissue-specific differences in ecto-nucleotidase activities may affect ATP and adenosine signaling such that delays in degradation of ATP could enhance stimulation of P_2 receptors while rapid metabolism could result in quick cessation of such signaling and enhanced signaling at adenosine receptors.

4.2 Inhibitors of Adenosine Metabolism as Therapeutic Agents

Intracellular metabolism is a key point of regulation of endogenous adenosine levels. Inhibitors of ADA and AK can increase endogenous adenosine levels in certain

conditions leading to enhanced stimulation of all adenosine receptors. This may or may not be of more benefit than A_1AR agonists since the roles of A_{2B}, A_3, and even A_{2A} adenosine receptors in neuroprotection are unclear. Using ADA and AK inhibitors may be a viable therapeutic strategy as some are beneficial in ischemia, seizure and pain models.

4.2.1 Adenosine Deaminase Inhibitors

The two most widely used inhibitors of ADA are EHNA (nM activity) and DCF (pM activity) (Geiger *et al.*, 1997). Under normal metabolic conditions EHNA had no effect on adenosine levels or hippocampal neuronal activity (Pak *et al.*, 1994). However, in rat brain global ischemia, DCF enhanced adenosine release and nucleotide recovery (Phillis and O'Regan, 1996). As well, DCF given pre-ischemia reduced CA1 neuronal damage in gerbils (Phillis and O'Regan, 1989) and given post-ischemia caused a reduction in cerebral ischemic injury in newborn rats (Gidday *et al.*, 1995). This finding indicates that ADA may be more active during conditions of elevated adenosine production and inhibitors of ADA may be more effective enhancers of endogenous adenosine under these conditions.

Much work remains to make a case for the therapeutic utility of ADA inhibitors. There are examples in both rat (Delaney *et al.*, 1993) and gerbil (Phillis and Clough-Helfman, 1990) models of cerebral ischemia where DCF was not neuroprotective. Furthermore, there is a curious lack of effect of ADA inhibitors in seizure (Zhang *et al.*, 1993) and pain models (Geiger *et al.*, 1997).

4.2.2 Adenosine Kinase Inhibitors

The most commonly used AK inhibitors are ITU, d-ITU and 5'-NH_2dAdo, each active at nM levels (Geiger *et al.*, 1997). ITU was an effective enhancer of endogenous adenosine levels in brain under basal conditions whereas EHNA was not (Pak *et al.*, 1994). As mentioned earlier, AK may experience substrate inhibition or non-competitive inhibition during energy depletion (Decking *et al.*, 1997). This may account for observations that AK inhibition was not effective in some disease models with pathophysiological levels of endogenous adenosine. For example, systemic ITU failed to protect CA1 neurons against global ischemia in gerbils (Phillis and Smith-Barbour, 1993). Alternatively, this could be due to the limited ability of ITU to cross the blood-brain barrier compared to d-ITU (Geiger *et al.*, 1997) since d-ITU protected rats against transient focal ischemia (Jiang *et al.*, 1997). ITU injected into the rat prepiriform cortex protected from bicuculline methiodide-induced seizures, in contrast to the effects of DCF (Zhang *et al.*, 1993). Systemic d-ITU protected against pentylenetetrazol-induced seizures. These data suggest that AK inhibitors may be more useful than ADA inhibitors in the treatment of seizures.

AK inhibitors may also be more effective than ADA inhibitors as antinociceptive agents. Intrathecal 5'-NH_2dAdo, but not DCF or EHNA, enhanced opioid-induced antinociception in mice (Keil II and DeLander, 1994). DCF did enhance antinociception produced by exogenous adenosine, again supporting the idea that ADA inhibitors are more effective at elevated adenosine levels, whereas AK inhibitors are more effective at basal adenosine levels.

Figure 4: Extracellular Fates of ATP and Adenosine

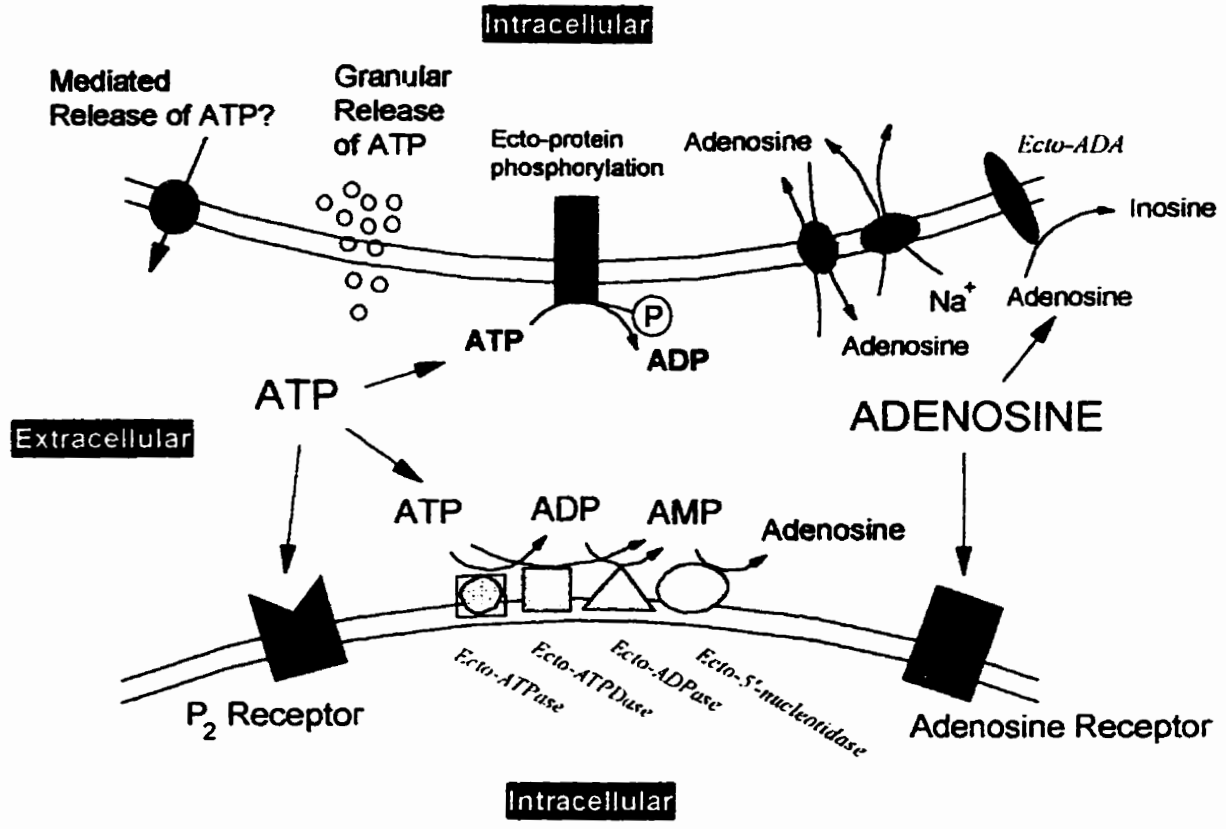

Both ATP and adenosine can be released from cells. Adenosine can act at cell surface receptors, be taken up into cells or broken down to inosine by ecto-adenosine deaminase. ATP can activate P_2 receptors, act as a substrate for ecto-protein phosphorylation or be catabolized by the ecto-enzymes ecto-ATPase, ecto-ADPase, ecto-apyrase and ecto-5'-nucleotidase to form adenosine.

4.3 Nucleoside/Adenosine Transporters

Nucleoside transporters (NTs) are integral membrane proteins that mediate the flux of nucleosides from one side of a membrane to the other. The major role of NTs is to satisfy cellular metabolic demands for nucleosides. Cells such as erythrocytes that do not have the ability to synthesize nucleosides *de novo* rely on uptake and salvage of nucleosides and nucleotides. Other cells utilize both pathways to varying degrees (Jones, 1980) and require mechanisms for nucleoside uptake. Another important role for NTs is to allow the cellular uptake of nucleoside analogs used as part of anti-cancer or anti-viral chemotherapy. For example, DCF, used for lymphoma and leukemia, acyclovir, used for Herpes virus, and AZT, used for HIV, all enter cells *via* NTs. There is evidence that the activity of NTs is an important determinant of cytotoxic activity of these drugs (Cass, 1995). Finally, NTs are important in adenosine pharmacology. The actions of adenosine at its receptors are dependent on the concentration of interstitial adenosine. As well as factors such as release and metabolism of ATP and adenosine, extracellular adenosine levels also depend heavily on its uptake and release through NT proteins.

The first NTs were identified on human erythrocytes in the early 1970s (Cass and Paterson, 1972; 1973). In the 1980s, with better methods of studying initial transport rates, other subtypes were discovered (Cass, 1995) and currently 8 subtypes have been identified and divided into 2 broad families, equilibrative and concentrative (table 5).

Equilibrative transport is driven by the transmembrane nucleoside concentration gradient and such transporters are responsible for both uptake and release of nucleosides. They have been further divided into 2 subtypes based on inhibitor sensitivities, both of

which have been cloned and functionally identified in brain. Equilibrative transporters are widely distributed and may be ubiquitous (Cass, 1995).

Under normal cellular energy conditions concentrative transporters mediate the inward flux of nucleosides coupled with Na^+ ions; they may be termed active Na^+/nucleoside symporters. They have a more limited distribution than equilibrative transporters, for the most part being confined to specialized tissues such as kidney, intestine and choroid plexus (Cass, 1995). Thus far, 6 subtypes have been identified based on different permeant selectivities and 2 of these have been cloned. The distribution of concentrative transporters in brain is poorly understood as only a few reports have documented Na^+-dependent nucleoside transport in the CNS.

4.3.1 Equilibrative Nucleoside Transporters

The first NT identified from human erythrocytes was found to be an equilibrative transporter (Cass and Paterson, 1972), or a facilitated diffusion NT. The NT activity of this protein was later found to be sensitive to inhibition by a nucleoside analog called nitrobenzylthioinosine (NBMPR) (Cass and Paterson, 1974). In the 1980s an equilibrative NT system insensitive to inhibition by NBMPR was identified, first in neoplastic cells (Belt, 1983). These two equilibrative NTs are now termed *es* for equilibrative and NBMPR-sensitive and *ei* for equilibrative and NBMPR-insensitive (Vijayalakshmi and Belt, 1988). They have very similar substrate selectivities and kinetics, and are present together on a number of cell types (Cass, 1995).

4.3.1.1 es Nucleoside Transport

The *es* transporter from human erythrocytes was purified (Kwong *et al.*, 1988) and recently cloned from human placenta (Griffiths *et al.*, 1997) and rat jejunum (Yao *et al.*, 1997). The rat cDNA (rENT1) predicts a protein of 457 amino acid residues and molecular weight 49,984 Da while the human cDNA (hENT1) predicts a 456 amino acid, 50,249 Da protein; the two amino acid sequences are 78% similar. Both species homologs predict 11 transmembrane (TM) domains, each connected by short hydrophilic segments. Exceptions in both human and rat are between TM 1 and 2 and TM 6 and 7 which are separated by extracellular loops of 41 amino acids and intracellular loops of 66 amino acids, respectively. rENT1 contains 2 additional putative glycosylation sites in the large extracellular loop compared with hENT1 suggesting that interspecies differences in glycosylation could explain why photoaffinity labeling experiments showed differences between the molecular weights of human (55,000 Da) and rat (62,000 Da) *es* transporters. There is some evidence that multiple isoforms of *es* exist, at least in human, based on the reactivity of an *es* polyclonal antibody in human placenta (Barros *et al.*, 1995).

Cloned ENT1 from both human and rat exhibit broad permeant selectivity. The endogenous nucleosides adenosine, uridine, cytidine, guanosine, inosine and thymidine, as well as some cytotoxic nucleoside analogs inhibited uridine influx through hENT1 (Boumah *et al.*, 1994; Griffiths *et al.*, 1997a) and rENT1 (Yao *et al.*, 1997) expressed in *Xenopus* oocytes. The K_M for uridine influx was 0.24 mM for hENT1 (Griffiths *et al.*, 1997a), and 0.15 mM for rENT1 (table 6) (Yao *et al.*, 1997).

The *es* transporter exhibits some selectivity for adenosine relative to other endogenous nucleosides in CNS tissues (Geiger and Fyda, 1991). The cloned hENT1

gave a mediated flux of adenosine 3-4 times that for uridine (Griffiths *et al.*, 1997a), consistent with these observations. Identification of transporters selective for adenosine is important when considering the role of specific transporter subtypes in regulating interstitial adenosine concentrations. Kinetic studies have indicated that *es* transporters in guinea pig cortical synaptosomes had a K_M for influx of 17 μM for adenosine. For rat erythrocytes the K_M was estimated at 12 μM (Griffith and Jarvis, 1996). In studies that controlled for metabolism of adenosine or used the metabolically stable enantiomer L-adenosine, the K_M for adenosine in rat cortical synaptosomes was about 40 μM (Gu *et al.*, 1992) while in human synaptosomes it was 89 μM (Gu *et al.*, 1993), double the value for rat.

Both rENT1 and hENT1 were sensitive to low nM concentrations of NBMPR with a K_i previously estimated at 0.1-1 nM (Thorn and Jarvis, 1996). However, ENT1 displayed species differences in sensitivity to the inhibitors dipyridamole (DPR) and dilazep (DZP). hENT1 was sensitive to DPR and DZP inhibition in cRNA-injected *Xenopus* oocytes with IC_{50} values of 140 nM and 60 nM, respectively, while rENT1 was insensitive at concentrations up to 1 μM (Yao *et al.*, 1997). This must be taken into consideration when using rat models to evaluate DPR and DZP for therapeutic use in humans. On the other hand, these data validate the use of NBMPR in rat models.

Table 6: Kinetics of Uridine Uptake Through Equilibrative Transporters Expressed in *Xenopus* Oocytes

	K_M (mM)	V_{max} (pmol/min per oocyte)
rENT1	0.15	18
hENT1	0.24	18
rENT2	0.30	14
hENT2	0.20	6.4

Data taken from Griffiths *et al.* (1997a,b) and Yao *et al.* (1997).

The *es* transporter appears to be metabolically regulated. A number of reports have shown that PKC and perhaps PKA can alter nucleoside uptake, release, and [^{3}H]NBMPR binding sites in different systems. Phorbol esters decreased NBMPR-sensitive adenosine transport and [^{3}H]NBMPR binding in T84 intestinal epithelial cells (Mun *et al.*, 1998). In chromaffin cells, adenosine transport, measured by flow cytometry, was inhibited by close to 50% in response to phorbol esters and forskolin-stimulated PKA activity (Sen *et al.*, 1998); a decrease in [^{3}H]NBMPR binding sites was also noted (Delicado *et al.*, 1991). Similarly, in HL-60 leukemia cells, 6 hour phorbol ester treatment caused a 30% decrease in [^{3}H]NBMPR binding sites and a 20-fold decrease in uridine uptake (Lee, 1994). Adenosine release may also be affected by PKC activation. In DDT$_1$ MF-2 cells, A_1AR activation increased nucleoside release by a PKC-dependent mechanism (Sinclair and Parkinson, submitted). Several compounds in

addition to DPR, DZP and NBMPR have been reported to inhibit *es* transporters. Since ethanol has been shown to inhibit *es*, endogenous adenosine may mediate some of its depressant effects (Nagy *et al.*, 1990). In addition, tamoxifen, an estrogen receptor antagonist used in the adjunctive treatment of breast cancer, inhibited *es* NTs in MCF-7 breast cancer cells raising the possibility that part of its anti-proliferative effects may be due to inhibition of DNA synthesis from lack of nucleoside salvage (Cai and Lee, 1996).

Functionally, *es* NTs have been detected in many regions throughout brains of different species. Various CNS cell types including neurons (Sweeney, 1996) and astrocytes (Gu *et al.*, 1996) have *es* activity. Characterization of *es* NT distribution in the CNS has been made possible by radiolabeled ligands such as [^{3}H]NBMPR and [^{3}H]DPR. [^{3}H]NBMPR was considered the best available marker for *es* systems prior to the cloning of ENT1 from rat and human and the development of antibodies (Geiger and Fyda, 1991). In the report of Bisserbe *et al.* (1985), high levels of [^{3}H]NBMPR binding in rat brain were seen in striatum, pyriform cortex, thalamus, superior colliculus, substantia nigra, nucleus of the solitary tract and substantia gelatinosa of the dorsal spinal cord. Moderate to low levels were seen in amygdala and certain nuclei of the thalamus and low levels were seen in cerebellum and hippocampus. Results were similar in guinea pig and further indicated high [^{3}H]NBMPR binding in area postrema, parietal cortex and hypothalamus (Deckert *et al.*, 1988). A_1AR receptor distribution correlated well in most cases with [^{3}H]NBMPR binding suggesting *es* transporters are important in regulating A_1AR stimulation (Deckert *et al.*, 1988). Notable exceptions were hippocampus and cerebellum, where A_1ARs are reportedly abundant (Olah and Stiles, 1995) yet [^{3}H]NBMPR binding was low.

Table 5: Nucleoside Transporter Subtypes

	Equilibrative		Concentrative					
	es	*ei*	N1	N2	N3	N4	N5	N6
Cloned	rENT1 hENT1	rENT2 hENT2	rCNT2 hCNT2	rCNT1 hCNT1	SNST1	-	-	-
Selectivity	Broad	Broad	Purines Uridine	Pyrimidines	Broad	Pyrimidines Guanosine	Formycin B	Guanosine
NBMPR Sensitivity	+	-	-	-	-	-	+	+
Na^+:nucleoside Stoichiometry	N.A.	N.A.	1:1	1:1	2:1	1:1	N.D.	N.D.
Distribution	Nearly ubiquitous	Nearly Ubiquitous	Kidney Intestine Spleen Liver Macrophage Monocytes Leukemia L1210 cells	Kidney Intestine	Choroid plexus Intestine	Human kidney	Human leukemia cells	Human leukemia cells

4.3.1.2 ei Nucleoside Transport

In contrast to *es* NTs, little was known about the structure and tissue distribution of *ei* prior to its cloning. Recently, cDNAs encoding the *ei* NT were isolated from human (hENT2) placenta (Griffiths *et al.*, 1997b) and leukemia cells (Crawford *et al.*, 1998), and rat jejunum (Yao *et al.*, 1997). The putative structure of ENT2 is very similar to ENT1. Both the rat and human homologs encode 456 amino acid peptides of 50,232 Da and 50,173 Da, respectively, and are about 50% identical to hENT1/rENT1. Like ENT1, ENT2 cDNAs predict 11 TM domains with shorter hydrophilic loops connecting TM 1 and 2 (28 residues for hENT2 and 27 for rENT2 *vs.* 41 for rENT1/hENT1) and longer loops connecting TM 6 and 7 (80 residues for rENT2/hENT2 *vs.* 66 for rENT1/hENT1). Both rENT2 and hENT2 have two putative glycosylation sites in the loop connecting TM 1 and 2, one of which is conserved in hENT1 (Griffiths *et al.*, 1997b).

Like ENT1, ENT2 can transport a broad range of nucleoside permeants. All endogenous nucleosides were able to inhibit [^{3}H]uridine influx through rENT2, however cytidine was less effective than in experiments with rENT1 (Yao *et al.*, 1997). The K_M for uridine influx through rENT2 was 0.30 mM (table 6) (Yao *et al.*, 1997). This affinity for uridine is in close agreement to results with hENT2, which yielded a K_M for influx of 0.20 mM (Griffiths *et al.*, 1997b). While NBMPR (1 μM) abolished all uridine influx through rENT1, 86% of activity remained in rENT2 expressing oocytes (Griffiths *et al.* 1997b). DPR and DZP were also effective inhibitors hENT1, while they were relatively ineffective as inhibitors of hENT2 (Griffiths *et al.*, 1997b) and rENT2 (Yao *et al.*, 1997) at 1 μM. Recall that this intraspecies difference in susceptibility to DPR and DZP is

smaller in rat because of the surprising lack of effect of nanomolar concentrations of these inhibitors on rENT1.

The *ei* NT subtype has been identified functionally in CNS preparations from a number of species including rabbit (Jones and Hammond, 1996), rat (Lee and Jarvis, 1988a) and guinea pig (Lee and Jarvis, 1988b) cortical synaptosomes, and human fetal astrocytes (Gu *et al.*, 1996). Species differences in CNS proportions of *es* to *ei* have been documented. In rabbit synaptosomes, 65% of equilibrative uridine influx was through an *es* system while in guinea pig and rat synaptosomes, most uridine influx through equilibrative NTs was *via* the *ei* subtype (Jones and Hammond, 1995). Further species differences in relative substrate affinities between *es* and *ei* may exist in CNS tissues. In guinea pig synaptosomes, the affinity of uridine for *es* was 2.5-fold greater than for *ei* (Griffith and Jarvis, 1996) while in rabbit synaptosomes, the affinity of uridine for *ei* was 3-fold greater than for *es* (Jones and Hammond, 1995). There is some discrepancy in the data for rat. The affinity of uridine for *es* was only slightly greater than for *ei* in rat synaptosomes (Lee and Jarvis, 1988a) but in cloned transporters, uridine exhibited 2-fold greater affinity for rENT1 (*es*) over rENT2 (*ei*). Interestingly, uridine had a higher affinity for the cloned hENT2 than for hENT1. Care must be taken in extending interpretation of results among species because of differences in both relative levels and substrate affinities of *es* and *ei* in the CNS of different species.

In the mid 1980s it was proposed that [^{3}H]DPR may be a good ligand for labeling *ei* NTs in guinea pig and human but not rat. [^{3}H]DPR has 2-5-fold more binding sites in guinea pig brain than does [^{3}H]NBMPR (Griffith and Jarvis, 1996) and 35% more binding sites in human parietal cortex (Deckert *et al.*, 1994). In guinea pig, [^{3}H]DPR

binding was inhibited by 10% in cerebellar purkinje cells and by more than 65% in anterior hypothalamus, nucleus tractus solitarius, area postrema and arteries (Deckert *et al.*, 1987) by 500 nM NBMPR. This finding suggested that the remaining bound [^{3}H]DPR marked *ei* NTs. Overall, only 40% of [^{3}H]DPR binding was susceptible to inhibition by NBMPR in guinea pig brain. These results must be viewed with caution however because (i) [^{3}H]DPR has higher non-specific binding than does [^{3}H]NBMPR; (ii) the hydrophobic nature of [^{3}H]DPR may allow it to bind intracellular sites whereas [^{3}H]NBMPR is thought to bind to the extracellular surface of cell membranes only; and (iii) [^{3}H]DPR may bind other proteins such as glucose transporters. It is clear that the nature of the additional [^{3}H]DPR binding sites is poorly understood. In addition, the K_i values for nucleoside inhibition of [^{3}H]DPR binding are not consistent with the potency of DPR inhibition of nucleoside uptake in guinea pig synaptosomes (Griffith and Jarvis, 1996). With cDNA sequence information for rENT2 and hENT2, it is now possible to determine the distribution of mRNA for *ei* NTs in brain.

4.3.2 Concentrative Nucleoside Transporters

In the mid 1980s investigators began to notice that nucleosides including adenosine could be transported in an energy-dependent, nucleoside gradient-independent manner by Na^+-cotransport (Le Hir and Dubach, 1984). Attempts to determine permeant selectivity of such transport systems using nucleosides to inhibit uptake of a radioactive permeant have revealed 6 concentrative, or Na^+-dependent nucleoside transporter subtypes differentiated by permeant selectivity and sensitivity to inhibition by NBMPR (Griffith and Jarvis, 1996) (table 5). N1 NTs are concentrative, NBMPR-insensitive and

prefer purine nucleosides (formycin B); N2 NTs are concentrative, NBMPR-insensitive and prefer pyrimidine nucleosides (thymidine); N3 NTs are concentrative, NBMPR-insensitive and accept a broad range of nucleoside permeants; N4 NTs are similar to N2 but also accept guanosine; N5 NTs are concentrative and sensitive to low nM concentrations of NBMPR; and N6 NTs are concentrative, permeated only by guanosine and sensitive to inhibition by low nM concentrations of NBMPR.

4.3.2.1 N1 Nucleoside Transporters

N1 NTs have been identified functionally in a wide variety of tissues and cells including rat, mouse and hamster macrophages, rabbit and mouse intestine, cultured rat intestinal IEC-6 cells, rat and bovine kidney, rat liver and L1210 mouse leukemia cells (Griffith and Jarvis, 1996). Recently, cDNAs for N1 NTs have been isolated from rat jejunum (rCNT2; Yao *et al.*, 1996) and liver (SPNT; Che *et al.*, 1995). Modeling of the cDNA sequence predicts a 659 amino acid peptide with a molecular weight of 72 kDa. rCNT2 has 14 putative hydrophobic TM domains in contrast to 11 for ENT1 and ENT2. Unique to rCNT2 is an ATP/GTP binding motif and putative PKC and PKA phosphorylation sites, suggesting differential regulation of Na^+-dependent NT subtypes.

rCNT2 is a purine nucleoside selective transporter, however it is also able to transport uridine. When expressed in *Xenopus* oocytes, rCNT2 significantly enhanced adenosine uptake compared to the control; uptake of adenosine proceeded with a K_M of 6 μM and a V_{max} of 0.46 pmol/min per oocyte. The flux ratio of uridine to adenosine was 0.39 indicating adenosine is a preferred permeant (Yao *et al.*, 1996). This finding is of particular interest because of its implications for adenosine pharmacology.

4.3.2.2 N2 Nucleoside Transporters

In contrast to N1 NTs, N2 NTs have a more limited distribution, thus far having been detected only in kidney, intestine (Griffith and Jarvis, 1996) and placenta (Ritzel *et al.*, 1997). cDNAs encoding proteins with N2 NT activity have been isolated from rat jejunum (rCNT1; Huang *et al.*, 1994) and human placenta (hCNT1; Ritzel *et al.*, 1997). rCNT1 is 64% identical to rCNT2 and both transporters are considered members of the same gene family (CNT). The rCNT1 protein contains 648 amino acid residues and has a molecular weight of 71 kDa. Like rCNT2 it has 14 putative TM domains. While rCNT1 lacks PKC and PKA regulatory sites possessed by rCNT2, there are conserved phosphorylation sites in the two proteins and this may indicate co-regulation. The most divergent parts of the respective protein sequences for rCNT1 and rCNT2 are near the C- and N-termini. The functional significance of this finding is unknown.

rCNT1 is selective for pyrimidine nucleosides. Uridine uptake mediated by rCNT1 transiently expressed in COS-1 African green monkey kidney cells proceeded with a K_M of 21 μM and a V_{max} of 11 pmol/s per 10^6 cells; the K_M for thymidine was 12.5 μM (Fang *et al.*, 1996). Guanosine was unable to inhibit uridine uptake but interestingly, adenosine (a purine) was. Uptake of adenosine had a K_M of 15 μM but the V_{max} for adenosine uptake by rCNT1 was very low; though they had similar K_M values, the V_{max}/K_M ratio for adenosine was 0.01 compared to about 0.55 for uridine (Fang *et al.*, 1996).

With receptors for UTP and UDP identified in the CNS, the cellular transport of uridine is an important consideration for regulation of effects mediated by uracil nucleotides (Anderson and Parkinson, 1997). In addition, if adenosine is indeed an

inhibitor of rCNT1, pathophysiological concentrations of adenosine could decrease uridine uptake and salvage, and may affect signaling at P_2 receptors selective for UTP and UDP.

4.3.2.3 Other Concentrative Nucleoside Transporters

N3 nucleoside transport has been functionally identified in rabbit choroid plexus (Wu *et al.*, 1992), rat jejunum (Huang *et al.*, 1993) and Caco-2 cells (Belt *et al.*, 1993). A cDNA with N3-like activity was isolated from rabbit kidney and termed SNST1 (Pajor and Wright, 1992). SNST1 has no significant homology with the CNT gene family but is similar to the Na^+/glucose cotransporter SGLT1. SNST1 cRNA-injected *Xenopus* oocytes displayed only small increases in Na^+-dependent uridine uptake compared to water-injected oocytes (Griffith and Jarvis, 1996) and SNST1 transcripts were found only in heart and kidney, differing from the functional distribution of N3 NTs. This may mean that another uncloned transporter, perhaps a member of the CNT family, is also responsible for N3 activity.

Little is known about the remaining concentrative transporters. N4 activity has been identified only in human kidney (Gutierrez *et al.*, 1992) while the classification of the N5 system is based on preliminary results showing inhibition of Na^+-dependent formycin B uptake by low (<10 nM) concentrations of NBMPR in human leukemia cells (Griffith and Jarvis, 1996). Another concentrative nucleoside transporter sensitive to inhibition by NBMPR and selective for guanosine has recently been identified in human leukemia cells (Flanagan and Meckling-Gill, 1997). Cloning of these subtypes will aid in elucidation of their function and distribution.

4.3.2.4 Concentrative Nucleoside Transport in Brain

Without specific inhibitors of Na^+-dependent nucleoside transporters, there are no compounds suitable for use as markers in tissues. Consequently, tissue and cellular distributions of these transport systems are poorly understood. In rat brain, a component of Na^+-dependent adenosine uptake was seen in dissociated cells (Johnston and Geiger, 1989), cortical synaptosomes (Bender *et al.*, 1980), primary cultures of neurons and astrocytes (Hösli and Hösli, 1988) and dorsal brain stem synaptosomes (Lawrence *et al.*, 1994). In mouse brain, Na^+-dependent adenosine uptake was not observed in dissociated cells (Geiger and Fyda, 1991) but was seen in astrocytes (Bender *et al.*, 1994) and brain slices (Banay-Schwartz *et al.*, 1980). Cloning of rCNT1 and rCNT2 has provided the first molecular probes for Na^+-dependent concentrative nucleoside transporters in brain.

4.4 Adenosine Uptake Inhibitors as Neuroprotective Agents

The use of compounds to inhibit adenosine uptake through nucleoside transporters could be beneficial in cerebral ischemia or seizure. Adenosine transport inhibitors (ATIs) provide a site-specific potentiation of endogenous adenosine levels that have been elevated due to decreased ATP synthesis or increased ATP use, thereby avoiding unwanted A_1AR stimulation in cardiovascular tissues and the associated side effects discussed earlier. In contrast to A_1AR agonists, this strategy allows stimulation of all AR subtypes. It is unknown whether this is of added benefit to A_1AR stimulation only given the uncertain effects of A_2AR stimulation in cerebral ischemia (see section 3.2.2).

Propentofylline (PPF) was shown to be an inhibitor of adenosine influx in cultured rat hippocampal cells (Ohkubo *et al.*, 1991) and of three specific NT subtypes (*es*, *ei*, N1) in cultured cells (Parkinson *et al.*, 1993). It is thought that this property of PPF at least partially accounts for its ability to enhance endogenous adenosine levels (Andiné *et al.*, 1990) and to afford neuroprotection in animal models of stroke (Parkinson *et al.*, 1994). PPF given post-ischemia reduced hippocampal cell death in gerbil global ischemia (Miller and Hsu, 1992), reduced infarct volume in rat focal ischemia (Park and Rudolphi, 1994), decreased neuronal damage in a newborn rat model of ischemia/hypoxia (Gidday *et al.*, 1995), and improved glucose utilization in human stroke patients (Huber *et al.*, 1993). PPF also has other effects. It blocks ARs at high concentrations, inhibits cAMP phosphodiesterase and can enhance nerve growth factor release in brain (Parkinson *et al.*, 1994). Thus it is not clear whether blockade of adenosine transporters is entirely responsible for PPF-induced neuroprotective effects.

In order to validate the use of ATIs as neuroprotective agents, similar *in vivo* data to those described for PPF are required for more potent and selective ATI. NBMPR is one such compound with a sub-nanomolar K_d value for binding at *es* NTs. In mice, NBMPR decreased locomotion and seizures when given peripherally and enhanced antinociception when given intrathecally (Geiger and Fyda, 1991). In cats, NBMPR enhanced the sleep-inducing effects of endogenous adenosine (Porkka-Heiskanen *et al.*, 1997). Site-specific injection of NBMPR in cortex by microdialysis improved post-ischemic hypoperfusion in pig global ischemia (Gidday *et al.*, 1996) but intraperitoneal NBMPR failed to protect in a gerbil forebrain ischemia model (DeLeo *et al.*, 1988). The poor solubility of NBMPR was, however, not addressed in this study. Furthermore,

although NBMPR is lipophilic, its ability to cross the blood-brain barrier has not been reported. Clear data with NBMPR in ischemia models, accounting for blood-brain barrier penetrability and drug solubility, will determine the validity of using blockers of adenosine uptake through equilibrative transporters as a therapeutic strategy.

This chapter serves to provide background relevant to our interests in investigating distributions of nucleoside transport inhibitors in brain, with the overall goal of clarifying specific nucleoside transporter subtype functions based on observed distributions.

Hypotheses

Nitrobenzylthioinosine (NBMPR), an adenosine transport inhibitor with potential neuroprotective effects, crosses the blood-brain barrier in sufficient quantities to inhibit transporters with a K_i of approximately 1-5 nM.

This hypothesis will be tested in Chapter 2 using a radiolabeled tracer technique, as well as direct measurements of NBMPR in cerebrospinal fluid or brain extracts following peripheral injection of NBMPR-phosphate.

Each cloned nucleoside transporter subtypes is present in brain with a unique regional and cellular distribution. Distribution of mRNA for transporters closely resembles protein distribution.

These hypotheses will be tested using various molecular biological techniques probing for both mRNA and protein distributions of four distinct nucleoside transporter subtypes in brain.

[1]Chapter 2

Ability of Nitrobenzylthioinosine to Cross the Blood-Brain Barrier in Rats

Summary

Nucleoside transport inhibitors that cross the blood-brain barrier may be able to potentiate the neuroprotective effects of adenosine. We tested whether nitrobenzylthioinosine (NBMPR) crosses the blood-brain barrier in three types of experiments. First, intravenous injection of [^{3}H]NBMPR and [^{14}C]sucrose was performed. Brain volume of distribution and brain delivery were greater for [^{3}H]NBMPR than for [^{14}C]sucrose. Second, rats were injected intraperitoneally with NBMPR 5'-monophosphate (NBMPR-P), a prodrug form of NBMPR, or vehicle. Perchloric acid extracts of brains from rats treated with NBMPR-P inhibited [^{3}H]NBMPR binding in competition binding assays nearly three-fold more than extracts from brains of vehicle-treated animals. Third, cerebrospinal fluid (CSF) extracted from rats treated with NBMPR-P (10 mg/kg i.p.) contained 24.1 ± 4.4 nM NBMPR while levels were undetectable in CSF from vehicle-treated rats. We conclude that NBMPR may cross the blood-brain barrier in sufficient quantities to inhibit nucleoside transporters.

Introduction

Adenosine is an endogenous neuroprotective agent that stabilizes neuronal membrane potentials and has vasodilatory, anti-platelet and anti-neutrophil activities (Rudolphi *et al.*, 1992). Enhancing extracellular levels of endogenous adenosine by

[1] Anderson CM, Sitar DS, Parkinson FE (1996) Ability of nitrobenzylthioinosine to cross the blood-brain barrier in rats. Neurosci Lett 219:191-194.

inhibiting cellular uptake is a potential therapeutic intervention for conditions, such as stroke or seizure that are characterized by excessive neuronal excitation.

Inhibiting cellular uptake and enhancing endogenous levels of adenosine are thought to account for, or at least contribute to, the neuroprotective effects of the xanthine derivative propentofylline (Parkinson *et al.*, 1994). However, besides being a nucleoside transport inhibitor, propentofylline is also a phosphodiesterase inhibitor and an adenosine receptor antagonist. Investigations using inhibitors with higher selectivity than propentofylline are required to investigate further whether inhibition of nucleoside transport is associated with neuroprotection in experimental models of cerebral ischemia. However, the classical transport inhibitors nitrobenzylthioinosine (NBMPR) and dipyridamole are poorly soluble in aqueous solutions. The potent and water soluble transport inhibitor dilazep is metabolized by endogenous esterases (Geiger and Fyda, 1991) and also inhibits Na^+ and Ca^{2+} channel activity (Hoque *et al.*, 1995). Thus, these compounds are of limited usefulness for characterizing neuroprotective effects of nucleoside transport inhibitors.

In the present study, we tested whether [^{3}H]NBMPR crosses the blood-brain barrier in rats and determined the concentrations of NBMPR achieved in brain samples following intraperitoneal (i.p.) administration of NBMPR 5'-monophosphate (NBMPR-P), a water soluble prodrug form of NBMPR that is rapidly hydrolyzed to NBMPR following parenteral administration (Gati and Paterson, 1997).

Methods, Results and Discussion

In the first set of experiments, male Sprague-Dawley rats (350 g) were anesthetized with sodium pentobarbital (50 mg/kg i.p.). In a 5 sec interval, 260 µl of

phosphate-buffered saline (0.1 M; pH 7.4) containing 10 μCi [^{3}H]NBMPR and 5 μCi [^{14}C]sucrose were injected into the femoral vein. Blood samples (200 μl) were collected from the femoral artery at 0.25, 1, 2, 5, 10, 20 and 30 minutes after injection was completed. Animals were subsequently killed by decapitation; brains were removed, and each cerebral hemisphere was homogenized in NCS tissue solubilizer (9 ml/g) (Amersham). Plasma (0.1 ml) or brain (1.0 ml) samples were combined with 5 ml liquid scintillation cocktail (Beckman) and analyzed for ^{3}H and ^{14}C content. Pharmacokinetic parameters were derived, using the ESTRIP computer program (Brown and Manno, 1978), based on a two-compartment open model where plasma concentration at time t is: $C(t) = Ae^{-k_1 t} + Be^{-k_2 t}$, with A and B representing intercepts with the ordinate axis at time = 0, and k_1 and k_2 representing disposition rate constants. Brain volume of distribution (V_D) and brain delivery (BD) were calculated as described by Samii et al. (1994). V_D = dpm/g brain ÷ dpm/ml plasma; $BD = (V_D - V_o)\, C_p(T)$, where V_D is brain volume of distribution, V_o is the volume of distribution of a plasma volume marker and equals 10 μl/g (Yoshikawa and Pardridge, 1992), and $C_p(T)$ is the terminal plasma [^{3}H]NBMPR content.

Log-transformed plasma concentration versus time curves for [^{3}H]NBMPR and [^{14}C]sucrose were curvi-linear (Fig. 5) and consistent with the two-compartment open pharmacokinetic model chosen for analysis of disposition. Reflected by the extrapolated values, A and B (table 7), a smaller percentage of the injected dose of [^{3}H]NBMPR than of [^{14}C]sucrose remained throughout the 30 minute monitoring period. This may reflect [^{3}H]NBMPR binding to nucleoside transporters associated with cells such as erythrocytes

Figure 5: Plasma Disposition Curves for [^{3}H]NBMPR and [^{14}C]Sucrose

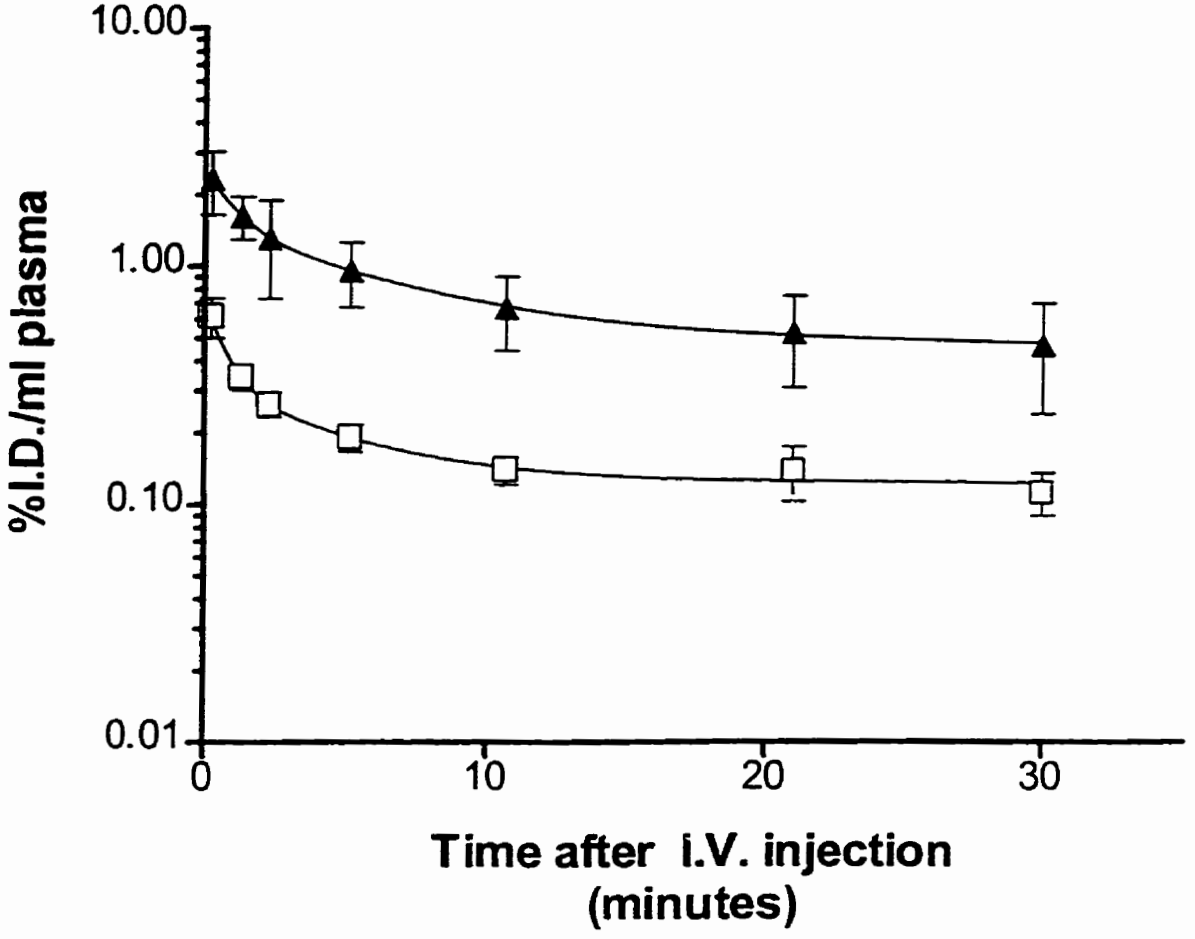

Plasma disposition curves for [^{3}H]NBMPR (open squares) and [^{14}C]sucrose (filled triangles). Points are means of 5 experiments and error bars represent standard error of the mean. Curves represent the best fit to a two-compartment pharmacokinetic model.

and endothelial cells. [^{3}H]NBMPR was eliminated from plasma with disposition half-lives ($t_{½}$) that were not significantly different from those of [^{14}C]sucrose (table 7). The brain volume of distribution (V_D) for [^{3}H]NBMPR was more than ten-fold greater than that for [^{14}C]sucrose and the brain delivery (in % injected dose/g brain) was 3.7 times greater than for [^{14}C]sucrose (table 7). Since ^{3}H was found in homogenized brain tissue, and both the brain volume of distribution and brain delivery were greater for [^{3}H]NBMPR than for [^{14}C]sucrose. However, it is also possible that our data reflect the presence of tritiated metabolites rather than [^{3}H]NBMPR in brain.

To address this concern, NBMPR content in brain tissue was determined by injecting male Sprague-Dawley rats (250 g) with 15 mg/kg NBMPR-P intraperitoneally. Animals were anesthetized with sodium pentobarbital (50 mg/kg i.p.) 45 minutes after injection and brains were perfused *in situ* with 0.1 M phosphate-buffered saline (PBS; pH 7.4) after a further 15 minutes to remove blood from the brain. Brains were removed, weighed and extracted with 0.1 M perchloric acid (PCA solution).

NBMPR concentrations in plasma and brain samples were determined using [^{3}H]NBMPR competition binding assays (Gati and Paterson, 1997). Outdated human blood was obtained from The Red Cross (Winnipeg, Canada) and ghost cell membranes were prepared as previously described (Gati and Paterson, 1997). [^{3}H]NBMPR (0.5 nM) and 10 μg membrane protein were incubated for 1 hour (22°C) in a final volume of 1.0 ml neutralized PCA solution. Non-specific binding was determined in the presence of 100 μM dilazep and a standard curve was constructed with graded concentrations of NBMPR (3 pM - 100 nM). Several dilutions of brain PCA extracts (1.25 - 10 fold) or

Table 7: Two-compartment Open Pharmacokinetic Modeling for [^{3}H]NBMPR

	[^{3}H]NBMPR	[^{14}C]Sucrose
A (%ID/ml)	0.555 ± 0.146	1.84 ± 0.47*
B (%ID/ml)	0.204 ± 0.032	1.06 ± 0.35*
k_1 (min^{-1})	0.998 ± 0.212	0.772 ± 0.168
k_2 (min^{-1})	0.022 ± 0.003	0.034 ± 0.005
Half-life (min)		
k_1	0.902 ± 0.270	1.09 ± 0.24
k_2	35.2 ± 6.6	22.4 ± 3.5
Brain V_D (µl/g brain)	963 ± 150 (6)	82.4 ± 8.1* (8)
Brain delivery (%ID/g brain)	0.11 ± 0.03 (4)	0.03 ± 0.01* (5)

Two-compartment open pharmacokinetic model for [^{3}H]NBMPR disposition. [^{3}H]NBMPR and [^{14}C]sucrose were injected intravenously and ^{3}H levels in plasma were assayed at different times. All values represent means ± SEM; n = 5 or as indicated in brackets. Parameters were determined from individual experiments by computer modeling of plasma disposition curves using the program ESTRIP. * $p<0.05$; student's unpaired t-test (two-tail).

plasma samples (300 - 30,000 fold) were prepared and analyzed for NBMPR. Assay mixtures were filtered through Whatman GF/B filters using a Brandel cell harvester and washed 3 times with ice-cold Tris-HCl (50 mM; pH 7.4, 25°C). Filters were then assayed for ^{3}H content by liquid scintillation counting. Data were analyzed by non-linear regression using Graphpad Prizm (version 1.0) (see inset, Fig. 6). An average inhibition constant for NBMPR of 1.1 nM was obtained. A detection limit of approximately 0.13 nM, or 1 pmol/g brain, was achieved; this is about 50-fold more sensitive than HPLC analysis of NBMPR (Gati and Paterson, 1997).

With this assay, NBMPR at a concentration of 59.4 ± 8.6 pmol/g brain was detected in brain samples from NBMPR-P treated rats (Fig. 6). However, an apparent NBMPR concentration of 22.1 ± 6.1 pmol/g brain was detected in samples from vehicle treated rats (Fig. 6), indicating the presence of a compound that was interfering with the [^{3}H]NBMPR competition binding assay.

We hypothesized that adenosine may be responsible since its levels in rats killed by decapitation are up to 50-fold greater than in rats killed by focused microwave irradiation (Delaney and Geiger, 1996), a method thought to more closely reflect levels in CSF of live rats. Adenosine levels were measured in brain extracts by high performance liquid chromatography (HPLC) as described previously (Delaney and Geiger, 1995), and found to be 7.4 ± 1.2 μM and 3.1 ± 1.5 μM ($p<0.05$, one-tailed student's t-test) in NBMPR-P and vehicle treated animals, respectively. This indicates that peripheral administration of NBMPR-P led to elevated brain concentrations of adenosine. We determined the inhibition constant (K_i) for adenosine-mediated inhibition of [^{3}H]NBMPR binding to ghost membranes to be 220 and 200μM in two separate experiments. There

Figure 6: Apparent NBMPR Content in Perchloric Acid Brain Extracts 60 Minutes after NBMPR-P Injection (15 mg/Kg i.p.)

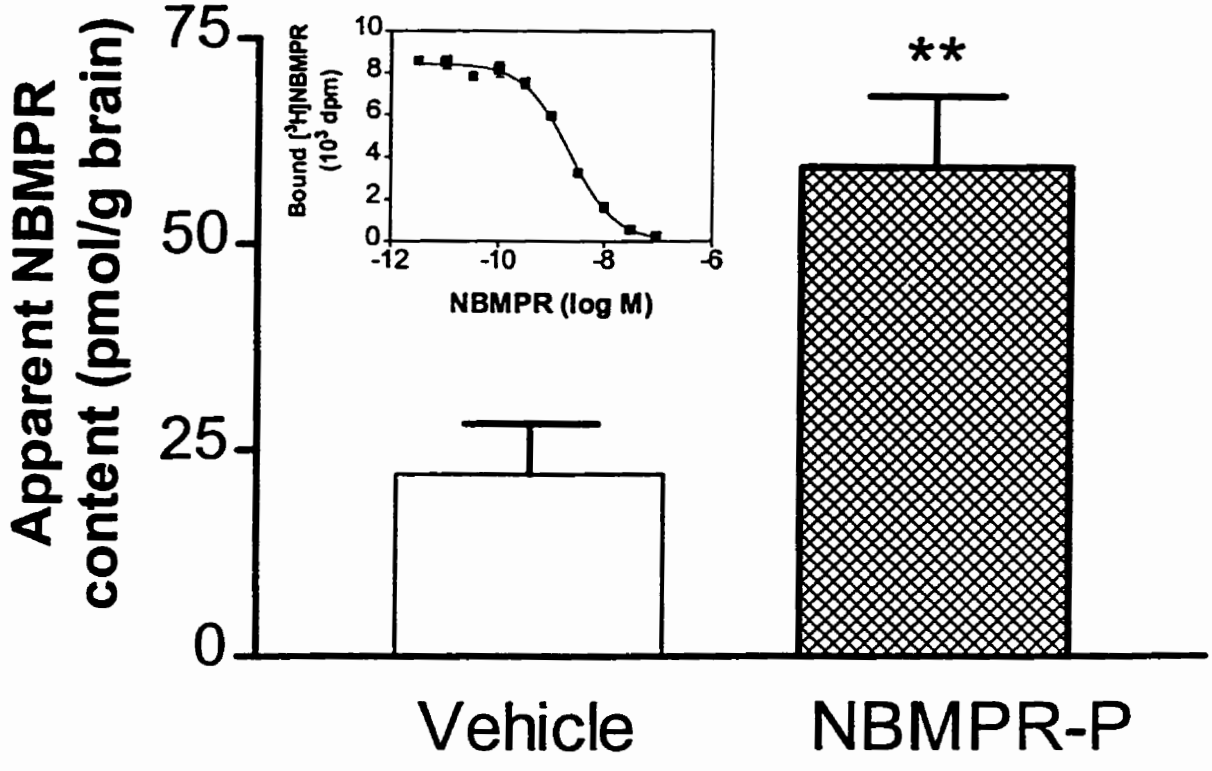

Apparent NBMPR content in brain PCA extracts 60 minutes following NBMPR-P (15 mg/kg i.p.) or vehicle administration. Values are plotted as mean ± SEM for 4 animals in each group. ** Indicates significance with $p<0.01$.

Inset: A representative dose-response curve for inhibition of [^{3}H]NBMPR binding to human erythrocyte ghost membranes by NBMPR. The K_i value obtained by a Cheng-Prusoff type calculation was 1.1 ± 0.3 nM.

was no appreciable metabolism of adenosine during incubation with ghost cell membranes (data not shown). Thus, the concentrations of adenosine in brain PCA extracts should inhibit [^{3}H]NBMPR binding by less than 5%, indicating that a substance other than, or in addition to, adenosine was present in PCA extracts and interfered with the NBMPR detection assay.

Since PCA extracts of brains from decapitated rats contained one or more substances that interfered with the NBMPR detection assay, we chose to measure NBMPR levels in cerebrospinal fluid (CSF), a source of brain perfusate samples which has equilibrated with cerebral interstitial fluid. NBMPR-P (10 mg/kg i.p.) was injected into male Sprague-Dawley rats (250 g). Animals were anesthetized with sodium pentobarbital (50 mg/kg i.p.) and CSF was extracted from the cisterna magna according to previously described methods (Walter *et al.*, 1988) 30 minutes following injection of NBMPR-P. Plasma samples were obtained and diluted as described above. Determination of NBMPR content of CSF samples, diluted 6 - 12 fold, or plasma samples was performed using the [^{3}H]NBMPR competition binding assay in a total reaction volume of 0.3 ml.

NBMPR concentrations of 4.74 ± 0.52 μM (mean ± SEM, n=5) and 24.1 ± 4.4 nM (n=5) in plasma and CSF, respectively, were measured in samples from rats treated with NBMPR-P. Both plasma and CSF samples from vehicle-treated animals showed no inhibition of [^{3}H]NBMPR binding to ghost cell membranes indicating the NBMPR detection assay was free of interfering compounds. The level of NBMPR, 24.1 nM, measured in CSF samples from NBMPR-P treated rats was 60-fold greater than the K_d value of 0.39 nM for NBMPR binding to rat brain slices (Bisserbe *et al.*, 1985). This

result suggests that following systemic injection of NBMPR-P, there may be sufficient NBMPR in the cerebral interstitium to inhibit nucleoside transporters and to affect endogenous adenosine levels.

Previous studies to evaluate central effects of NBMPR have indicated that the sedative effects of adenosine were potentiated in rat (Crawley *et al.*, 1983) but NBMPR was not neuroprotective in a gerbil model of cerebral ischemia (DeLeo *et al.*, 1988). However, the poor solubility of this compound was not addressed and no estimates of NBMPR levels in brain were made. Our study demonstrates that nanomolar concentrations of NBMPR reach brain tissue and CSF following peripheral administration of the prodrug form NBMPR-P. The high potency and selectivity of this compound make it an excellent candidate for testing the effects of nucleoside transport inhibitors *in vivo*.

[2]Chapter 3

Distribution of Equilibrative, Nitrobenzylthioinosine-sensitive Nucleoside Transporters in Brain

Summary

Nucleoside transport processes may play a role in regulating endogenous levels of the inhibitory neuromodulator adenosine in brain. cDNAs encoding species homologs of one member of the ENT gene family of equilibrative nucleoside transporters have recently been isolated from rat (rENT1) and human (hENT1) tissues. The current study used RT-PCR, northern blot, *in situ* hybridization and [^{3}H]nitrobenzylthioinosine ([^{3}H]NBMPR) autoradiography to determine the distribution of mRNA and protein for rENT1 and hENT1 in rat and human brain, respectively. Northern blot analysis in human brain using a 1.2 kb cDNA probe for hENT1 indicated a wide regional distribution for hENT1 mRNA. RT-PCR using hENT1-specific primers also showed a heterogeneous cellular distribution for hENT1 mRNA as bands were seen for mRNA from both human fetal neurons and astrocytes. RT-PCR with total RNA from rat brain regions using rENT1-specific primers confirmed this wide distribution of ENT1 in rat brain as well. ^{35}S-Labeled sense and antisense riboprobes, transcribed from a 153-bp segment of rENT1, were hybridized to fresh frozen coronal rat brain sections (14 μm). Hybridization of the antisense probe was widespread, confirming results seen with RT-PCR (rat) and northern blot (human). Message for rENT1 was seen in granule and pyramidal neurons

[2] Anderson CM *et al.* (1998) Distribution of equilibrative, nitrobenzylthioinosine-sensitive nucleoside transporters (ENT1) in brain. J Neurosci. (Submitted).

of the hippocampus, Purkinje and granule neurons of the cerebellum, and in cortical and striatal neurons. Other cell types including astrocytes, choroid plexus epithelial cells and smooth muscle cells, but not oligodendrocytes, also displayed signal for rENT1 by *in situ* hybridization. Film autoradiography with [^{3}H]NBMPR in rat brain indicated transporter density was highest in striatum and thalamus, intermediate in cerebral cortex and lowest in hippocampus and cerebellum, in contrast to results with *in situ* hybridization showing high rENT1 antisense riboprobe binding in all of these regions. We have previously reported the existence of mRNA for two members of the concentrative nucleoside transporter family (CNT) in rat brain. Our results here show a wide cellular and regional distribution of hENT1 mRNA in human brain, and rENT1 mRNA and protein in rat brain, indicating that control of adenosine levels is achieved by multiple transport processes.

Introduction

Several CNS effects including decreased alertness following prolonged wakefulness (Porkka-Heiskanen *et al.*, 1997) and neuroprotection in conditions such as stroke or seizure (von Lubitz *et al.*, 1997) have been associated with the inhibitory effects of the purine nucleoside adenosine. These effects are mediated by four adenosine receptor subtypes termed A_1, A_{2A}, A_{2B} and A_3.

Stimulation of adenosine A_1 receptors is inhibitory by stabilizing cellular ionic currents and decreasing excitatory neurotransmitter release. Through these mechanisms, adenosine can limit cellular damage due to toxic accumulation of Ca^{2+} during metabolic stress (Rudolphi *et al.*, 1992). Adenosine A_1 receptors may also mediate ethanol-induced

motor incoordination in cerebellum (Dar, 1997), contribute to synaptic plasticity in hippocampus (de Mendonça and Ribeiro, 1997) and produce antinociception in spinal cord (Sollevi, 1997). Stimulation of adenosine A_{2A} receptors has direct vasodilatory effects on cerebral vessels and inhibits neutrophil and platelet activities, leading to improved blood flow during times of reduced ATP synthesis (Miller and Hsu, 1992). Excitatory actions have also been described for A_{2A} receptors in brain (Sebastião and Ribeiro, 1996) as have antagonistic interactions with dopamine D_2 receptors in the basal ganglia (Ferré *et al.*, 1997). Roles for adenosine A_{2B} and A_3 receptors in the CNS are less clear.

Nucleoside transporters are thought to facilitate the salvage of extracellular nucleosides for synthesis of nucleotides. In brain, the role of nucleoside transport processes may be of further importance as regulators of endogenous adenosine levels and adenosine receptor stimulation. Endogenous adenosine levels rise significantly in brain during cerebral ischemia and can be potentiated by inhibiting pathways of adenosine degradation or nucleoside transport processes (Rudolphi *et al.*, 1992). The xanthine derivative, propentofylline, is an inhibitor of cellular adenosine uptake and has neuroprotective effects in animal models of stroke (Parkinson *et al.*, 1994).

Two broad categories of nucleoside transporters are equilibrative and Na^+-dependent (see Cass, 1995 for review). At least five Na^+-dependent subtypes exist, two of which have been cloned. Both rCNT1 (pyrimidine selective) and rCNT2 (purine selective) have been identified in rat brain by RT-PCR (Anderson *et al.*, 1996a). Equilibrative transporters are distinguished based on sensitivity to the inhibitor nitrobenzylthioinosine (NBMPR). *E*quilibrative, NBMPR-*i*nsensitive transporters are

termed *ei* and *e*quilibrative, NBMPR-*s*ensitive transporters are termed *es*. The *es* transporter has recently been cloned from rat jejunum and human placenta and termed rENT1 (Yao *et al.*, 1997) and hENT1 (Griffiths *et al.*, 1997), respectively. Both functional studies and autoradiography with [^{3}H]NBMPR have previously indicated the presence of *es* transport activity in rat brain (Geiger and Fyda, 1991).

Isolation of hENT1 and its rat homologue rENT1 has allowed investigation of the distribution and regulation of ENT1 mRNA synthesis in rat and human tissues. The goals of the present study were to identify and to localize mRNA for rENT1 in rat brain using RT-PCR and *in situ* hybridization, to compare mRNA distributions with [^{3}H]NBMPR binding site distribution in rat brain, and to use cDNA probes to determine the distribution and relative abundance of mRNA for hENT1 in human brain by northern blot.

Materials and Methods

Culture of human fetal neurons and astrocytes

For both neurons and astrocytes, brain specimens were obtained from fetuses of 14 to 15 weeks gestational age, with consent, from women undergoing elective termination of pregnancy. All protocols received approval from, and were performed in accordance with, The University of Manitoba Committee for the Protection of Human Subjects and the Human Ethics Committee of the Health Sciences Center Hospital.

Cultures of human neurons were established as described previously (Magnuson *et al.*, 1995). Briefly, the cells were mechanically dissociated, suspended in OptiMEM with 5% heat-inactivated fetal bovine serum, 0.2% N2 supplement (GIBCO), and 1%

antibiotic solution (penicillin G 10^4 units/ml, streptomycin 10 mg/ml, and amphotericin B 25 μg/ml in 0.9% NaCl) and plated in 75 cm^2 culture flasks. Cultures were maintained for at least 30 days, with fresh medium added every 3-4 days, prior to RNA isolation. These cultures were >70% neurons as determined by immunostaining for the neuronal marker microtubule-associated protein 2 (MAP-2).

For human fetal astrocytes, cells were mechanically dissociated, centrifuged at 270 *g* for 10 min, resuspended in Dulbecco's modified Eagle's medium (DMEM) containing 10% fetal calf serum (FCS), 1.0% L-glutamine and 0.2% antibiotic solution consisting of 1000 units/ml penicillin G, 10 mg/ml streptomycin and 25 μg/ml amphotericin B in 0.9% NaCl, and grown in 75 cm^2 culture flasks in 5% CO_2 at 37°C. Fresh media was added every 3-4 days. Seven-day-old cultures were placed on a rotary shaker for 2 h at 333 rpm at room temperature (25°C). Supernatants were discarded and the remaining cells were exposed to 0.05% trypsin and 0.53 mM EDTA. Cells were collected, centrifuged at 270 *g* for 10 min, resuspended in DMEM containing 10% FCS and placed into 75 cm^2 culture flasks. After 30 min, decanted cells were plated and allowed to grow to confluence for RNA isolation. These cells were >98% astrocytes as determined by immunostaining for glial fibrillary acidic protein (GFAP; Chemicon).

Reverse Transcriptase PCR

Total RNA was isolated from rat cortex, cerebellum, striatum, hippocampus and superior colliculus using the SNAP RNA isolation kit (Invitrogen) and treated with DNase I. Oligo$(dT)_{12-18}$ primer (300 ng) was annealed to the mRNA template (5 μg) and cDNA synthesis proceeded at 37°C for 60 minutes using 3 mM dNTPs, 6.7 μM dithiothreitol (DTT) and either 3.3 Units reverse transcriptase or 1μl H_2O in 60 μl of buffer containing 50 mM Tris-HCl (pH 8.3), 75 mM KCl, 3 mM $MgCl_2$.

For polymerase chain reaction cDNA template solutions (2 µl) were amplified in a mixture containing 200 µM dNTPs, 2 mM $MgCl_2$, 1 µM each of the 5' and 3' primers and 2.5 Units Taq DNA polymerase (Gibco/BRL) in a total volume of 100 µl. The amplification consisted of 30 cycles of: 30 s. at 94°C, 30 s. at 56°C and 1 min. at 72°C. A final 10 min. 72°C elongation step followed and samples were frozen or analyzed immediately by electrophoresis on a 1.0% agarose gel. DNA bands were viewed and photographed under UV light following ethidium bromide staining.

A 213-bp fragment of hENT1 from bases 907 to 1119 was amplified using the 5' primer 5'-CGGGGAGCAGGAGACCAAGT-3' and the 3' primer 5'-ACCTCAACAGT-CACGGCTGGAAA-3'. rENT1 was amplified using the 5' primer 5'-GGCCTGTGCAG-TTGTCATTC-3' and the 3' primer 5'-CCTCCTCTTGGCTCCTCTCC-3' to produce a 153-bp fragment from bases 637 to 789.

The presence of mRNA for glyceraldehyde-3-phosphate dehydrogenase (GAPDH), a ubiquitous housekeeping gene, was used to verify the quality of cDNA preparations, and was detected using the 5' primer 5'-GCTGGGGCTCACCTGAAGGG-3' and the 3' primer 5'-GGATGACCTTGCCCACAGCC-3' to amplify a 343-bp DNA product (bases 346 to 688) from the rat GAPDH cDNA (Tso et al., 1985).

Northern Blots

A human brain multiple tissue northern blot was purchased (Clontech) and probed with a 1.2 Kb fragment from hENT1 (bases 881 to 2021). hENT1 and β-actin cDNAs were labeled with ^{32}P using random primers and the Klenow fragment in the presence of [α-^{32}P]dCTP. Membranes were prehybridized at 42°C in 50% formamide, 5x SSPE (0.6 M NaCl, 40 mM $NaH_2PO_4 \cdot H_2O$, 4 mM EDTA, pH 7.4), 10x Denhardt's solution, 2% sodium dodecylsulfate (SDS) and 100 µg/ml denatured, sheared salmon testis DNA. After 3 hours, an excess of ^{32}P-labeled cDNA probe was added (~2 x 10^6 cpm/ml) and hybridization was allowed to proceed for 24 hours. Blots were rinsed several times with

2x SSC (0.3 M NaCl, 30 mM Na-citrate) containing 0.05% SDS at room temperature and then washed with high stringency at 60°C for 60 minutes in 0.1x SSC containing 0.1% SDS. Membranes were wrapped in plastic and exposed to x-ray film for 72 hours.

In Situ Hybridization

Male Sprague-Dawley rats (250 g) were sacrificed by decapitation and brains were removed and frozen. Fresh frozen sections (14 μm) were cut using a cryostat and placed on ProbeOn Plus microscope slides (Fisher). Sections were frozen at -80°C until use. Sections were fixed for 2 minutes in buffered 4% paraformaldehyde, permeabilized for 7 minutes with 0.0005% proteinase K at 37°C, acetylated for 10 minutes (0.25% v/v acetic anhydride in 0.1 M triethanolamine buffer, pH 8.0) and dehydrated in graded ethanol concentrations prior to hybridization.

RNA probes (riboprobes) were used to detect rENT1 in rat brain. RT-PCR was performed using the above 3' primer and a phosphorylated 5' primer 5'-phosphate-GGCCTGTGCAGTTGTCATTC-3' to generate a 153-bp monophosphorylated cDNA product from bases 637 to 789. This product was ligated into the pCR-Script Direct plasmid vector (Stratagene) to produce a directional clone such that *in vitro* transcription with T3 RNA polymerase produced a sense riboprobe while T7 RNA polymerase gave an antisense riboprobe. The Ambion Maxiscript kit was used to transcribe RNA from linearized/proteinase K-treated templates. Transcription proceeded for 60 minutes at 37°C with 0.5 mM each of ATP, GTP and CTP, 10 mM dithiothreitol (DTT), 400 μCi [α-^{35}S]UTP (NEN) and 0.5 Units T3 or T7 RNA polymerase in a total volume of 20 μl. Labeled RNA probes were ethanol precipitated, resuspended in solution containing 10 mM Tris-HCl (pH 8.0), 1 mM EDTA, 10 mM DTT and 1% SDS, and counted for ^{35}S content.

Hybridization was performed overnight at 55°C in a Microprobe hybridizer (Fisher). Hybridization solution contained 50% (v/v) formamide, 10% (w/v) dextran

sulfate, 0.3 M NaCl, 1x Denhardt's solution, 10 mM Tris-HCl (pH 8.0), 1 mM EDTA, 100 μg/ml denatured salmon sperm DNA, 0.5 mg/ml yeast tRNA and 10 mM DTT. Riboprobes were added to a concentration of 5 x 10^6 cpm/ml hybridization solution. Following hybridization sections were treated with RNase A (20 μg/ml) and washed with increasing temperature and decreasing salt concentration to a final wash for 30 minutes at 60°C in 0.1x SSC with 50 mM DTT. Sections were dehydrated in preparation for emulsion or film autoradiography. For film autoradiography, sections were exposed to Amersham Hyperfilm-βmax for 14 days and developed using Kodak D-19 developing solution. For emulsion autoradiography, slides were dipped in Kodak NTB-2 autoradiographic emulsion for 14 days and developed using a 1:1 dilution of Kodak D-19 developer. Sections were then counter-stained with the nuclear stain hematoxylin.

[^{3}H]NBMPR Autoradiography

Fresh frozen rat brain coronal sections (14 μM) were cut and placed on Superfrost Plus slides (Fisher) as described for *in situ* hybridization. Sections were thawed, fixed for 2 minutes in buffered 4% paraformaldehyde and rinsed twice for 5 minutes in ice-cold 0.1 M phosphate-buffered saline (PBS). Total binding was determined by incubating sections with 1 nM [^{3}H]NBMPR (NEN) at 20°C for 30 minutes in the presence of 2 Units/ml adenosine deaminase. Non-specific binding was determined using the same conditions with the addition of 10 μM nitrobenzylthioguanosine (NBTG). Following binding, sections were rinsed twice for 10 minutes each in ice-cold PBS and blown dry overnight at 4°C. Tritium signal was detected by exposing slides to Hyperfilm ^{3}H (Amersham) in x-ray cassettes for 3 weeks at 4°C.

Results

Regional identification of hENT1 mRNA in human brain

A multi-tissue northern blot of mRNA from various regions of human brain was probed using a ^{32}P-labeled 1.2 kb segment of the hENT1 cDNA. Results indicated a wide distribution of hENT1 mRNA in human brain (Fig. 7*A*). Relative mRNA levels were quantified using Kodak Digital Science 1D software. Standardization of hENT1 signals against β-actin for each region indicated highest hENT1 mRNA levels in amygdala and caudate nucleus. Intermediate levels were seen in corpus collosum, hippocampus, subthalamic nucleus and thalamus while the hENT1/β-actin ratio for substantia nigra was lowest and was approximately half of the maximum seen for the caudate nucleus. Bands were also detected at approximately 1.5 kb; this is due to residual β-actin signal from previous experiments.

RT-PCR was performed with RNA isolated from primary cultured human fetal neurons and astrocytes. A 213-bp product was seen in both cell types (Fig. 7*B*) indicating mRNA for hENT1 has a broad cellular distribution as well as a broad regional distribution. A larger product was also seen but did not remain following changes in PCR conditions (not shown).

Regional distribution of [^{3}H]NBMPR binding sites in rat brain

Film autoradiography using [^{3}H]NBMPR, a potent inhibitor of the *es* nucleoside transporter, was performed to localize *es* transporter protein in rat brain regions (Fig. 8).

A, an mRNA northern blot from human brain was probed with a ^{32}P-labeled 1.2 Kb fragment of hENT1. A wide regional distribution for hENT1 is indicated by hybridization to a 2.2 Kb RNA species in each region. The bar graph represents the ratio of mean band intensities for hENT1 to β-actin. Am, amygdala; CN, caudate nucleus; CC, corpus collosum; Hp, hippocampus; WB, whole brain; Sg, substatia nigra; SN, subthalamic nucleus; Th, thalamus. B, RT-PCR was performed with hENT1-specific primers using total RNA (5 μg) from cultured human fetal astrocytes and neurons. The band corresponding to hENT1 is 213-bp and was present in both cell types. No product was amplified from samples not treated with reverse transcriptase (RT).

Figure 7: Regional and Cellular distributions of mRNA for hENT1 in Human Brain

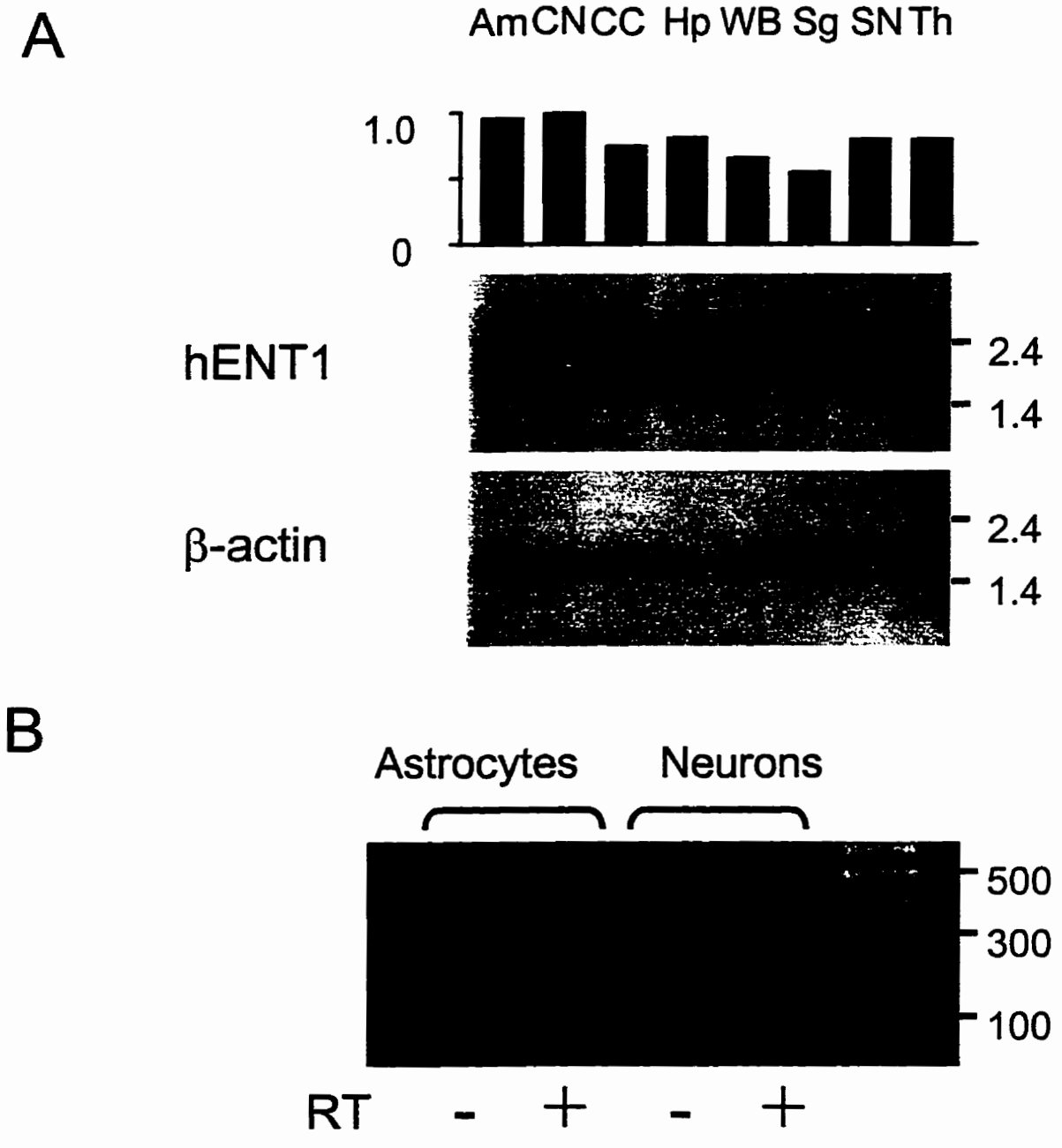

Figure 8: Distribution of [^{3}H]NBMPR Binding Sites in Rat Brain

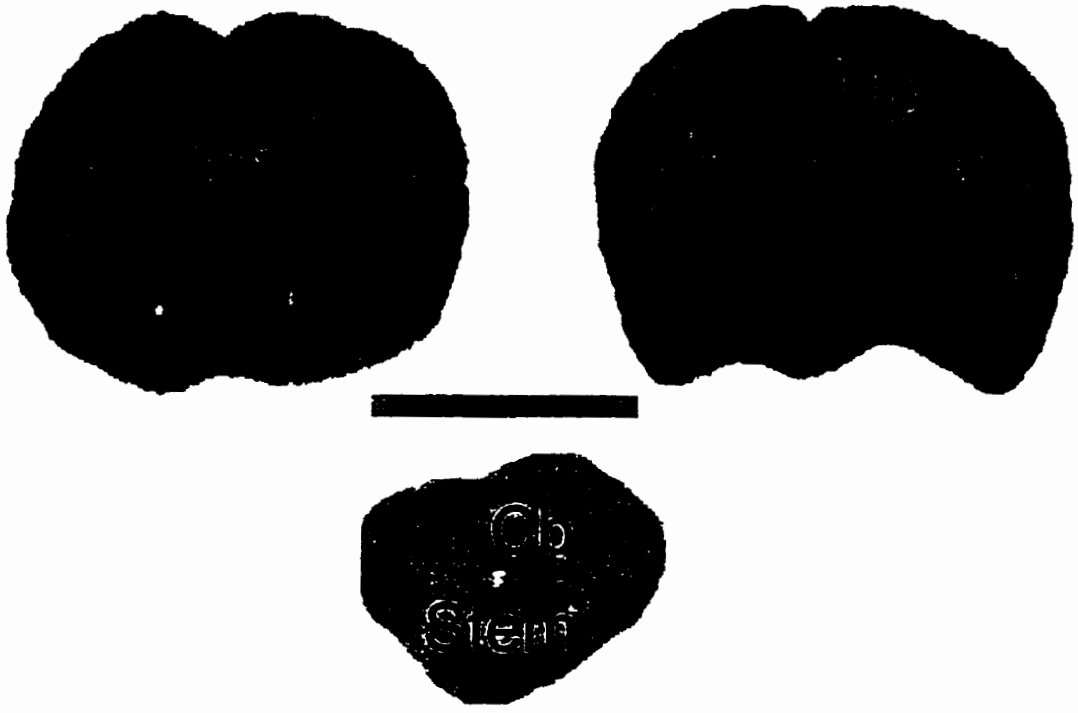

Brain slices were incubated with [^{3}H]NBMPR (1 nM) for 30 minutes at 20°C in the presence of adenosine deaminase. The film shows moderate to high binding of [^{3}H]NBMPR throughout much of the brain (background color indicated by horizontal strip). Note the high binding site densities in striatum (Str) and thalamus (Th) and the very low density in hippocampus (Hp) and cerebellum (Cb). CC, corpus callosum; Cx, cerebral cortex.

As determined by image analysis performed by the Scion Image graphics program, highest binding site density, indicating high expression of *es* nucleoside transporters, was seen in the paraventicular nucleus, medial thalamic nuclei and rhomboid and reuniens thalamic nuclei. Optical densities of approximately 70% of these maximum values were seen in lateral thalamic nuclei and the caudate putamen while binding site density in the cerebral cortex was 60% of the maximum. Lowest [^{3}H]NBMPR binding densities were detected in cerebellum and hippocampus. Optical densities in both regions were approximately 40% of the maximum. The film background had an optical density reading 33% of the maximum. These results are in agreement with those reported previously (Geiger and Nagy, 1984; Bisserbe *et al.*, 1985).

Regional identification of rENT1 mRNA in rat brain using RT-PCR

RT-PCR was performed using RNA from rat brain tissues and primers specific for rENT1. A 153-bp PCR product was seen in all regions tested including cortex, cerebellum, striatum, hippocampus and superior colliculus (Fig. 9). The product was absent in samples not treated with reverse transcriptase indicating the absence of contaminating genomic DNA. The presence of the housekeeping gene, GAPDH (Fig. 9), and agarose gel electrophoresis (not shown) indicated that RNA samples were of good quality. Agarose gel band intensities were compared to GAPDH for each region to give an estimate of relative abundance of rENT1 mRNA for each region. While rENT1:GAPDH intensity ratios were fairly consistent among regions tested, it was highest in superior colliculus (1.0) followed closely by hippocampus (0.96). Striatum was intermediate (0.85) while cerebellum (0.81) and cortex (0.80) were lower.

Figure 9: Regional Distribution of rENT1 mRNA in Rat Brain

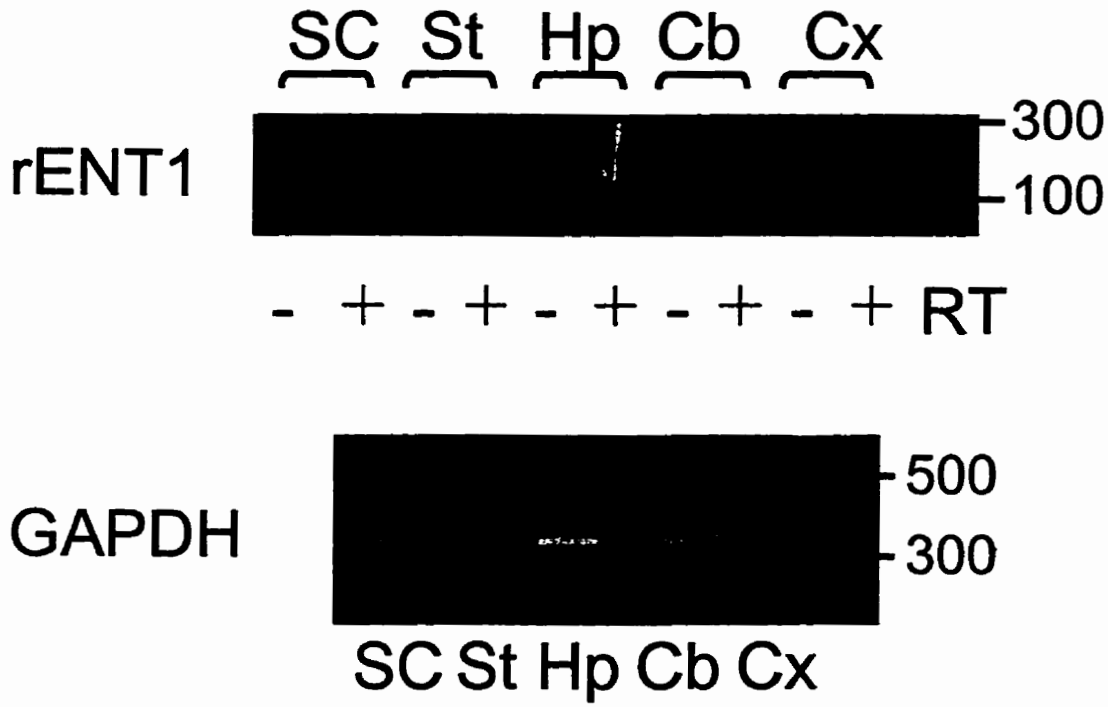

Total RNA was isolated from superior colliculus (SC), striatum (St), hippocampus (Hp), cerebellum (Cb) and cerebral cortex (Cx), and subjected to RT-PCR with primers specific for rENT1. The expected product of 153-bp was seen in all regions tested. No product was seen in samples not treated with reverse transcriptase (RT) indicating good RNA quality.

Distribution of rENT1 mRNA in rat brain using in situ hybridization

^{35}S-labeled cRNA probes transcribed from a 153-bp segment of the rENT1 cDNA were used for *in situ* hybridization. A high level of antisense sequence binding was seen throughout rat brain. Binding of the sense sequence in parallel sections was negligible. Hippocampus exhibited extensive antisense sequence binding (Fig. 10), as did striatum, cortex, cerebellum (Fig. 11) and thalamus (not shown) indicating a widespread presence of rENT1 mRNA in rat brain. This is in agreement with the human data from Fig. 7 and RT-PCR from Fig. 9. The habenular nucleus displayed a particularly strong hybridization signal for rENT1 mRNA (Fig. 12*G, H*).

In hippocampus, a strong specific signal was seen in the granule neurons of the dentate gyrus and the pyramidal neurons of the CA1 through CA4 subfields (Fig. 10). Both granule and Purkinje neurons of the cerebellum also contain rENT1 transcripts (Fig 11*A-D*). Hybridization signals were also detected with about 50% of neurons in cortex, striatum (Fig. 11*E-H*) and thalamus. Co-localization studies with markers for specific neurotransmitters are required to identify the types of neurons expressing rENT1 in these regions.

There is also evidence that rENT1 mRNA is present in astrocytes. The subpial layers of the brain bound antisense riboprobe, suggesting rENT1 may be present in subpial astrocytes (Fig. 11*A-D*, cerebellum). Dense cellular silver grain aggregations were also seen in the molecular layers of the cerebellum and dentate gyrus, as well as the stratum radiatum of the hippocampus. Corpus callosum did not appear to display any appreciable specific binding of the antisense rENT1 riboprobe (not shown), suggesting oligodendrocytes do not express rENT1.

Sense and antisense cRNA probes were transcribed from a 153-bp cDNA fragment of rENT1 ligated into the PCR-Script direct vector and were hybridized to 14 μm fresh frozen coronal rat brain sections. A and B represent results of in situ hybridization obtained with the sense cRNA probe for rENT1 while C and D are results with the antisense probe (20x magnification). Nuclei were stained with hematoxylin as seen in bright-field images A and C. B and D are dark-field images in which cRNA probes are detected by silver grains which appear white. Note the broad neuronal distribution of rENT1 mRNA in hippocampus as indicated by a strong hybridization signal for the antisense cRNA probe (D). The sense probe did not produce a hybridization signal (B). DG, dentate gyrus; CA1, CA1 subfield; CA3, CA3 subfield.

Figure 10: Distribution of rENT1 mRNA in Rat Hippocampus

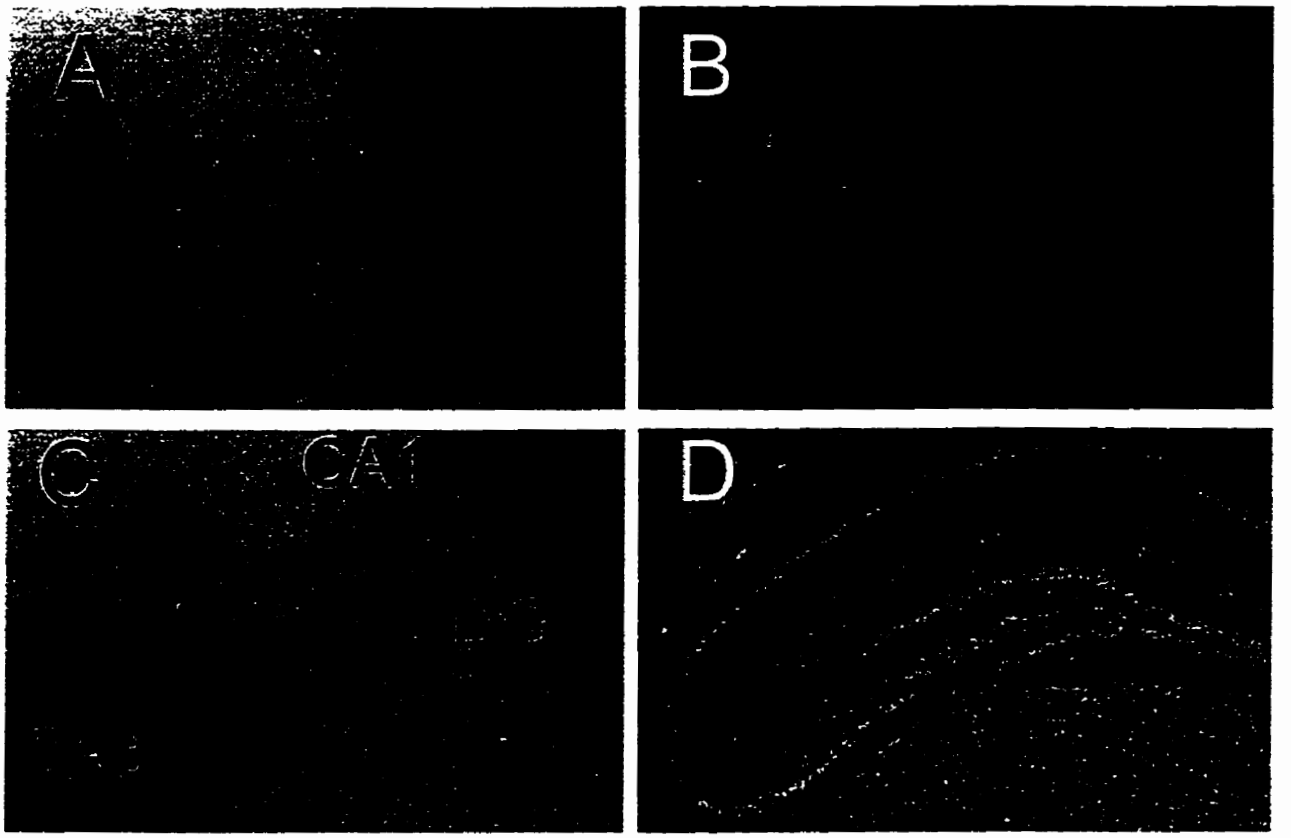

Sense and antisense cRNA probes were transcribed from a 153-bp cDNA fragment of rENT1 ligated into the PCR-Script direct vector and were hybridized to 14 μm fresh frozen coronal rat brain sections. Nuclei were stained with hematoxylin as seen in bright-field images A, C and E to H. B and D are dark-field images in which cRNA probes were detected by silver grains, which appear white. A and B represent results of in situ hybridization obtained with the sense cRNA probe for rENT1 in cerebellum while C and D are results with the antisense probe in cerebellum (40x magnification). The Purkinje (Pk) and granule cell layers (Gr) both displayed specific antisense probe binding (D). Sense probe binding was negligible (B). The pial layers (PL) of the cerebellum also contain rENT1 mRNA. E represents sense probe treatment and F represents antisense probe treatment of cerebral cortical sections (400x magnification). Silver grains appear black and indicate that approximately 50% of neurons in the cerebral cortex contain mRNA for rENT1 (F). Sense probe binding was negligible (E). G represents sense probe treatment and H represents antisense probe treatment of dorsal lateral striatal sections (400x magnification). Again, approximately 50% of neurons contained mRNA for rENT1 (H). For F and H, black arrowheads indicate rENT1-positive cells while white arrowheads show rENT1-negative cells.

Figure 11: Distribution or rENT1 mRNA in Rat Cerebellum, Cerebral Cortex and Striatum

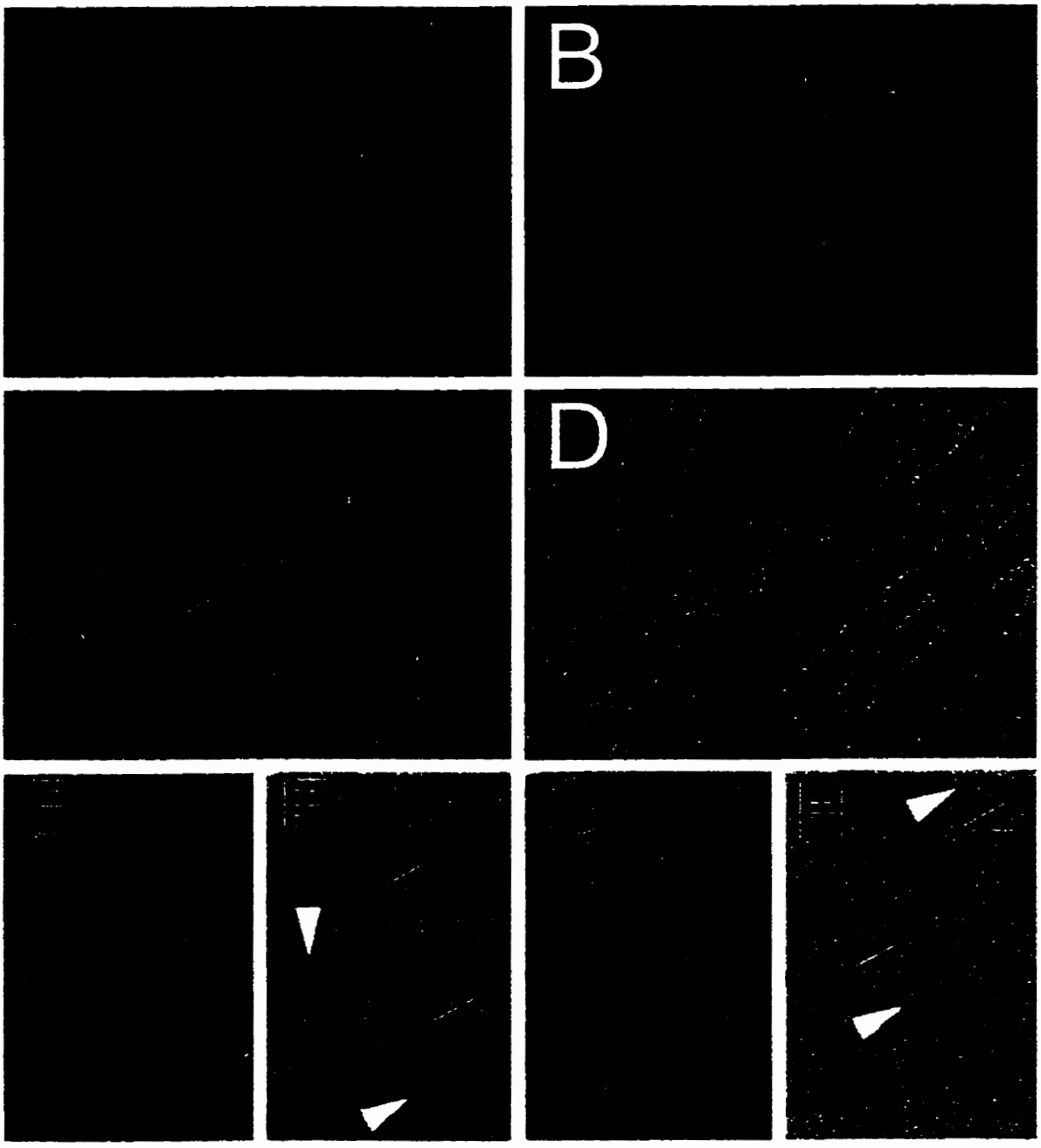

Sense and antisense cRNA probes were transcribed from a 153-bp cDNA fragment of rENT1 ligated into the PCR-Script direct vector and were hybridized to 14 μm fresh frozen coronal rat brain sections. Nuclei were stained with hematoxylin as seen in bright-field images A, C, E and G. B, D, F, and H are dark-field images in which cRNA probes were detected by silver grains, which appear white. A to D represent results of in situ hybridization obtained with the antisense cRNA probe for rENT1 in a cerebral artery (A, B) and vein (C, D) (100x magnification). A strong hybridization signal was seen in the arterial wall (B) but only a slight signal was seen in the vein wall (D). Ar, artery; V, vein. Sections in E and F were treated with the sense rENT1 cRNA probe while G and H received the antisense probe (100x magnification). Antisense binding was high in the choroid plexus as well as the habenula nucleus (H). Again, sense probe binding was negligible (F). CP, choroid plexus; Hb, habenular nucleus.

Figure 12: Distribution of rENT1 mRNA in Rat Cerebral Blood Vessels and Choroid Plexus

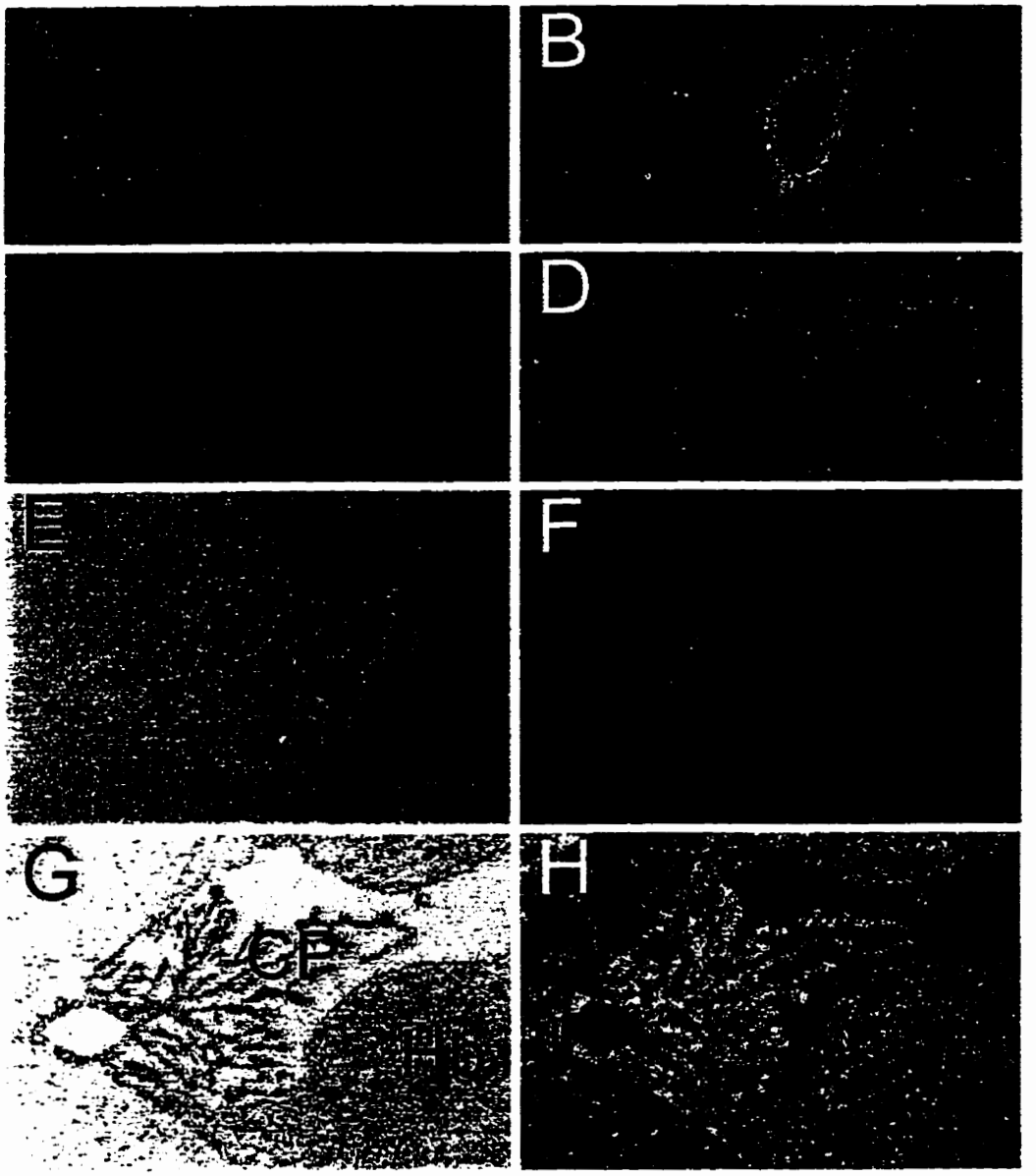

rENT1 antisense hybridization signal was strong in arterial walls while that for the sense probe was low. Low signal strength was seen in veins. These observations indicate high expression of rENT1 in smooth muscle cells but low expression of rENT1 in endothelial cells (Fig. 12).

Choroid plexus, a highly vascularized tissue consisting of epithelial cells, also displayed a high level of rENT1 antisense hybridization signal (Fig. 12*E-H*). Choroid plexus regulates passage across the blood-brain barrier and may be important in removing nucleosides from brain.

Discussion

The regional and cellular distributions of equilibrative, NBMPR-sensitive, nucleoside transporters (ENT1) were investigated in the present study. hENT1 mRNA is distributed widely throughout human brain and appears to be present in both neurons and astrocytes. In agreement, RT-PCR and *in situ* hybridization revealed a wide regional distribution of rENT1 mRNA in rat brain and indicated that rENT1 mRNA is present in many cells types including neurons, astrocytes, smooth muscle cells and epithelial cells. The distribution of rENT1 mRNA is not ubiquitous, however, as some neurons of the cerebral cortex and striatum as well as oligodendrocytes of the corpus collosum did not appear to express rENT1.

Until the successful cloning of rENT1 (Yao *et al.*, 1997), the best method of determining *es* nucleoside transporter distribution was by using [^{3}H]NBMPR, an inhibitor of nucleoside transport through *es* systems with a K_i of 0.1 – 1 nM (Griffith and Jarvis, 1996). We found that both [^{3}H]NBMPR and antisense rENT1 riboprobe binding were

moderate to high in rat cortex, thalamus and striatum. An interesting finding of this study is that while *in situ* hybridization revealed abundant mRNA for rENT1 in rat cerebellum and hippocampus, particularly pyramidal neurons and dentate gyrus granule cells, [^{3}H]NBMPR autoradiography indicated low levels of rENT1 protein in these regions. The explanation for this contradiction will require further study but several possibilities exist. Hippocampus and cerebellum may express a homologous protein with high similarity to ENT1 in the sequence corresponding to our hybridization probe. A homology search with the sense sequence of our probe indicated no significant similarity to any known coding sequences. It is also possible that only a small proportion of ENT1 mRNA is being translated. Alternatively, there may be an mRNA splice variant or post-translational modification resulting in an ENT1 isoform not recognized by NBMPR. At least one previous study found evidence for heterogeneity of NBMPR binding sites in mammalian brain (Hammond and Clanachan, 1985). Interestingly, the degree of disparity between rENT1 message and [^{3}H]NBMPR binding sites may vary by species. In contrast to low levels in rat, human hippocampus and cerebellum express a moderate number of [^{3}H]NBMPR binding sites (Glass *et al.*, 1996).

Despite low [^{3}H]NBMPR binding in rat cerebellum as determined by this and other studies (Geiger and Nagy, 1984; Bisserbe *et al.*, 1985), there is some functional evidence for *es* adenosine transport in this region. Low nM concentrations of NBMPR inhibited approximately 50% of [^{3}H]adenosine uptake in cultured cerebellar granule cells (Sweeney, 1996). This suggests our results obtained by *in situ* hybridization reflect transport activity in rat cerebellum. While NBMPR has been found to inhibit adenosine uptake and neuronal activity in hippocampus (Ohkubo, *et al.*, 1991; Haas and Greene,

1988; Hada *et al.*, 1996), NBMPR concentrations used (1-10 μM) were too high to differentiate between *es* and *ei* transporters.

Functional data support the presence of *es* adenosine transport on both neurons (Gu and Geiger, 1992; Lee and Jarvis, 1988) and astrocytes (Gu and Geiger, 1996). In agreement, our results indicate that hENT1 and rENT1 mRNAs are present in both cell types in human and rat. Such a broad cellular distribution suggests an important role for *es* transporters in nucleoside uptake for metabolic salvage. In addition, we found rENT1 mRNA to be present in cells previously reported to be rich in adenosine receptors. Rat hippocampal pyramidal cells, cerebellar Purkinje cells, and thalamic, cortical and striatal neurons all have rENT1 mRNA and are reported to exhibit extensive binding of [^{3}H]cyclohexyladenosine, a marker for adenosine A_1 receptors (Bisserbe *et al.*, 1985). This suggests that rENT1 is important for regulation of extracellular adenosine levels and adenosine receptor stimulation in these brain regions. Regulation of adenosine receptor stimulation by rENT1 could have many functional implications in the CNS.

One implication of this control by rENT1 may be observable during ethanol intoxication. Adenosine A_1 receptors are thought to mediate ethanol-induced motor incoordination in the cerebellum (Dar, 1990). This may be partly due to inhibition of *es* adenosine uptake by ethanol at concentrations reached following excessive ingestion of ethanol (Clark and Dar, 1989; Nagy *et al.*, 1990). We have shown that rENT1 is present in cerebellar cells expressing adenosine A_1 receptors, providing support that ethanol blockade of *es* transport would enhance adenosine levels in the vicinity of cerebellar A_1 receptors.

It is likely that rENT1 represents an important mechanism of extracellular adenosine regulation in hippocampus and striatum, regions sensitive to ischemic damage and rich in neuroprotective adenosine receptors (Miller and Hsu, 1992). Inhibitors of adenosine uptake through *es* transporters may be neuroprotective in cerebral ischemia by potentiating endogenous adenosine levels, which can rise up to 100-fold during periods of reduced ATP synthesis. The neuroprotective effects of the drug propentofylline in ischemic models have been attributed, at least in part, to its ability to block *es* adenosine transport (Parkinson *et al.*, 1994). NBMPR is a more potent and selective *es* transport inhibitor that has recently been found to cross the blood-brain barrier in rats (Anderson *et al.*, 1996b). Cortical NBMPR administration improved post-ischemic hypoperfusion in pigs (Gidday *et al.*, 1996). Further success with NBMPR in animal ischemic models along with our data showing a wide regional and cellular distribution of rENT1 will support the development of *es* transport inhibitors as neuroprotective agents in cerebral ischemia.

Besides neuroprotection and ethanol-induced motor incoordination, adenosine has been implicated in many CNS processes including apoptosis, antinociception, synaptic plasticity and sleep. The present study suggests that rENT1 is a major contributor to adenosine regulation in brain regions responsible for these effects.

[3]Chapter 4

Distribution of mRNA encoding a nucleoside transporter insensitive to inhibition by nitrobenzylthioinosine (ENT2) in rat and human brain

Summary

Nucleoside transporters may play a role in regulating levels of extracellular adenosine and adenosine receptor activity. Two members of the equilibrative nucleoside transporter family have recently been cloned. ENT1 is potently inhibited by nitrobenzylthioinosine (NBMPR) ($K_i \approx 1$ nM) and was previously found to have a wide distribution in rat and human brain. ENT2 is insensitive to inhibition by NBMPR at low nanomolar concentrations and there is little previous data describing its distribution in the CNS. The present study examined the expression of ENT2 in rat and human brain. Northern analysis using a 178-bp cDNA probe from hENT2 gave 2 hybridization signals of about 1 kb and 4.4 kb in every region examined. RT-PCR showed the expected 178-bp product in primary cultures of both human neurons and astrocytes. RT-PCR for rENT2 in dissected rat brain regions showed a 211-bp band in each region tested. *In situ* hybridization revealed a strong hybridization signal in regions including hippocampus, cortex and cerebellum. Evidence that astrocytes contain mRNA for rENT2 was provided by hybridization in molecular and some subpial layers of the brain. Our results indicate a wide cellular and regional distribution for ENT2 in both rat and human brain, similar to ENT1, indicating that control of adenosine levels in brain is achieved by multiple transport processes.

[3] Anderson, C.M. *et al.* (1998) Manuscript in preparation.

Introduction

Adenosine is a ubiquitous purine nucleoside and an important inhibitory neuromodulator in the CNS. Actions of adenosine at its four identified plasma membrane receptors are implicated in processes as diverse as antinociception, sleep and synaptic plasticity (Guieu *et al.*, 1997). Because of the wide range of effects of adenosine in the CNS, processes that control endogenous adenosine levels are important and may be considered as a therapeutic targets to enhance adenosine receptor stimulation.

Transport of adenosine across plasma membranes is an important determinant of extracellular endogenous adenosine levels and, therefore, of the degree of adenosine receptor stimulation. Nucleoside transport processes are membrane-bound proteins that mediate nucleoside influx and/or efflux. Two broad categories of nucleoside transporters (NTs) exist: concentrative and equilibrative. Concentrative transporters are proteins that mediate the influx of nucleosides coupled to the inward movement of Na^+ ions. At present, two members of the concentrative NT gene family have been cloned, CNT1 (concentrative, NT1; Huang *et al*, 1994; Ritzel *et al*, 1998), a pyrimidine nucleoside-selective NT, and CNT2 (Che *et al*, 1995; Yao *et al*, 1996), a purine nucleoside-selective NT. Equilibrative NTs are facilitated diffusion carriers that allow nucleosides to cross membranes in either direction according to their concentration gradients. Two equilibrative NT subtypes accepting both purine and pyrimidine nucleosides as well as a number of synthetic nucleoside analogs have been cloned and termed ENT1 (Griffiths *et al*, 1997a; Yao *et al*, 1997) and ENT2 (Griffiths *et al*, 1997b; Yao *et al*, 1997; Crawford *et al*, 1998). Functionally, ENT1 and ENT2 are differentiated based on their sensitivity to inhibition by the nucleoside analog nitrobenzylthioinosine (NBMPR). ENT1 is also

termed *es* (sensitive to low nanomolar concentrations of NBMPR) and ENT2 is also termed *ei* (insensitive to low nanomolar concentrations of NBMPR).

Both cloned concentrative NTs were detected in rat brain by RT-PCR (Anderson *et al*, 1996a) and ENT1 was detected in human brain by northern analysis and RT-PCR, and in rat brain by *in situ* hybridization and [^{3}H]NBMPR autoradiography (Anderson *et al*, submitted). Previously, detection of *ei* NTs in brain was accomplished by functional transport assays using radiolabeled nucleoside analogs in the absence of Na^+ ions and in the presence of enough NBMPR to inhibit *es* but not *ei* transporters. In addition, [^{3}H]dipyridamole autoradiography in species with high sensitivity of *ei* to dipyridamole, such as guinea pig and human, may be able to identify *ei* NTs (Deckert *et al*, 1987); as dipyridamole has low affinity for *ei* in rat, such experiments are not possible with this species. While functional studies in rat brain preparations have indicated a higher proportion of *ei* activity compared to *es* activity (Jones and Hammond, 1995), little is known about the regional or cellular distribution of *ei* NTs in rat and human CNS. The cloning of rat and human cDNAs for *ei* NTs (rENT2 and hENT2) has allowed such investigations and in the present study, we examined the regional and cellular distributions of ENT2 mRNA in rat and human CNS preparations.

Materials and Methods

Culture of human fetal neurons and astrocytes

For both neurons and astrocytes, brain specimens were obtained from fetuses of 14 to 15 weeks gestational age, with consent, from women undergoing elective termination of pregnancy. All protocols received approval from, and were performed in

accordance with, The University of Manitoba Committee for the Protection of Human Subjects and the Human Ethics Committee of the Health Sciences Center Hospital.

Cultures of human neurons were established as described previously (Magnuson *et al.*, 1995). Briefly, the cells were mechanically dissociated, suspended in OptiMEM with 5% heat-inactivated fetal bovine serum, 0.2% N2 supplement (GIBCO), and 1% antibiotic solution (penicillin G 10^4 units/ml, streptomycin 10 mg/ml, and amphotericin B 25 μg/ml in 0.9% NaCl) and plated in 75 cm^2 culture flasks. Cultures were maintained for at least 30 days, with fresh medium added every 3-4 days, prior to RNA isolation. These cultures were >70% neurons as determined by immunostaining for the neuronal marker microtubule-associated protein 2 (MAP-2).

For human fetal astrocytes, cells were mechanically dissociated, centrifuged at 270 x *g* for 10 min, resuspended in Dulbecco's modified Eagle's medium (DMEM) containing 10% fetal calf serum (FCS), 1.0% L-glutamine and 0.2% antibiotic solution consisting of 1000 units/ml penicillin G, 10 mg/ml streptomycin and 25 μg/ml amphotericin B in 0.9% NaCl, and grown in 75 cm^2 culture flasks in 5% CO_2 at 37°C. Fresh media was added every 3-4 days. Seven-day-old cultures were placed on a rotary shaker for 2 h at 333 rpm at room temperature (25°C). Supernatants were discarded and the remaining cells were exposed to 0.05% trypsin and 0.53 mM EDTA. Cells were collected, centrifuged at 270 x *g* for 10 min, resuspended in DMEM containing 10% FCS and placed into 75 cm^2 culture flasks. After 30 min, decanted cells were plated and allowed to grow to confluency for RNA isolation. These cells were >98% astrocytes as determined by immunostaining for glial fibrillary acidic protein (GFAP; Chemicon).

Reverse Transcriptase PCR

Total RNA was isolated from rat cortex, cerebellum, striatum, hippocampus and superior colliculus using the SNAP RNA isolation kit (Invitrogen) and treated with DNase I. Oligo$(dT)_{12-18}$ primer (300 ng) was annealed to the mRNA template (5 μg) and cDNA synthesis proceeded at 37°C for 60 minutes using 3 mM dNTPs, 6.7 μM dithiothreitol (DTT) and either 3.3 Units reverse transcriptase or 1μl H_2O in 60 μl of buffer containing 50 mM Tris-HCl (pH 8.3), 75 mM KCl, 3 mM $MgCl_2$.

For polymerase chain reaction cDNA template solutions (2 μl) were amplified in a mixture containing 200 μM dNTPs, 2 mM $MgCl_2$, 1 μM each of the 5' and 3' primers and 2.5 Units Taq DNA polymerase (Gibco/BRL) in a total volume of 100 μl. The amplification consisted of 30 cycles of: 30 s. at 94°C, 30 s. at 56°C and 1 min. at 72°C. A final 10 min. 72°C elongation step followed and samples were frozen or analyzed immediately by electrophoresis on a 1.0% agarose gel. DNA bands were viewed and photographed under UV light following ethidium bromide staining.

A 178-bp fragment of hENT2 from bases 729 to 906 (Griffiths *et al*, 1997b) was amplified using the 5' primer 5'-CCAGTCTGATGAGAACGGGATTC-3' and the 3' primer 5'-GAAGACCAACACAAGGCACAGC-3'. rENT2 was amplified using the 5' primer 5'-CTGGAAGTTTGCCCGTTAC-3' and the 3' primer 5'-CGACAAAGACCGAAGGTT-3' to produce a 211-bp fragment from bases 800 to 1010.

The presence of mRNA for glyceraldehyde-3-phosphate dehydrogenase (GAPDH), a ubiquitous housekeeping gene, was used to verify the quality of cDNA preparations, and was detected using the 5' primer 5'-GCTGGGGCTCACCTGAAGGG-3' and the 3' primer 5'-GGATGACCTTGCCCACAGCC-3' to amplify a 343-bp DNA product (bases 346 to 688) from the rat GAPDH cDNA (Tso et al., 1985).

other cloned member of the ENT gene family. The search also failed to detect any other cloned rat sequence. This product was ligated into the pCR-Script Direct plasmid vector (Stratagene) to produce a directional clone such that *in vitro* transcription with T3 RNA polymerase produced a sense riboprobe while T7 RNA polymerase gave an antisense riboprobe. The Ambion Maxiscript kit was used to transcribe RNA from linearized/proteinase K-treated templates. Transcription proceeded for 60 minutes at 37°C with 0.5 mM each of ATP, GTP and CTP, 10 mM dithiothreitol (DTT), 400 μCi [α-^{35}S]UTP (NEN) and 0.5 Units T3 or T7 RNA polymerase in a total volume of 20 μl. Labeled RNA probes were ethanol precipitated, resuspended in solution containing 10 mM Tris-HCl (pH 8.0), 1 mM EDTA, 10 mM DTT and 1% SDS, and counted for ^{35}S content.

Hybridization was performed overnight at 55°C in a Microprobe hybridizer (Fisher). Hybridization solution contained 50% (v/v) formamide, 10% (w/v) dextran sulfate, 0.3 M NaCl, 1X Denhardt's solution, 10 mM Tris-HCl (pH 8.0), 1 mM EDTA, 100 μg/ml denatured salmon sperm DNA, 0.5 mg/ml yeast tRNA and 10 mM DTT. Riboprobes were added to a concentration of 5 x 10^6 cpm/ml hybridization solution. Following hybridization sections were treated with RNase A (20 μg/ml) and washed with increasing temperature and decreasing salt concentration to a final wash for 30 minutes at 60°C in 0.1x SSC with 50 mM DTT. Sections were dehydrated in preparation for emulsion or film autoradiography. For film autoradiography, sections were exposed to Amersham Hyperfilm-βmax for 14 days and developed using Kodak D-19 developing solution. For emulsion autoradiography, slides were dipped in Kodak NTB-2 autoradiographic emulsion for 14 days and developed using a 1:1 dilution of Kodak D-19 developer. Sections were then counter-stained with the nuclear stain hematoxylin.

Results

Identification of hENT2 RNA in human brain

A random-primed, ^{32}P-labeled 178-bp cDNA from the large intracellular loop between transmembrane domains 6 and 7 (bases 729-906) of hENT2 was used to probe a human brain northern blot with poly(A)$^+$ RNA from multiple regions. Two major bands were obtained in all brain regions tested (Fig. 13*A*). The major RNA species was approximately 1 kb in length and an average 18-fold more abundant than the other RNA band which appeared at 4.4 kb. A third faint band at 2.6 kb was detected in all tissues as well. The relative abundances of both major bands were determined by densitometry with Kodak 1D software. Numbers in brackets indicate intensity (corrected for background) relative to β-actin. For the 1 kb band, the order of intensity was hippocampus (1.26) > subthalamic nucleus (1.11) > caudate nucleus (1.03) > amygdala (0.98) > thalamus (0.96) > corpus collosum (0.88) > substantia nigra (0.74). For the 4.4 kb band, the order was hippocampus (0.15) = thalamus (0.15) > amygdala (0.12) > subthalamic nucleus (0.11) > substantia nigra (0.061) > caudate nucleus (0.023) > corpus collosum (0.019).

RT-PCR was performed with total RNA isolated from human fetal neurons and astrocytes. A product of 178-bp was expected and was seen in both cell types (Fig. 13*B*). A second product of about 380-bp was also detected. These data indicate that hENT2 mRNA is present in both astrocytes and neurons in a wide variety of brain regions.

Regional identification of rENT2 in rat brain by RT-PCR

RT-PCR was performed with total RNA isolated from various regions of rat brain using primers specific for rENT2. The expected 211-bp product was detected in all regions tested including cerebral cortex, cerebellum, hippocampus, striatum and superior colliculus (Fig. 14). The presence of a 350-bp product for the housekeeping gene GAPDH was used to verify the quality of RNA preparations for RT-PCR. Relative intensities of the 211-bp bands standardized against the appropriate GAPDH bands were measured and found to be high in superior colliculus (1.0), moderate in hippocampus (0.78) and cerebral cortex (0.73) and low in striatum (0.63) and cerebellum (0.59).

Distribution of rENT2 mRNA in rat brain using in situ hybridization

Sense and antisense ^{35}S-labeled cRNA probes were synthesized from linearized plasmids containing a 211-bp cDNA insert from rENT2 and used in *in situ* hybridization with frozen coronal rat brain sections (14 μm). In general, a strong hybridization signal was detected throughout rat brain with the antisense riboprobe while sense probes exhibited only low levels of hybridization.

In hippocampus, strong labeling was seen in the granule cells of the dentate gyrus and pyramidal cells (Fig. 15). The dentate gyrus molecular layer and stratum radiatum displayed a moderate hybridization signal. In cerebellum, the most prominent signal was in the granule cells (Fig. 16). In a minority of animals, Purkinje cells were more densely labeled than granule cells (not shown), suggesting there may be variability among animals in rENT2 expression in these cells. rENT2 antisense cRNA probes bound to virtually all cells of the cerebral cortex (Fig. 17), showing rENT2 to be nearly ubiquitous

A, A poly(A)$^+$ RNA northern blot for multiple regions of human brain was probed with a radiolabeled 178-bp fragment of rENT2 unique from rENT1. Two RNA species were detected with the major band appearing at about 1 kb and a less intense band at 4.4 kb. β-actin was detected at 2.0 kb. Am, amygdala; CN, caudate nucleus; CC, corpus collosum; Hp, hippocampus; WB, whole brain; Sg, substatia nigra; SN, subthalamic nucleus; Th, thalamus. B, RT-PCR was performed with hENT2-specific primers using total RNA (5 μg) from cultured human fetal astrocytes and neurons. The expected band corresponding to hENT2 is 178-bp and was present in both cell types. A second product of about 380-bp was also amplified. No product was amplified from samples not treated with reverse transcriptase (RT).

Figure 13: Regional and Cellular Distribution of mRNA for hENT2 in Human Brain

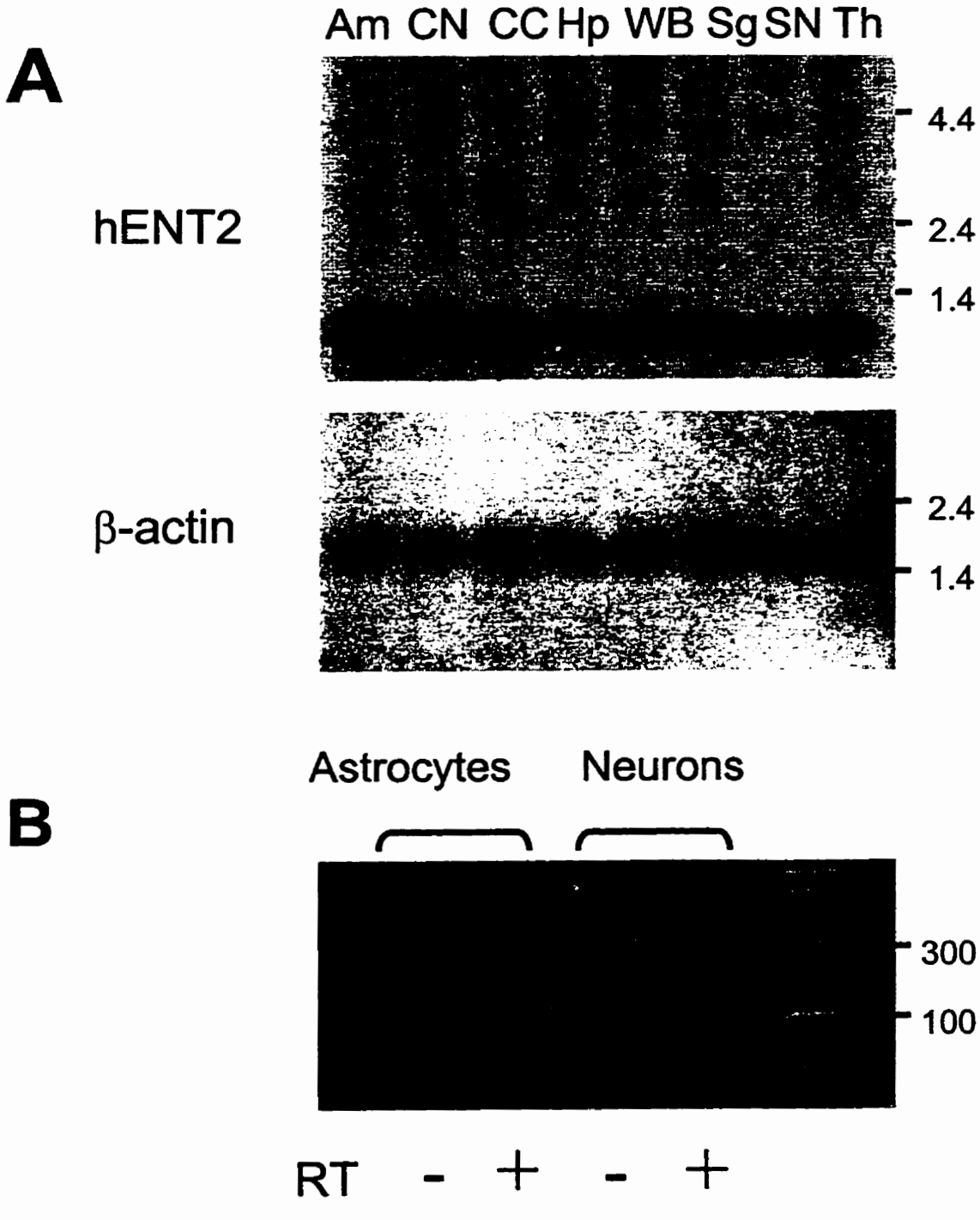

Figure 14: Regional Distribution of rENT2 mRNA in Rat Brain

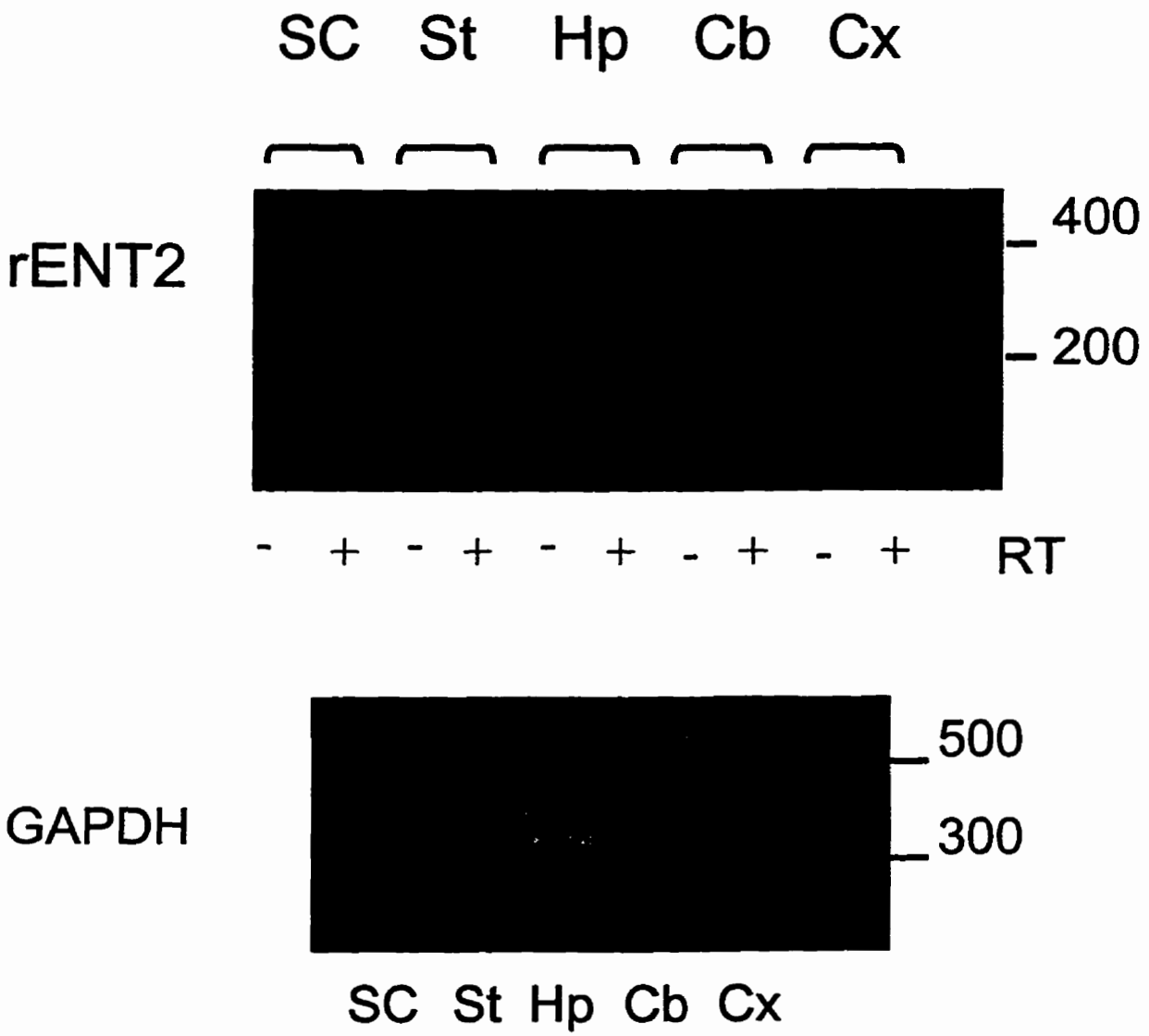

Total RNA was isolated from superior colliculus (SC), striatum (St), hippocampus (Hp), cerebellum (Cb) and cerebral cortex (Cx), and subjected to RT-PCR with primers specific for rENT2. The expected product of 211-bp was seen in all regions tested. No product was seen in samples not treated with reverse transcriptase (RT) indicating good RNA quality.

Sense and antisense cRNA probes were transcribed from a 211-bp cDNA fragment of rENT2 ligated into the PCR-Script direct vector and were hybridized to 14 μm fresh frozen coronal rat brain sections. A and B represent results of in situ hybridization obtained with the sense cRNA probe for rENT2 while C and D are results with the antisense probe (20x magnification). Nuclei were stained with hematoxylin as seen in bright-field images A and C. B and D are dark-field images in which cRNA probes are detected by silver grains which appear white. Note the broad neuronal distribution of rENT1 mRNA in hippocampus as indicated by a strong hybridization signal for the antisense cRNA probe (D). Signal was also seen in the dentate gyrus molecular layer (ML) and stratum radiatum (SR). The sense probe did not produce a hybridization signal (B). DG, dentate gyrus; CA1, CA1 subfield; CA3, CA3 subfield.

Figure 15: Distribution of rENT2 mRNA in Rat Hippocampus

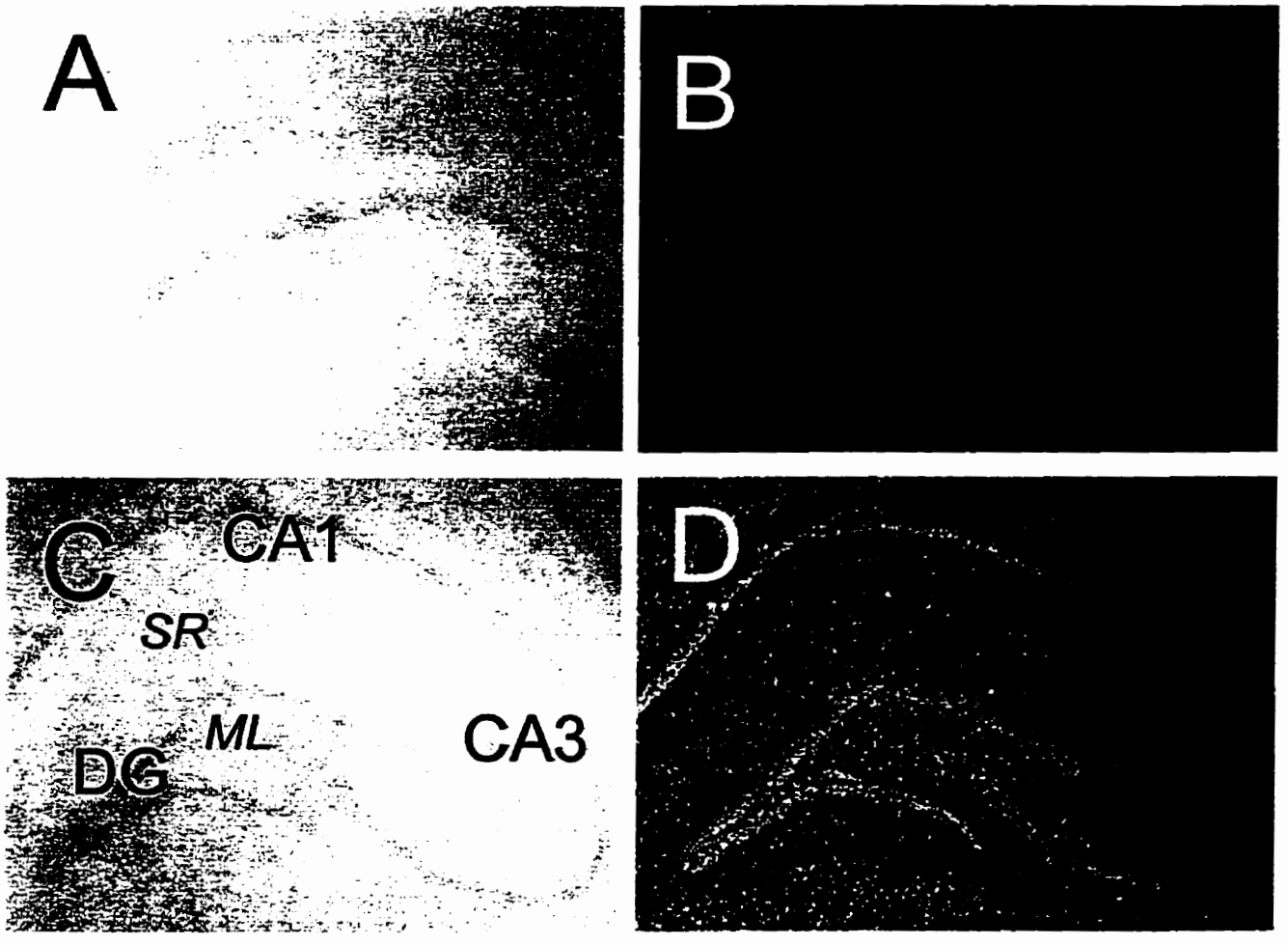

Sense and antisense cRNA probes were transcribed from a 211-bp cDNA fragment of rENT2 ligated into the PCR-Script direct vector and were hybridized to 14 μm fresh frozen coronal rat brain sections. Nuclei were stained with hematoxylin as seen in bright-field images A and C. B and D are dark-field images in which cRNA probes were detected by silver grains, which appear white. A and B represent results of in situ hybridization obtained with the sense cRNA probe for rENT1 in cerebellum while C and D are results with the antisense probe in cerebellum (100x magnification). The Purkinje (Pk) and granule cell layers (Gr), as well as the molecular layer (ML), all displayed specific antisense probe binding (D). Sense probe binding was negligible (B).

Figure 16: Distribution of rENT2 mRNA in Rat Cerebellum

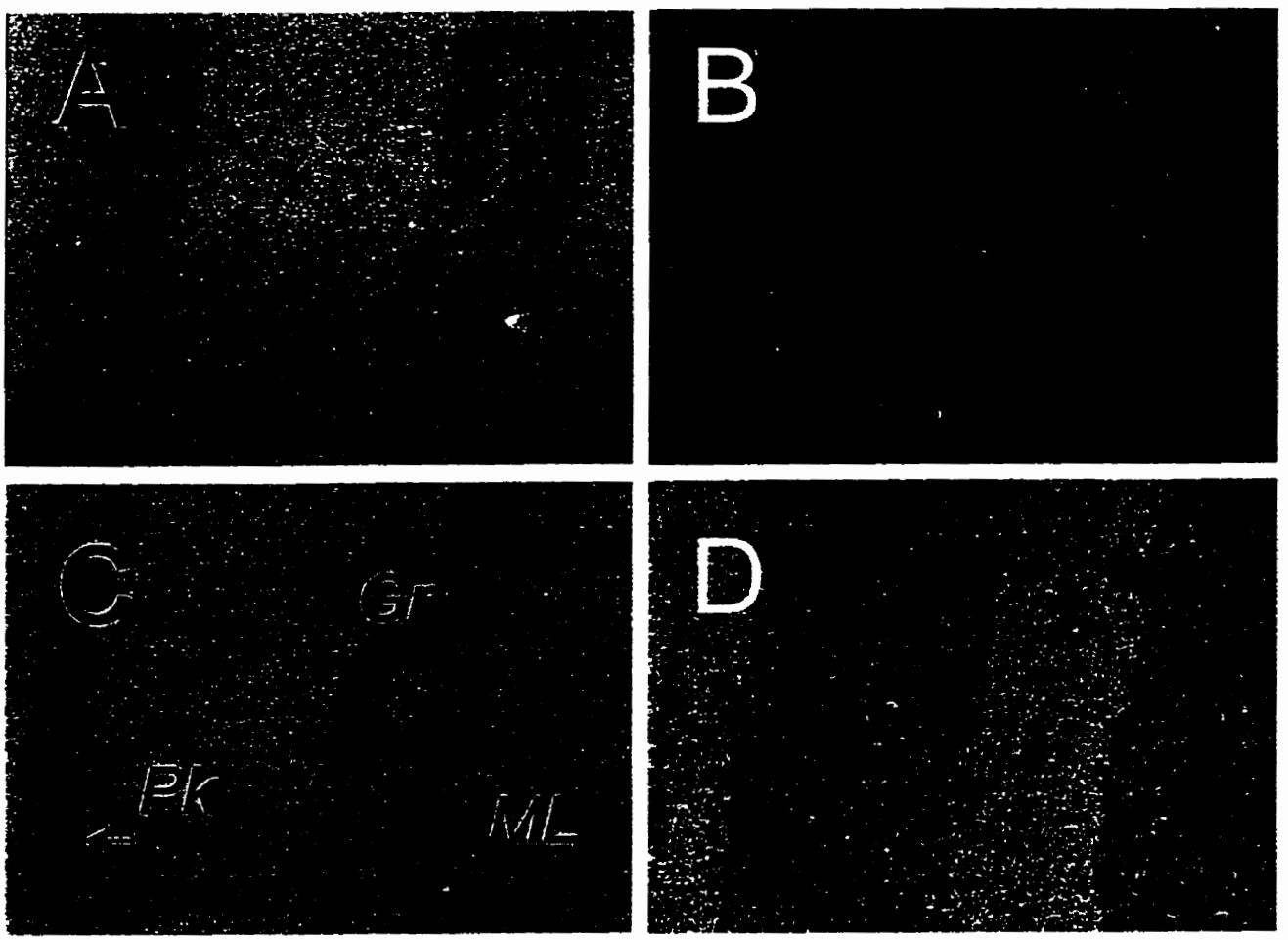

Figure 17: rENT2 mRNA in Cerebral Cortical Cells

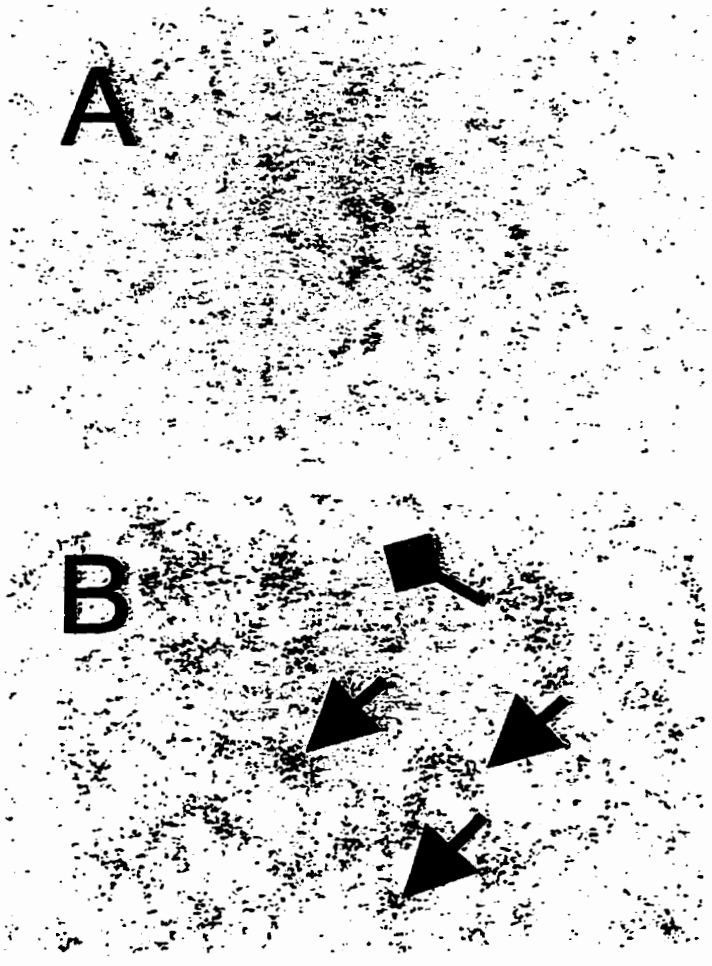

A represents sense probe treatment and B represents antisense probe treatment of cerebral cortical sections (400x magnification). Silver grains appear black and indicate that approximately 80-90% of neurons in the cerebral cortex contain mRNA for rENT2. Sense probe binding was negligible (B). In B, arrowheads indicate rENT2-positive cells while the diamond-shaped head shows an rENT2-negative cell.

throughout the layers of the cortex. Similar results were seen in thalamus and striatum (not shown).

rENT2 was detected in non-neuronal cell types in rat brain as well. Signal was seen in the molecular layers of the dentate gyrus and cerebellum as well as in some subpial layers, suggesting the presence of rENT2 in astrocytes, in agreement with human RT-PCR data. rENT2 was also detected in arterial walls within brain tissues (Fig. 18*A,B*). As well, choroid plexus, a highly vascularized tissue responsible for regulating cerebrospinal fluid (CSF) composition, displayed a strong hybridization signal for rENT2 (Fig. 18*C-F*); thus, rENT2 may play a role in regulating nucleoside concentrations in CSF.

Discussion

We have shown that ENT2, or *ei* NTs have a wide distribution in rat and human brain. A poly(A)$^+$ RNA northern blot of different regions of human brain probed with a 178-bp cDNA from a region unique to hENT2 indicated that hENT2 is present throughout the brain. RT-PCR showed the expected 178-bp product in both neurons and astrocytes. *In situ* hybridization and RT-PCR in rat brain both indicated a wide regional and cellular distribution for rENT2, in agreement with the data for hENT2. rENT2 appeared to be expressed in a wide variety of cell types including neurons, astrocytes, smooth muscle cells and possibly choroid plexus epithelial cells. Only about 10% of cells in the rat cerebral cortex and striatum did not express rENT2.

In the absence of selective ligands or specific antibodies, the cloning of ENT2 from rat and human provided the first specific probes for these transporters. A previous report found 2.6 kb transcripts when using a full-length hENT2 cDNA to probe a

multiple tissue human northern blot (Crawford *et al*, 1998). The same study found the predominant hybridization signal to be at approximately 4 kb. Our results support this finding as we found that this band is more prominent than the 2.6 kb band which appeared only very faintly on our blot. There is a slight discrepancy in the size we report (4.3-4.4 kb) compared with that of Crawford *et al.* (4 kb). By far the most intense hybridization signal appeared on our blot between 0.8 and 1 kb. This is likely a transcript encoding the 326 residue HNP36 protein, a growth factor-induced delayed early response gene of unknown function that uses an initiation codon downstream to that used for full-length ENT2. Uridine uptake assays showed that only the full-length ENT2, and not the truncated HNP36, possessed nucleoside transport activity (Crawford *et al.*, 1998). A sequence homology search for our hENT2 probe did not detect hENT1 confirming that we were not seeing signal from the other cloned member of the ENT gene family. Alternatively this 1 kb band could be a degradation product, although that is unlikely because there was no evidence of degradation of the β-actin mRNA.

RT-PCR in human fetal neurons and astrocytes produced the expected 178-bp product. The neuron preparation, however, contained 10-20% astrocytes so we can only definitively conclude that hENT2 is present in astrocytes, which were not contaminated with neurons. A second product of about 380-bp was amplified as well. The origin of this product is not known. It is not likely that it is derived from hENT1 since the PCR primers were chosen to minimize this likelihood. It is possible that there is an alternatively spliced mRNA from the same gene as the cloned hENT2. Because this band

Sense and antisense cRNA probes were transcribed from a 211-bp cDNA fragment of rENT2 ligated into the PCR-Script direct vector and were hybridized to 14 μm fresh frozen coronal rat brain sections. Nuclei were stained with hematoxylin as seen in bright-field images A, C, and E. B, D, F and G are dark-field images in which cRNA probes were detected by silver grains, which appear white. C and D show the hybridization signal after in situ hybridization with the antisense cRNA probe for rENT2 in choroid plexus sections. A and B received the sense probe and displayed no appreciable signal (100x magnification). A strong antisense hybridization signal was seen in arterial walls (G) while sense binding was negligible (E, F) (100x magnification).

Figure 18: Distribution of rENT2 mRNA in Rat Cerebral Arteries and Choroid Plexus

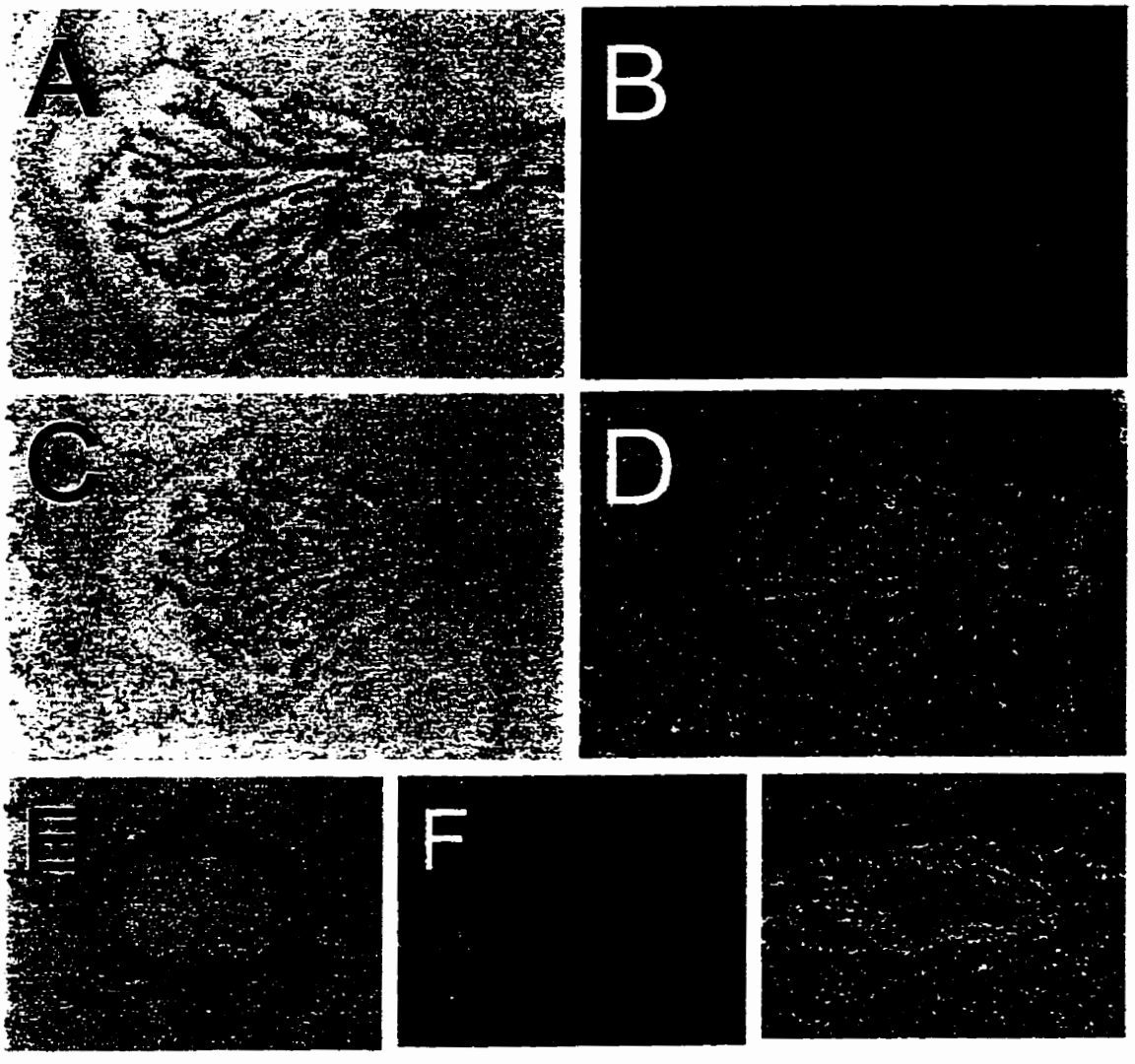

was not amplified from samples not treated with reverse transcriptase, we can conclude that the unknown band is not due to contaminating genomic DNA.

In agreement with RT-PCR in cultured human fetal astrocytes, *in situ* hybridization indicated the presence of rENT2 in brain regions rich in astrocytes such as cerebellar and hippocampal molecular layers and subpial layers. Co-staining with glial fibrillary acidic protein (GFAP) is required to confirm this finding.

Our study found hENT2 transcript in total RNA isolated from cultured human neurons and astrocytes and supported a similar distribution of rENT2 in rat brain. This is in agreement with previous studies in rat cortical synaptosomes (Lee and Jarvis, 1988a; Gu and Geiger, 1992) and human astrocytes (Gu *et al.*, 1996), all of which found significant levels of NBMPR-insensitive nucleoside uptake in the absence of Na^+ ions. *In situ* hybridization indicated that about 90% of cells in the cortex had message for rENT2. This is greater than the 50% reported for rENT1 (Anderson *et al.*, submitted) and suggests that rENT2 is the predominant nucleoside transport process in rat brain. This has been reported previously in functional studies as well. For example, Lee and Jarvis (1988a) found 60% of equilibrative [^{14}C]uridine uptake to be through *ei* type NTs in cerebral cortical synaptosomes from rat. This *es*:*ei* ratio appears to be species-dependent however, as rabbit cortical synaptosomes exhibited 65% *es* activity (Jones and Hammond, 1995). Human brain also has higher *es* activity than *ei* while guinea pig closely resembles rat in that *ei* predominates.

This is the first study to report the distribution of *ei* NTs in human or rat brain. We have found a widespread distribution of ENT2 throughout the brain of both species including regions known to express adenosine receptors richly. It is possible that rENT2

is important in the regulation of extracellular adenosine levels and therefore the degree of adenosine receptor stimulation. As stated, functional assays in brain tissues have detected adenosine transport activity *via ei* transporters. In addition, there have been many reports describing effects of dipyridamole, a non-selective inhibitor of *ei*, on adenosine receptor activation in brain. Because dipyridamole also inhibits *es* transporters, a function for *ei* is not yet clear. Its identity to HNP36 may mean that ENT2 is a delayed early response gene product. Selective inhibitors or strategies to determine function, such as ENT2 knockouts or antisense knockdowns, are required to clarify further the role of ENT2 in brain.

[4]Chapter 5

Demonstration of the existence of mRNAs encoding the N1/*cif* (CNT2) and N2/*cit* (CNT1) concentrative nucleoside transporters in rat brain

Summary

Nucleoside transport may be involved in the regulation of extracellular levels of adenosine, an inhibitory neuromodulator in the central nervous system. At least two functionally distinct equilibrative (Na^+-independent) nucleoside transport processes are present in rat brain. In addition, Na^+-dependent, or concentrative, nucleoside transport in rat brain has also been documented. Recently, two Na^+/nucleoside cotransporter cDNAs were cloned. A cDNA encoding a pyrimidine-selective nucleoside transporter (rCNT1) was cloned from rat jejunum and subsequently, a purine-selective transporter cDNA (rCNT2) was isolated from rat liver. In the present study we tested various regions of rat brain including choroid plexus, posterior hypothalamus, hippocampus, striatum, superior colliculus, cortex, brain stem and cerebellum for the presence of mRNA for rCNT1 or rCNT2. Total RNA was isolated and reverse transcriptase polymerase chain reaction (RT-PCR) was performed using primers designed to amplify the rCNT1 nucleotide sequence from base 1593 to 1911 (309-bp) or the rCNT2 nucleotide sequence from base 1228 to 1462 (235-bp). Agarose gel electrophoresis of rCNT1 RT-PCR products indicated a product of the expected size in all brain tissues investigated. Southern blot analysis, restriction digests and cDNA sequencing confirmed that these products were derived from rCNT1 mRNA. Agarose gel electrophoresis of rCNT2 RT-PCR reactions indicated products of the predicted size in all brain regions tested. The sequence of this product was identical to that of bases 1228 to 1462 of the rCNT2 sequence.

---

[4] Anderson CM *et al.* (1996) Demonstration of the existence of mRNAs encoding N1/*cif* and N2/*cit* sodium/nucleoside cotransporters in rat brain. Mol Brain Res 42:358-361.

These experiments demonstrate the presence of both rCNT1 and rCNT2 mRNA in rat brain and suggest that at least two functionally distinct Na^+-dependent nucleoside transporters are present in brain.

Introduction

Nucleoside transport processes are membrane-bound carrier proteins that mediate the transfer of nucleosides across biological membranes. At present, seven nucleoside transporter subtypes have been characterized (for review see Cass, 1995). These have been broadly divided into equilibrative/Na^+-independent and concentrative/Na^+-dependent transporters. Equilibrative transporters are further classified into *es* and *ei*, based on sensitivity or insensitivity, respectively, to inhibition by nanomolar levels of the nucleoside analog nitrobenzylthioinosine (NBMPR) (Vijayalakshmi and Belt, 1988). Five Na^+-dependent transporters have been identified to date and are primarily distinguished by permeant selectivity. N1/*cif* transporters are purine-selective, N2/*cit* and N4/*cit* are pyrimidine-selective, and N3/*cib* and N5/*cs* accept both purines and pyrimidines as permeants (Cass, 1995).

Nucleoside transport processes are important components of nucleoside salvage pathways, providing cells with nucleosides that are required for cellular metabolism. In addition, adenosine is an endogenous nucleoside with inhibitory neuromodulatory effects in the central nervous system (CNS) (Fredholm and Hedqvist, 1980; Snyder, 1985). The CNS actions of adenosine are mediated by A_1 and A_2 plasma membrane receptors and adenosine levels in brain are regulated by metabolism and by nucleoside transport processes (Geiger and Fyda, 1991).

Na^+-dependent nucleoside transport in dissociated brain cells (Johnston and Geiger, 1989) as well as in brain stem and choroid plexus (Bender *et al.*, 1994; Bender *et al.*, 1981; Lawrence *et al.*, 1994; Spector and Huntoon, 1984; Wu *et al.*, 1992) has been

reported. To date, there have been no data describing specific Na^+-dependent nucleoside transporter subtypes in brain other than the observation of broadly-selective, N3/*cib* activity in rabbit choroid plexus (Wu *et al.*, 1992). A pyrimidine-selective, N2/*cit* transporter cDNA was recently cloned from rat jejunum epithelium by expression screening in *Xenopus* oocytes and termed rCNT1 (Huang *et al.*, 1994). Subsequently, a cDNA encoding an N1/*cif* transporter, termed rCNT2, or SPNT, was isolated from rat jejunum (Yao *et al.*, 1996) and bile canalicular membranes (Che *et al.*, 1995), respectively. rCNT2 has 64% amino acid identity to rCNT1, indicating that the two Na^+-dependent transporters are from the same gene family. In the present study, we have used reverse transcriptase polymerase chain reaction (RT-PCR) to demonstrate the presence of mRNAs for both rCNT1 and rCNT2 in rat brain.

Materials and Methods

Isolation of Total RNA

Male, Sprague-Dawley rats weighing 250-300 g were used in this study. The animals were obtained from The University of Manitoba Central Animal Care facility, Winnipeg, Canada.

Animals were sacrificed by decapitation, dissections proceeded on ice, and all tissues were immediately frozen on dry ice to minimize RNA degradation by endogenous ribonucleases. The guanidinium isothiocyanate method (Chomczynski and Sacchi, 1987) was used to isolate total RNA from rat jejunum, cerebral cortex, cerebellum, striatum, hippocampus, superior colliculus, brain stem, choroid plexus, and posterior hypothalamus. Briefly, frozen tissues were placed in 4 M guanidinium isothiocyanate (GIBCO) containing 0.1 M β-mercaptoethanol (Sigma), and homogenized. Total RNA was extracted in the aqueous phase from the homogenate following the addition of 2 M sodium acetate (pH 4.0) and phenol:chloroform (5:1) (Sigma). RNA was precipitated

with isopropanol (Sigma, USA), resuspended in denaturing solution and re-precipitated for increased purity. The pellet was washed in 75% ethanol, resuspended in an appropriate volume of diethylpyrocarbonate (DEPC) treated distilled de-ionized water, and stored at -80°C. The concentration of RNA was determined by spectrophotometric absorbance at 260 nm and its purity was assessed from the ratio of its absorbance at 260 nm to that at 280 nm; all ratios were greater than 1.7. Structural integrity was monitored by agarose gel electrophoresis.

Northern and Southern Blots

For northern blots, 10 μg of total RNA from each tissue or brain region was run on a denaturing 1.0% agarose (Promega) gel with 18% formaldehyde (Sigma, USA). Gels were stained with ethidium bromide (0.2 μg/ml) (Sigma) and photographed under ultraviolet light. Gels were soaked in 0.05 N NaOH for 20 minutes and 20x SSC (3 M sodium chloride, 0.3 M sodium citrate, pH 7.0) for 45 minutes and RNA was transferred to GeneScreen™ nylon membranes (DuPont/NEN). RNA was fixed to membranes by baking at 80°C. Membranes were prehybridized for 3 hours at 42°C in 50% formamide (Boehringer Mannheim, Canada) solution containing 5x Denhardt's solution (Sigma), 5x SSC, 1% sodium dodecylsulfate (SDS) (Boehringer Mannheim), and 100 μg/ml denatured salmon testis DNA (Sigma). Following overnight hybridization in the presence of random primed, ^{32}P-labeled denatured cDNA probes, membranes were washed with high stringency for 90 minutes at 68°C in 0.2x SSC/0.1% SDS solution and placed on Kodak XAR X-ray film in a cassette with intensifying screen at -80°C for 48 hours.

For Southern blots, gels were stained with ethidium bromide and photographed. They were treated with 0.5 N NaOH/1.5 M NaCl denaturing solution for 45 minutes then neutralized in 1 M Tris-Cl (pH 7.4) for a further 45 minutes. The transfer of DNA to

nylon membranes, hybridization of cDNA probes, washing of membranes and autoradiography proceeded as described above for northern blots.

Reverse Transcriptase Polymerase Chain Reaction (RT-PCR)

Total RNA from jejunum, cerebral cortex, cerebellum, brain stem, hippocampus and striatum was treated with 0.005 μg/μl DNase I (Pharmacia) in the presence of 10 mM $MgCl_2$, 1 mM dithiothreitol (Boehringer Mannheim) and 0.025 units/μl ribonuclease inhibitor (Promega). The resulting mixture was extracted with phenol:chloroform (5:1) and precipitated with 0.1 volume 3 M sodium acetate (pH 5.2) and 2.5 volumes 100% ethanol. DNase treatment was not performed with RNA from choroid plexus, posterior hypothalamus or superior colliculus due to the limited quantities of RNA obtained. Total RNA (DNase I treated or untreated) from each tissue (10 μg) was reverse transcribed. Briefly, RNA was annealed to 100 ng/μl oligo(dT) primer (Stratagene) and treated with Moloney murine leukemia viral reverse transcriptase (1 unit/μl) (GIBCO) in the presence of 6.7 mM dithiothreitol and a 4 mM dNTP mixture. The resulting first strand cDNA (3 μl) was added to 200 μM dNTP mixture, 1.5 mM $MgCl_2$, 1 μM of each primer and 2.5 units of Taq DNA polymerase (GIBCO). PCR consisted of an initial 5 minute denaturing step (94°C), followed by a 5 minute primer annealing step (54°C) and 30 cycles of: 30 sec. at 94°C, 30 sec. at 55°C and 1 minute at 72°C. A final 10 minute elongation step (72°C) was performed and the samples were cooled to -9°C. The resulting amplified DNA (25 μl) was run on a 1.2% agarose gel. rCNT1 product gels underwent Southern blot analysis. In control reactions that were not treated with reverse transcriptase, all steps were the same except sterile, DEPC-treated water was added in place of reverse transcriptase. For some experiments, RNase A (~15 μg/μl) was added to RNA samples, prior to RT-PCR, in order to verify an mRNA origin of products.

PCR Primers and cDNA Probes

Rat rCNT1 cDNA was detected using the 21-mer 5' primer 5'-CCGGTAGTGGC-TGAGTTGCTG-3' and the 21-mer 3' primer 5'-ACAGGCGTTTAGCAGGGACAC-3' to amplify a 309-bp DNA product (bases 1593 to 1911) of rCNT1. This was detected on Southern blots with a 612-bp (bases 1309 to 1920) ^{32}P-labeled rCNT1 cDNA probe (Huang *et al.*, 1994) isolated from the plasmid pBluescript (Stratagene) by restriction digestion with the enzymes Acc I and BamH1 (both from GIBCO).

Rat rCNT2 cDNA was detected using the 20-mer 5' primer 5'-TCTGCTCATCC-GTCCCTACC-3' and the 22-mer 3' primer 5'-CTTCACTCCCTCCTTGCTCTTG-3' to amplify a 235-bp DNA product (bases 1228 to 1462) of SPNT. A second 19-mer sense primer with sequence 5'-ACTTCTGTGAAAGACTTCA-3' was used with the 3' primer to amplify a 1468-bp product (bases 1228 to 2694).

The presence of mRNA for glyceraldehyde-3-phosphate dehydrogenase (GAPDH), a ubiquitous housekeeping gene, was used to verify the quality of cDNA preparations and was detected using the 20-mer 5' primer 5'-GCTGGGGCTCACCTGA-AGGG-3' and the 20-mer 3' primer 5'-GGATGACCTTGCCCACAGCC-3' to amplify a 343-bp DNA product (bases 346 to 688) from the rat GAPDH cDNA (Tso *et al.*, 1985).

rCNT1 and rCNT2 PCR primers were synthesized by the GIBCO Custom Primers Laboratory. GAPDH primers were synthesized by The University of Manitoba Oligonucleotide Synthesis Facility.

RT-PCR Product Sub-cloning and Sequencing

Polymerase chain reaction was performed as described above. Products were run on 1.2% agarose gels, viewed by ethidium bromide staining and bands of interest were excised from the gels. Gel slices were immediately frozen at -80°C, then thawed and centrifuged at 13,000 x *g* for 15 minutes. Supernatants were collected and DNA was

precipitated with 95% ethanol following extraction with chloroform:isoamyl alcohol (24:1).

The pCR-Script™ cloning kit (Stratagene) was used to sub-clone the PCR products. Gel-purified RT-PCR products amplified from cortex RNA were blunted with *Pfu* DNA polymerase (Stratagene) and ligated into the Srf I restriction site of the pCR-Script vector, as per the manufacturer's protocol. Transformation into *E. coli* was performed and cells with inserted PCR products were selected as white or light blue, ampicillin-resistant colonies on LB-agar plates treated with isopropyl-β-D-thio-galactopyranoside (IPTG), 5-bromo-4-chloro-3-indoyl-β-D-galactopyranoside (X-gal) (GIBCO) and ampicillin (50 μg/ml). Cells were grown to saturation in LB-broth containing ampicillin (50 μg/ml) and plasmids were isolated and purified with the Wizard ™ DNA clean-up system (Promega).

Purified plasmids were sequenced using both T7 and T3 sequencing primers by the DNA Sequencing Laboratory at the University of Alberta.

Results

RT-PCR with rCNT1 primers

No evidence for the presence of mRNA for rCNT1 in rat brain was found by northern analysis of total RNA (data not shown). Agarose gel electrophoresis indicated RT-PCR products of the expected size (309-bp) were amplified from RNA isolated from jejunum and rat brain regions. Southern blot analysis of these RT-PCR products using a ^{32}P-labeled 612-bp segment of rCNT1 revealed hybridization signals in all brain regions tested (Fig. 19*A*). Qualitatively, the strongest hybridization signals were seen with RT-PCR products from brain stem, choroid plexus, cortex and hippocampus while the weakest signals were observed with products from striatum and superior colliculus (Fig.

Total RNA was isolated from dissected rat brain regions and jejunum and treated with (Panel A) or without (Panel B) reverse transcriptase. Southern blot analysis of PCR products obtained with rCNT1-specific primers was performed with a ^{32}P-labeled 612-bp cDNA fragment of rCNT1. Reverse transcriptase-treated RNA samples show a 309-bp product in all regions, while the product is absent in RNA samples not treated with reverse transcriptase. Panel C: Agarose gel electrophoresis showed that a 343-bp product was obtained from RT-PCR performed with GAPDH primers. **Abbreviations:** J = Jejunum, Cx = Cerebral cortex, Cb = Cerebellum, Hp = Hippocampus, St = Striatum, Sm = Brain stem, SC = Superior colliculus, PH = Posterior hypothalamus, CP = Choroid plexus.

Figure 19: Distribution of mRNA for rCNT1 in Rat Brain

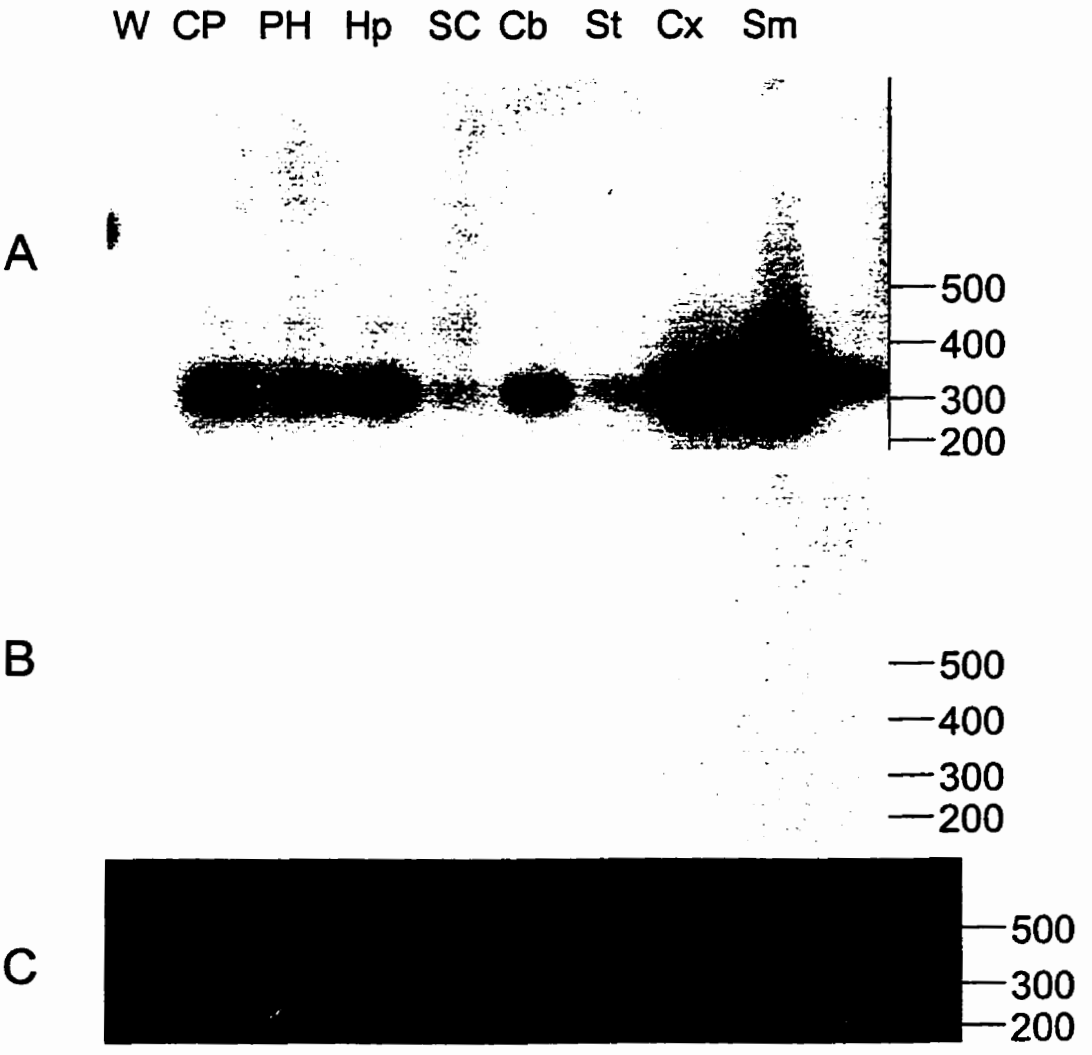

19*A*). Intermediate levels of hybridization intensity were seen with posterior hypothalamus and cerebellum RT-PCR products. For RNA samples that had been incubated with DEPC-treated water in place of reverse transcriptase, no hybridization signals were seen on Southern blots (Fig. 19*B*), indicating that mRNA, and not contaminating genomic DNA, was the source of the amplification products. GAPDH mRNA was detected using RT-PCR with every tissue extraction tested indicating good quality RNA preparations (Fig.19*C*). PCR was also performed with GAPDH-specific primers on RNA samples that were incubated with DEPC-treated water in place of reverse transcriptase and no products were detected (data not shown).

The RT-PCR product amplified from cortex RNA was digested with the restriction enzyme Stu I. Two fragments of sizes consistent with digestion of the 309-bp rCNT1 RT-PCR product into 212-bp and 97-bp fragments were obtained (Fig. 20). The cortex RT-PCR product was sub-cloned and sequenced, and the nucleotide sequence obtained exactly matched that predicted from the published rCNT1 sequence (Huang *et al.*, 1994).

RT-PCR with rCNT2 primers

RT-PCR was performed using primers designed to amplify a 235-bp segment of rCNT2. A reaction product of the expected size was seen in all brain regions tested (Fig. 21*A*). The 235-bp product was not evident following PCR with RNA samples not treated with reverse transcriptase indicating that mRNA was the source of the 235-bp product (Fig. 21*B*).

The cortex RT-PCR product was digested with Alw44 I, an enzyme predicted to cut once within the full-length rCNT2 nucleotide sequence; two fragments consistent with 162-bp and 73-bp fragment sizes predicted by the published rCNT2 nucleotide sequence were obtained (Fig. 22). Nucleotide sequencing of the sub-cloned RT-PCR

Figure 20: Stu I Restriction Digest of Cortex rCNT1 RT-PCR Product

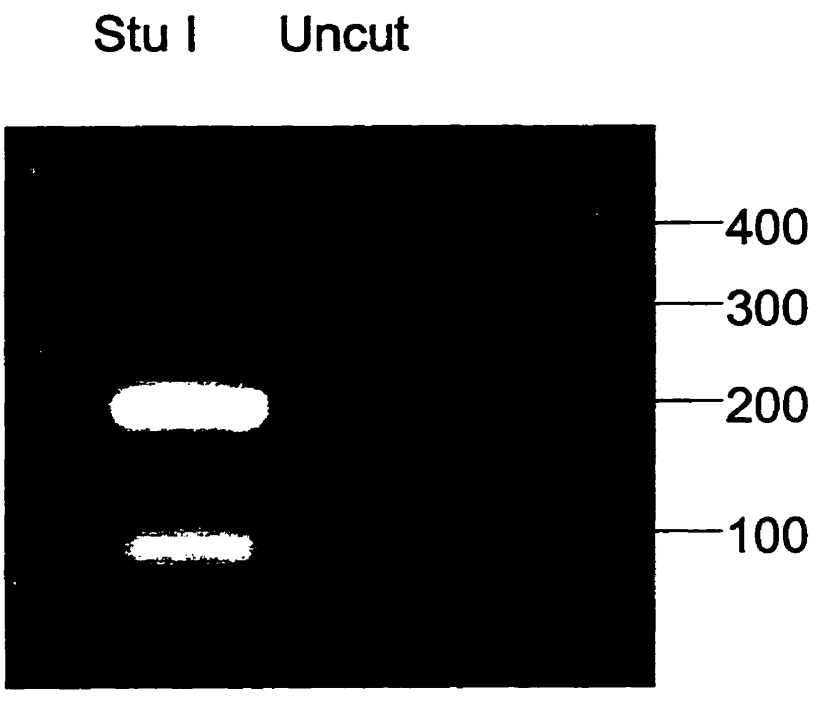

Following RT-PCR performed with cerebral cortex RNA, a 309-bp product was digested with Stu I. Agarose gel electrophoresis of the resulting mixture indicated that the cut produced two fragments consistent with the 212-bp and 97-bp predicted sizes.

Total RNA was isolated from dissected rat brain regions and jejunum, and treated with (Panel A) or without (Panel B) reverse transcriptase. Agarose gel electrophoresis of PCR products obtained with rCNT2-specific primers indicated a 235-bp product in jejunum and each brain region for RNA treated with reverse transcriptase; this product was not obtained with RNA samples that were not treated with reverse transcriptase. A 316-bp product was present in CP, PH and SC in the presence or absence of reverse transcriptase treatment. **Abbreviations:** As in legend for figure 19, W = Water.

Figure 21: Distribution of mRNA for rCNT2 in Rat Brain Using RT-PCR

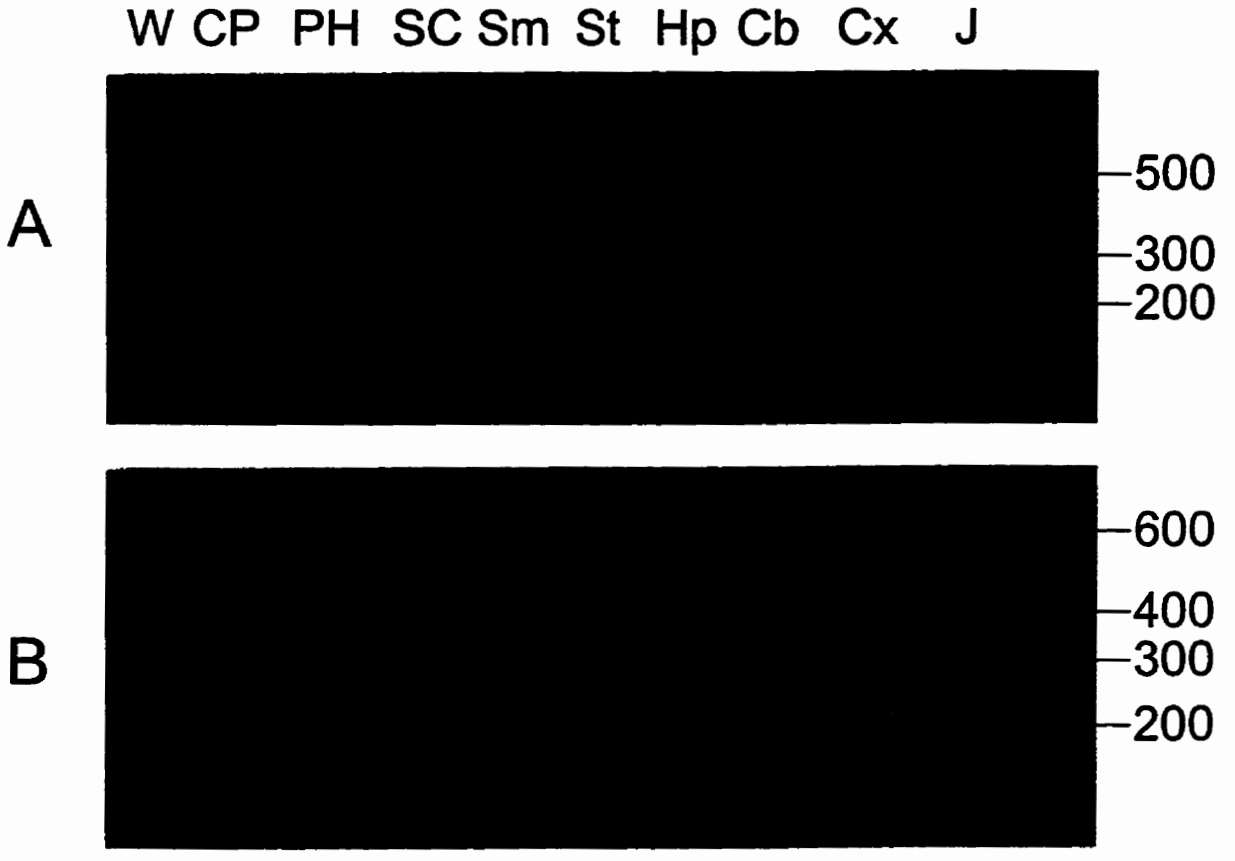

Figure 22: Alw44 I restriction digest of cortex 235-bp rCNT2 RT-PCR product

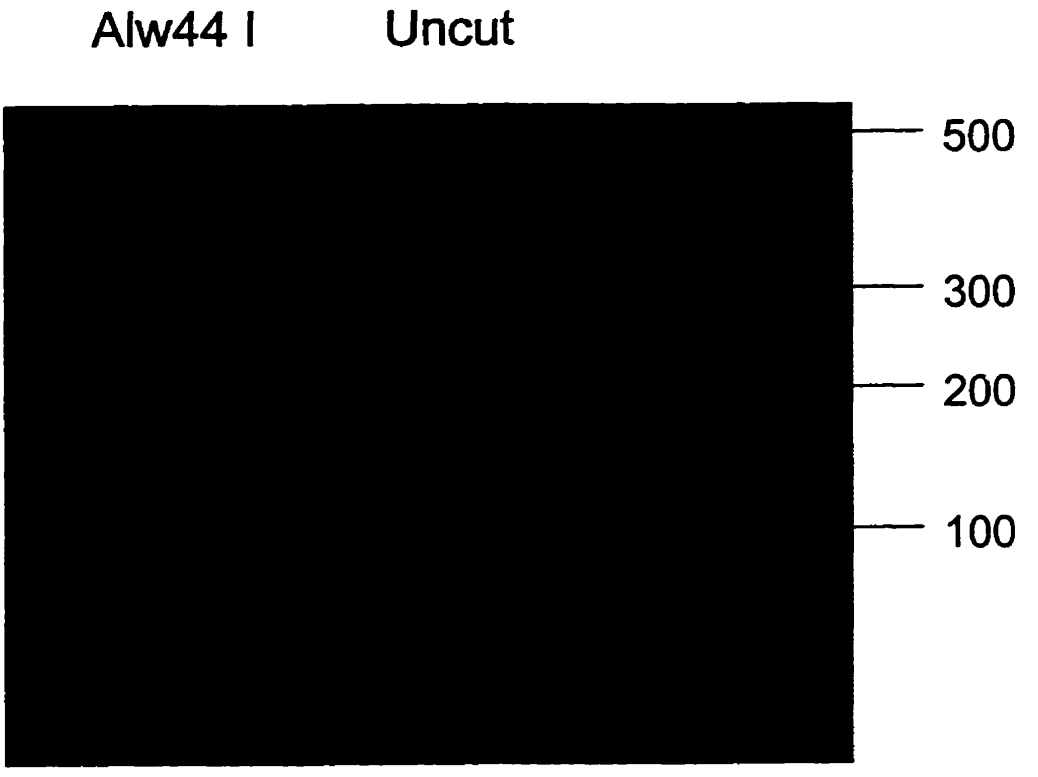

Following RT-PCR performed with cerebral cortex RNA, a 235-bp product was digested with Alw44 I. Agarose gel electrophoresis of the resulting mixture shows that the cut produced two fragments consistent with the 162-bp and 73-bp predicted sizes.

product confirmed that it is 235-bp in length and identical to the predicted product (data not shown).

A second PCR product of approximately 300-bp was obtained with RNA from choroid plexus, posterior hypothalamus and superior colliculus, samples that were not treated with DNase I (Fig. 21*A*). The product was obtained in the absence of reverse transcriptase treatment (Fig. 21*B*), or following RNase treatment of RNA (data not shown), indicating that its source was contaminating genomic DNA. Nucleotide sequencing of this larger RT-PCR product showed that it was 316-bp in length and had an identical sequence to the 235-bp product except for an in-frame 81-bp insert after position 115[5] (Fig. 23).

Discussion

This study represents the first identification of specific subtypes of Na^+-dependent nucleoside transporters in mammalian brain. Specifically, the results demonstrate the presence of mRNAs for two Na^+/nucleoside cotransporter subtypes in rat brain. Messenger RNAs for rCNT1, which encodes an N2/*cit* transporter, and for rCNT2, which encodes an N1/*cif* transporter were identified with RT-PCR analysis. While rCNT2 RT-PCR products were amplified similarly from several brain regions, the amounts of rCNT1 RT-PCR product, detected by Southern blot, varied among brain regions tested.

Since there are no selective radioligands for Na^+-dependent transporters, the distribution of these transporters in CNS was previously evaluated by functional studies. Bender *et al.* (1981) reported a 35% decrease in adenosine uptake in cerebral cortical synaptosomes when Na^+ ions were removed and Lawrence *et al.* (1994) reported a greater than 90% decrease in adenosine uptake in brain stem synaptosomes in the absence of Na^+ ions. This correlates well with the findings of this study, which demonstrate the

[5] The nucleotide sequence of this cDNA has been submitted to the GenBank™/EMBL Data Bank with accession number U67084.

Figure 23: Nucleotide Sequence of 316-bp rCNT2 RT-PCR Product (following page)

Total RNA from cerebral cortex was analyzed by RT-PCR. A 316-bp product was obtained, isolated and sub-cloned. Nucleotide sequencing was performed using both T7 and T3 DNA sequencing primers. The sequence is identical to the 235-bp product until base 115, at which point an 81-bp sequence is inserted. The two sequences merge again at base 116 of the 235-bp product and at base 197 of the 316-bp product.

5'

1- TCTGCTCATC CGTCCCTACC TTGCAGACAT GACCCTCTCT GAAATCCATG CAGTGATGAC

61- TGGAGGCTTT GCTACTATAG CAGGCACAGT GTTGGGAGCC TTCATATCCT TTGGG ***insert***

116- ***begins*** GTGAG GCACAGTCAA CAGAATCGCT CTTGGTGCAC CCACGTTGAT CCCTATAGTG

171- GTGCTAATCC CCATCTGGCT TTACGG ***insert ends*** ATTG ATGCATCATC CTTGATTTCT

221- GCCTCAGTGA TGGCTGCCCC TTGTGCACTT GCCTTGTCCA AACTGGTATA TCCAGAAGTA

281- GAAGAGTCCA AGTTCAAGAG CAAGGAGGGA GTGAAG

3'

presence of mRNA for rCNT1 and rCNT2 in these brain regions. Additionally, Na^+-dependent uptake of adenosine by cultured mouse astrocytes has been described (Bender *et al.*, 1994), and indicates that glial cells may transcribe mRNA for Na^+-dependent nucleoside transporters.

The regions of brain investigated in the present study were chosen according to previous indications of high or low *es* and/or *ei* activity and Na^+-dependent nucleoside transport activity (Bender *et al.*, 1981; Johnston and Geiger, 1989; Spector and Huntoon, 1984; Wu *et al.*, 1992). High densities of [^{3}H]NBMPR and [^{3}H]dipyridamole binding sites, indicative of high *es* and/or *ei* activity, were reported in superior colliculus, choroid plexus, striatum, hypothalamus, cerebellum and cortex (Bisserbe *et al.*, 1985; Deckert *et al.*, 1987; Geiger and Fyda, 1991). rCNT1 and rCNT2 transcripts were present in all these regions, suggesting that cell types within these tissues may possess many transporter subtypes. Hippocampus was investigated because of its low [^{3}H]NBMPR and [^{3}H]dipyridamole binding site densities (Bisserbe *et al.*, 1985), indicating low *es* and *ei* activity. In the present study, mRNAs for both rCNT1 and rCNT2 were identified in hippocampus, suggesting that Na^+-dependent transporters may be the predominant mechanism by which nucleosides are transported in this region.

The function of Na^+-dependent nucleoside transporters in brain is unclear. Other active transport systems in CNS serve to transport neuroactive substances into neurons or glia as a mechanism of inactivation of chemical messengers. Adenosine receptors are abundant in regions of rat brain where rCNT1 and rCNT2 have been identified, suggesting that Na^+-dependent nucleoside transporters may be involved in the regulation of adenosine receptor activation by endogenous adenosine. It was previously believed that rCNT1 is selective for adenosine and pyrimidine nucleosides (Cass, 1995). However, it has recently been shown that adenosine is transported more slowly than uridine or thymidine in mammalian (COS-1) cells transiently transfected with rCNT1 (Fang *et al.*, 1995); similar results were seen in *Xenopus* oocytes injected with mRNA

from rat jejunum (Yao *et al.*, 1996). If adenosine is also a poor permeant for rCNT1 in rat brain, it may be cleared slowly from the interstitium in areas containing rCNT1 transporters, thereby resulting in prolongation of adenosine receptor-mediated effects. Alternatively, rCNT2 and/or rCNT1 may play a role in neural systems containing P_2 purinoceptors. P2X, P2Y and P2U receptors are activated by ATP and have been identified in CNS tissues in rat (Zimmerman, 1994). P2U receptors are also activated by UTP. This is of interest considering the ability of rCNT1 to transport uridine, although a signaling role for UTP has not been described.

The processes involved in adenosine formation, metabolism, receptor stimulation and transport are all possible points of intervention for enhancing the receptor-mediated effects of adenosine. The cloning and sequencing of N1/*cif* and N2/*cit* Na^+/nucleoside cotransporter cDNAs has provided valuable tools to investigate the presence and distribution of mRNAs for these transporters.

CHAPTER 6

[6]Chapter 6

Distribution of concentrative nucleoside transporters (CNT) in rat brain: An in situ hybridization and immunocytochemical study

Summary

Much evidence exists showing that purine nucleosides and nucleotides are important signaling molecules in the CNS. There is building evidence that this is also the case for uridine (pyrimidine) nucleotides. Therefore, transport of purine and pyrimidine nucleosides is an important consideration in the extracellular regulation of these compounds. We have determined the distribution of two concentrative nucleoside transporter subtypes, rCNT1 and rCNT2, in rat brain using immunocytochemistry and *in situ* hybridization with ^{35}S-labeled cRNA probes. *In situ* hybridization showed a wide distribution for both rCNT1 and rCNT2 mRNA with varying signal intensities among regions. For rCNT1, low levels were seen in hippocampal granule and pyramidal cells and the molecular layers. Low levels were also detected in cerebellar granule, Purkinje and molecular layers. A small percentage (10-20%) of cells in the cerebral cortex and striatum were positive for rCNT1 mRNA. rCNT2 mRNA was most abundant in granule cells in the dentate gyrus, cerebellum and layer II of the cortex and in pyramidal cells in the hippocampus. Cerebellar Purkinje cells were also positive. In contrast to rCNT1, cerebellar and hippocampal molecular layers exhibited very low signal relative to the neuronal layers of the hippocampus and cerebellum. About 40-50% of cells in the cerebral cortex and striatum were positive for rCNT2. Immunocytochemistry localized

[6] Anderson, C.M. *et al.* (1998) Manuscript in preparation.

rCNT1 and rCNT2 to cells bodies and supported the distributions seen by *in situ* hybridization.

Introduction

Both purine and pyrimidine nucleosides and nucleotides have been implicated in signaling in the CNS. Four plasma membrane receptors for adenosine, a purine nucleoside, have been identified in the CNS and a growing body of evidence supports the pyrimidine nucleotides UDP and UTP, as well as the purine nucleotides ADP and ATP as endogenous signaling molecules.

Important considerations for the regulation of receptor-mediated actions of nucleosides and nucleotides are metabolism and transport across the cell membrane. Transport of nucleosides is achieved by two broad categories of nucleoside transport proteins: equilibrative and concentrative. Equilibrative transporters are facilitated diffusion protein carriers that shuttle nucleosides across the cell membrane in either direction according to the concentration gradient. Two equilibrative transporter subtypes that accept both purine and pyrimidine nucleosides as permeants have been cloned from human tissues to date and are termed hENT1 (Griffiths *et al.*, 1997a) and hENT2 (Griffiths *et al.*, 1997b; Crawford *et al.*, 1998). The rat cDNAs were subsequently isolated and termed rENT1 and rENT2 (Yao *et al.*, 1997). Concentrative nucleoside transporters are energy dependent Na^+/nucleoside symporters and are classified according to their permeant selectivities and sensitivity to inhibition by the nucleoside analog NBMPR. Currently, six subtypes are recognized. N1 is purine selective, N2 is pyrimidine selective, N3 accepts a broad range of nucleoside permeants, N4 is pyrimidine

and guanosine selective, N5 accepts a broad range of nucleoside permeants and is sensitive to inhibition by NBMPR, and N6 is guanosine selective and sensitive to inhibition by NBMPR. Two members of this CNT gene family have been cloned from rat. An N2 cDNA was isolated from jejunum and termed rCNT1 (Huang *et al.*, 1994) and N1 was cloned from liver (Che *et al.*, 1995) and jejunum (Yao *et al.*, 1996) and termed rCNT2.

There is some functional evidence for concentrative, or Na^+-dependent nucleoside transport in rat brain (Johnston and Geiger, 1989; Bender *et al.*, 1981; Lawrence *et al.*, 1994). In addition, we have recently demonstrated the presence of mRNA for rCNT1 and rCNT2 in rat brain regions by RT-PCR (Anderson *et al.*, 1996a). The objective of the present study was to determine the regional and cellular distributions of rCNT1 and rCNT2 mRNA and protein in rat brain using *in situ* hybridization and immunocytochemistry.

Materials and Methods

In Situ Hybridization

Male Sprague-Dawley rats (250 g) were sacrificed by decapitation and brains were removed and frozen. Fresh frozen sections (14 μm) were cut using a cryostat and placed on ProbeOn Plus microscope slides (Fisher). Sections were frozen at -80°C until use. Sections were fixed for 2 minutes in buffered 4% paraformaldehyde, permeabilized for 7 minutes with 0.0005% proteinase K at 37°C, acetylated for 10 minutes (0.25% v/v acetic anhydride in 0.1 M triethanolamine buffer, pH 8.0) and dehydrated in graded ethanol concentrations prior to hybridization.

RNA probes (riboprobes) generated by reverse transcriptase PCR were used to detect rCNT1 and rCNT2 in rat brain. For rCNT1, the 5' primer 5'-phosphate-CTTCTTGATGGTCGCCTGC-3' and the 3' primer 5'-GCGGTGTCCAGAGATAGCC-3' were used to generate a 231-bp monophosphorylated cDNA product from bases 444 to 674. For rCNT2, the 5' primer 5'-phosphate-TCTGCTCATCCGTCCCTACC-3' and the 3' primer 5'-CTTCACTCCCTCCTTGCTCTTG-3' were used to generate a 235-bp monophosphorylated cDNA product from bases 1228 to 1562. These products were ligated into the pCR-Script Direct plasmid vector (Stratagene) to produce a directional clone such that *in vitro* transcription with T3 RNA polymerase produced sense riboprobes while T7 RNA polymerase gave antisense riboprobes. The Ambion Maxiscript kit was used to transcribe RNA from linearized/proteinase K-treated templates. Transcription proceeded for 60 minutes at 37°C with 0.5 mM each of ATP, GTP and CTP, 10 mM dithiothreitol (DTT), 400 μCi [α-^{35}S]UTP (NEN) and 0.5 Units T3 or T7 RNA polymerase in a total volume of 20 μl. Labeled RNA probes were ethanol precipitated, resuspended in solution containing 10 mM Tris-HCl (pH 8.0), 1 mM EDTA, 10 mM DTT and 1% SDS, and counted for ^{35}S content.

Hybridization was performed overnight at 55°C in a Microprobe hybridizer (Fisher). Hybridization solution contained 50% (v/v) formamide, 10% (w/v) dextran sulfate, 0.3 M NaCl, 1x Denhardt's solution, 10 mM Tris-HCl (pH 8.0), 1 mM EDTA, 100 μg/ml denatured salmon sperm DNA, 0.5 mg/ml yeast tRNA and 10 mM DTT. Riboprobes were added to a concentration of 5 x 10^6 cpm/ml hybridization solution. Following hybridization sections were treated with RNase A (20 μg/ml) and washed with increasing temperature and decreasing salt concentration to a final wash for 30 minutes at

60°C in 0.1x SSC with 50 mM DTT. Sections were dehydrated in preparation for emulsion or film autoradiography. For film autoradiography, sections were exposed to Amersham Hyperfilm-βmax for 14 days and developed using Kodak D-19 developing solution. For emulsion autoradiography, slides were dipped in Kodak NTB-2 autoradiographic emulsion for 14 days and developed using a 1:1 dilution of Kodak D-19 developer. Sections were then counter-stained with the nuclear stain hematoxylin.

Immunohistochemistry

Polyclonal antiserum for rCNT2 was prepared by Commonwealth Biotechnologies (Richmond, VA). Rabbits were injected with synthetic immunogenic peptide from the carboxyl terminal of rCNT2 (LNGTNMPSFSGPWQDC; amino acids 624-638). Antiserum used was from the third bleed because these samples had the highest antibody titer. For rCNT1, an affinity-purified anti-GST fusion protein bearing residues 21-78 of rCNT1 as well as an affinity-purified antibody generated against residues 505-524 of rCNT1 were obtained from Dr. S. Baldwin, University of Leeds.

Fresh frozen sections (5 μm) were cut from male Sprague-Dawley rat brains, placed on Superfrost Plus slides (Fisher) and frozen at –80°C until use. Sections were fixed with 4% paraformaldehyde for 5 min and permeabilized with 0.1% triton X-100 for 10 min Endogenous peroxidase activity was inhibited by treatment with 0.5% H_2O_2 for 25 min and non-specific binding sites were blocked with blocking solution containing 2% bovine serum albumin and 10% normal goat serum for 30 min All treatments were at room temperature unless otherwise indicated. Following this, sections were treated overnight with blocking solution, normal rabbit serum or diluted primary antisera generated against either rCNT1 or rCNT2. Sections were then washed thoroughly with

0.1 M phosphate-buffered saline (PBS) and treated with biotinylated goat anti-rabbit IgG (Boerhinger;1000x dilution) for 60 min After washing again with PBS, streptavidin-linked horse-radish peroxidase (Boerhinger; 2000x dilution) was placed on the sections for 45 min Binding distribution of the primary antibody was determined by the brown product formed by the reaction of the peroxidase with the substrate diaminobenzidine (DAB). Sections were subsequently dehydrated with graded ethanol concentrations, cover-slipped, viewed and photographed.

Western Blots

Membrane protein fractions were prepared by centrifuging tissue homogenates at 1000 x *g* for 10 minutes at 4°C and then centrifuging the supernatant for 1 hour at 100,000 x *g* at 4°C. Protein concentrations were measured using the Lowry method and 20 μg were loaded in to each well of a 10% polyacrylamide gel containing 0.2% sodium dodecylsulfate (SDS). The samples were electroblotted onto PVDF membranes for 1 hour at 4°C and membranes were placed in blocking solution containing 2% bovine serum albumin and 2.5% skim milk powder overnight at 4°C. Primary antibodies were diluted either 500x (antiserum, rCNT2) or 4000x (affinity-purified, rCNT1) in blocking solution and incubated with the membranes for 3 hours at room temperature. Blots were washed 4 times for 5 min each in phosphate-buffered saline containing 0.1% Tween 20 (PBS-T) and incubated with biotinylated goat anti-rabbit IgG diluted 1500x in blocking solution for 1 hour. Following a further 4 washes in PBS-T, membranes were incubated with streptavidin linked horse-radish peroxidase (POD; 2500x dilution) for 1 hour in blocking solution. Blots were finally washed and treated either with the Boehringer-

Mannheim chemiluminescence substrate for 1 min and exposed to film for 10-60 min, or with diaminobenzidine (DAB) to achieve a colour reaction.

Results

Distribution of rCNT2 mRNA using in situ hybridization

In situ hybridization was performed on frozen 14 μm coronal rat brain sections with ^{35}S-labeled sense and antisense cRNA probes transcribed from a 235-bp cDNA from rCNT2. Message for rCNT2 was detected by hybridization of the antisense riboprobe. The sense probe displayed low non-specific binding to tissue sections.

Varying levels of hybridization signal intensity were seen throughout rat brain. Highest levels were detected in the granule cells of the dentate gyrus (Fig. 24). A more moderate signal appeared in other regions of the hippocampus. The pyramidal cells of the CA1 and CA2 subfields displayed roughly 50% of the hybridization intensity of the dentate gyrus granule cells as determined by densitometry performed by Scion Image software. In general, the CA3 and CA4 pyramidal cells had approximately only 25% of the signal intensity of dentate gyrus granule cells.

A strong hybridization signal, comparable to that of the dentate gyrus granule cells, appeared in cerebellar granule cells (Fig. 25). Examination of sections under high magnification indicated that Purkinje cells also appear to contain rCNT2 transcripts (not shown).

Layer II cortical granule cells also were heavily labeled with silver grains, indicating high levels of rCNT2 mRNA (Fig. 26) while a moderate level of hybridization occurred throughout the rest of the cortex where approximately 40-50% of cells were

positive for rCNT2 mRNA. Results were similar in striatum and thalamus (not shown). Co-localization studies with cell-specific markers are required to determine cell types.

There is no evidence that rCNT2 is present on astrocytes. There is minimal signal in the molecular layers of the dentate gyrus and cerebellum. The same is true for the stratum radiatum of the hippocampus and the subpial layers of the brain (Fig. 25,26), all areas of relatively dense astrocyte populations. Choroid plexus epithelial cells, however, do appear to be a non-neuronal cell type possessing mRNA for rCNT2 (Fig. 26). rCNT2 may be important for the transport of purine nucleosides into or out of the brain.

Distribution of rCNT2 using immunocytochemistry

Antiserum raised against an immunogenic rCNT2 peptide was used in western blots. Immunoblotting with plasma membrane protein fractions from lung, heart, kidney and brain indicated one major band at approximately 80-90 kDa (Fig. 27). Levels of this protein were highest in heart and kidney while lung and brain homogenates gave rise to faint signals with the rCNT2 antiserum.

The same antiserum was used for immunocytochemistry with 5 μm frozen coronal rat brain sections to look at rCNT2 protein expression. Substantial immunostaining was seen in hippocampus, cerebellum, cerebral cortex and choroid plexus, in agreement with *in situ* hybridization data. No colour product was formed in control sections treated with normal rabbit serum in place of the antiserum.

A consistent level of colour was detected on the cell bodies of the dentate gyrus granule cells and on the pyramidal cells (Fig. 28). Staining appeared darker around the cell perimeter indicating the transporter is located on the cell membrane (Fig. 28*C*).

Cerebellar granule cells stained positive with rCNT2 antiserum (Fig. 29), again agreeing with data obtained with *in situ* hybridization. Purkinje cells appeared negative for rCNT2. Some cell bodies in the cerebellar molecular layer were stained.

As seen with rCNT2 *in situ* hybridization, there is staining throughout the cortex with particularly dense staining of cells in layer II (Fig. 30).

Choroid plexus cell bodies were stained by the rCNT2 antiserum (Fig. 30*E*), again agreeing with *in situ* hybridization and suggesting that rCNT2 may be important in regulating purine nucleoside levels in brain.

Distribution of rCNT1 using in situ hybridization

In situ hybridization was performed on frozen rat brain sections using ^{35}S-labeled sense and antisense riboprobes transcribed from a 231-bp cDNA from rCNT1. A signal of variable intensity throughout the brain was seen with the antisense probe while the sense probe produced no hybridization signals.

The antisense probe produced a hybridization signal throughout the hippocampus. Figure 31 is representative of the distribution seen for rCNT1 antisense binding. The granule cells of the dentate gyrus and the pyramidal cells appear to have rCNT1 mRNA but generally produced signals of similar intensity to the molecular layer and stratum radiatum, providing evidence that rCNT1 may be present on astrocytes. This is in contrast to rCNT2, which was prominent in granule and pyramidal cells and not evident in the molecular layer and stratum radiatum (see Fig. 24).

A hybridization signal was present in the cerebellum as well. Generally, low levels of antisense binding were detected in the granule cells and Purkinje cells (Fig. 32).

Signal was also seen in the molecular layer and subpial layers, a further indication that rCNT1 may be present on astrocytes.

Hybridization signal was detected in cerebral cortex and striatum as well. Examination of sections at high magnification indicated silver grain aggregation on 10-20% of cell bodies in these regions (not shown).

Distribution of rCNT1 using immunocytochemistry

Two affinity-purified antibodies raised in rabbits against a GST fusion protein bearing residues 21-78 of rCNT1 (AB1) or residues 505-524 (AB2) of rCNT1 were tested on western blots containing plasma membrane protein isolated from lung, heart, kidney and brain. AB1 recognized a band of 80-90 kDa in all four tissues with greatest intensity in heart and kidney Fig. 33). Similar results were seen with AB2 but a second band of 70-75 kDa, the expected size of the unmodified rCNT1 protein, was also detected (not shown).

Both antibodies were used in immunocytochemistry with rat brain sections. AB2 gave a signal in every cell (Fig. 34). This signal appeared to result from an interaction with cell nuclei and thus, is not likely to represent the distribution of rCNT1. Immunocytochemistry with AB1 gave rise to membrane staining. It produced a positive signal in the hippocampus (Fig. 35), similar to *in situ* hybridization for rCNT1. Staining in the dentate gyrus molecular layer and stratum radiatum was less than predicted from *in situ* hybridization, however. AB1 produced a signal in cerebellar granule cells, Purkinje cells and other brain regions such as cerebral cortex (Fig. 36), thalamus and striatum (not

shown) showed some cells stained positive for rCNT1 AB1. Co-staining studies are needed to determine the cells types stained.

Discussion

This is the first study to investigate the distribution of mRNA and protein for two members of a concentrative nucleoside transporter gene family, rCNT1 and rCNT2, in rat brain sections. *In situ* hybridization showed rCNT2 to be abundant in cortical and cerebellar granule cells, the granule and pyramidal cells of the hippocampus and in choroid plexus cells. Results of immunocytochemistry with an rCNT2 antibody supported these results. rCNT1 seemed to be more widely distributed at lower levels. mRNA for rCNT1 was present in hippocampus and cerebellum like rCNT2 but unlike rCNT2 appeared in cell layers where glial cells are present. Immunocytochemistry with an antibody for rCNT1 showed a similar distribution except for a lower than expected signal in the molecular layers of the cerebellum and hippocampus.

Since rCNT1 and rCNT2 are members of the same gene family and share 64% amino acid identity (Che *et al.*, 1995), it is important to consider the degree of homology between the probes used for each sequence. The probe used for rCNT1 did not identify the rCNT2 sequence in a BLAST homology search, indicating the rCNT1 probe is selective for rCNT1. The rCNT2 probe is 76% identical to the rCNT1 sequence at the nucleic acid level between bases 1116 and 1359. Slides were washed with high stringency (0.1x SSC, 60°C, 30 min) to minimize hybridization of the rCNT2 probe to rCNT1 mRNA.

Immunocytochemistry was performed with antibodies for both rCNT1 and rCNT2 that each recognized one major band on western blots at 80-90 kDa. The predicted size of both rCNT1 and rCNT2 proteins is approximately 72 kDa. It is possible that the translated rCNT1 and rCNT2 proteins are modified and migrate at a slower rate. For instance, rCNT2 has five prospective N-linked glycosylation sites and relative mobility is decreased with glycosylation. To show that glycosylation is responsible, an enzyme deglycosylation step would have to be taken prior to SDS-PAGE.

There is limited previous evidence for concentrative nucleoside transport in brain. Rat dissociated brain cells (Johnston and Geiger, 1989), rat cortical synaptosomes (Bender *et al.*, 1981), rat brain stem synaptosomes (Lawrence *et al.*, 1994) and mouse astrocytes (Bender *et al.*, 1994) have all been shown to have a component of Na^+-dependent (concentrative) nucleoside uptake. The most consistent evidence for Na^+-dependent nucleoside transport in brain is in choroid plexus (Spector and Huntoon, 1984; Wu *et al.*, 1992). Our previous results with RT-PCR (Anderson *et al.*, 1996a) showed rCNT1 and rCNT2 amplification products throughout rat brain and, with the results of the present study, are in agreement with the earlier reports of Na^+-dependent nucleoside transport in brain. With the exception of brain stem, which was not investigated, both rCNT1 and rCNT2 were detected in the regions where functional Na^+-dependent transport had been previously documented.

The functional significance of the distributions of these transporters is unknown. Hippocampus is a brain region selectively vulnerable to ischemic damage. Since hippocampus is also rich in A_1ARs, endogenous adenosine could be effective neuroprotectant. Since rCNT2 appears to be present in hippocampus, it may play a role

in regulating adenosine levels. ENT1 and ENT2 mRNA are also present in hippocampus (unpublished data) thus adenosine levels may be regulated by multiple coexisting transporters. In ischemia, perturbations of the cellular energy state and Na^+ gradient would be expected to inhibit rCNT2-mediated adenosine uptake and maybe even cause reversal of rCNT2 promoting release of adenosine and enhancement of neuroprotective effects; reversal of the transporters has been demonstrated *in vitro* (Borgland and Parkinson, 1997).

rCNT1 has a high affinity for adenosine but transport of adenosine proceeds very slowly, prompting one group to call adenosine an inhibitor of rCNT1 (Fang *et al.*, 1996). Uridine, however, is transported by rCNT1 with a V_{max} approximately 60-fold greater than for adenosine (Fang *et al.*, 1996). This may be of importance given findings that uridine nucleotides may be signaling molecules in brain *via* P_2 receptors (Anderson and Parkinson, 1997). As nucleotides are metabolized extracellularly, CNT1 may facilitate reuptake of the nucleoside product of UDP or UTP. CNT1 may be a cellular marker of cells using UDP or UTP as signaling molecules.

The discovery of the presence of concentrative nucleoside transporters in different areas of rat brain is an important step in understanding how endogenous nucleosides, including adenosine, are regulated and may have importance for signaling actions of nucleotides.

Sense and antisense cRNA probes were transcribed from a 235-bp cDNA fragment of rCNT2 ligated into the PCR-Script direct vector and were hybridized to 14 μm fresh frozen coronal rat brain sections. *A* and *B* represent results of *in situ* hybridization obtained with the sense cRNA probe for rCNT2 while *C* and *D* are results with the antisense probe (20x magnification). Nuclei were stained with hematoxylin as seen in bright-field images *A* and *C*. *B* and *D* are dark-field images in which cRNA probes are detected by silver grains which appear white. A strong hybridization signal for rCNT2 was seen in neuronal layers of the hippocampus as indicated by binding of the antisense cRNA probe (*D*). Signal was low the dentate gyrus molecular layer (*ML*) and stratum radiatum (*SR*). The sense probe did not produce a hybridization signal (*B*). *DG*, dentate gyrus; *CA1*, CA1 subfield; *CA3*, CA3 subfield.

Figure 24: Distribution of rCNT2 mRNA in Rat Hippocampus

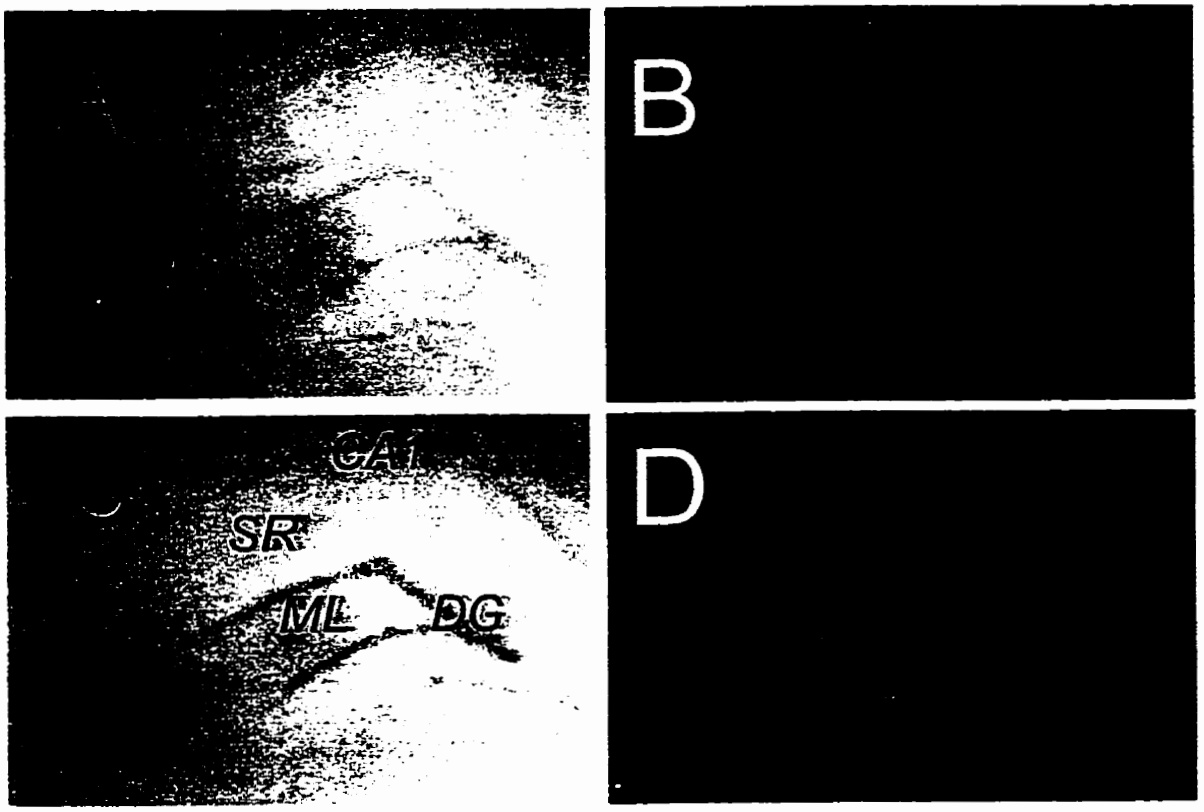

Sense and antisense cRNA probes were transcribed from a 235-bp cDNA fragment of rCNT2 ligated into the PCR-Script direct vector and were hybridized to 14 μm fresh frozen coronal rat brain sections. Nuclei were stained with hematoxylin as seen in bright-field images *A* and *C*. *B* and *D* are dark-field images in which cRNA probes were detected by silver grains, which appear white. *A* and *B* represent results of *in situ* hybridization obtained with the sense cRNA probe for rCNT2 in cerebellum while *C* and *D* are results with the antisense probe in cerebellum (40x magnification). The granule cell layer (*Gr*) and Purkinje cells (*Pk*) all displayed specific antisense probe binding (*D*). Signal in molecular layers (*ML*) and subpial layers (*PL*) was low. Sense probe binding was negligible (*B*).

Figure 25: Distribution of rCNT2 mRNA in Rat Cerebellum

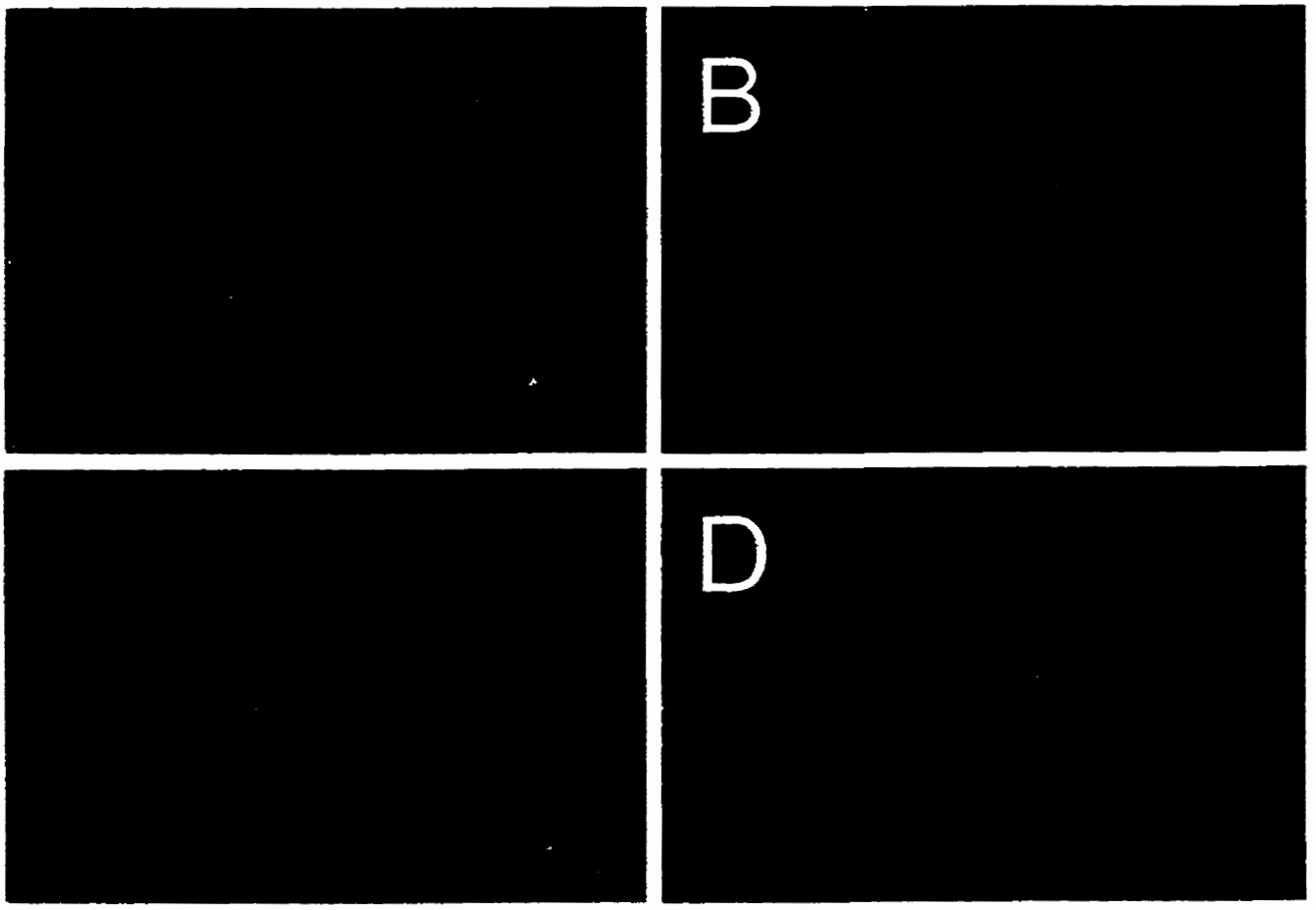

Sense and antisense cRNA probes were transcribed from a 235-bp cDNA fragment of rCNT2 ligated into the PCR-Script direct vector and were hybridized to 14 μm fresh frozen coronal rat brain sections. Nuclei were stained with hematoxylin as seen in bright-field images *A, C, E* and *F*. *B, D, G* and *H* are dark-field images in which cRNA probes were detected by silver grains, which appear white. *A* and *B* represent results of *in situ* hybridization obtained with the sense cRNA probe for rCNT2 in cortex layer II on either side of the bisection line of the 2 cerebral hemispheres, while *C* and *D* are results with the antisense probe in cortex layer II (100x magnification) and show substantial hybridization signal (*D*). Sense probe binding was negligible (*B*). *E* and *F* represent results in other cortical layers (400x magnification). *F* was treated with the antisense probe and shows 40-50% of cells positive for rCNT2 while sense probe binding was negligible (*E*). Triangular arrowheads represent cells positive for rCNT2 mRNA and diamond-shaped arrowheads represent negative cells. *G* shows sense probe treatment of a choroid plexus section. Binding of the sense probe was low while the antisense probe produced a strong hybridization signal (*H*). *PL*, Subpial layer.

Figure 26: Distribution of rCNT2 mRNA in Rat Cerebral Cortex and Choroid Plexus

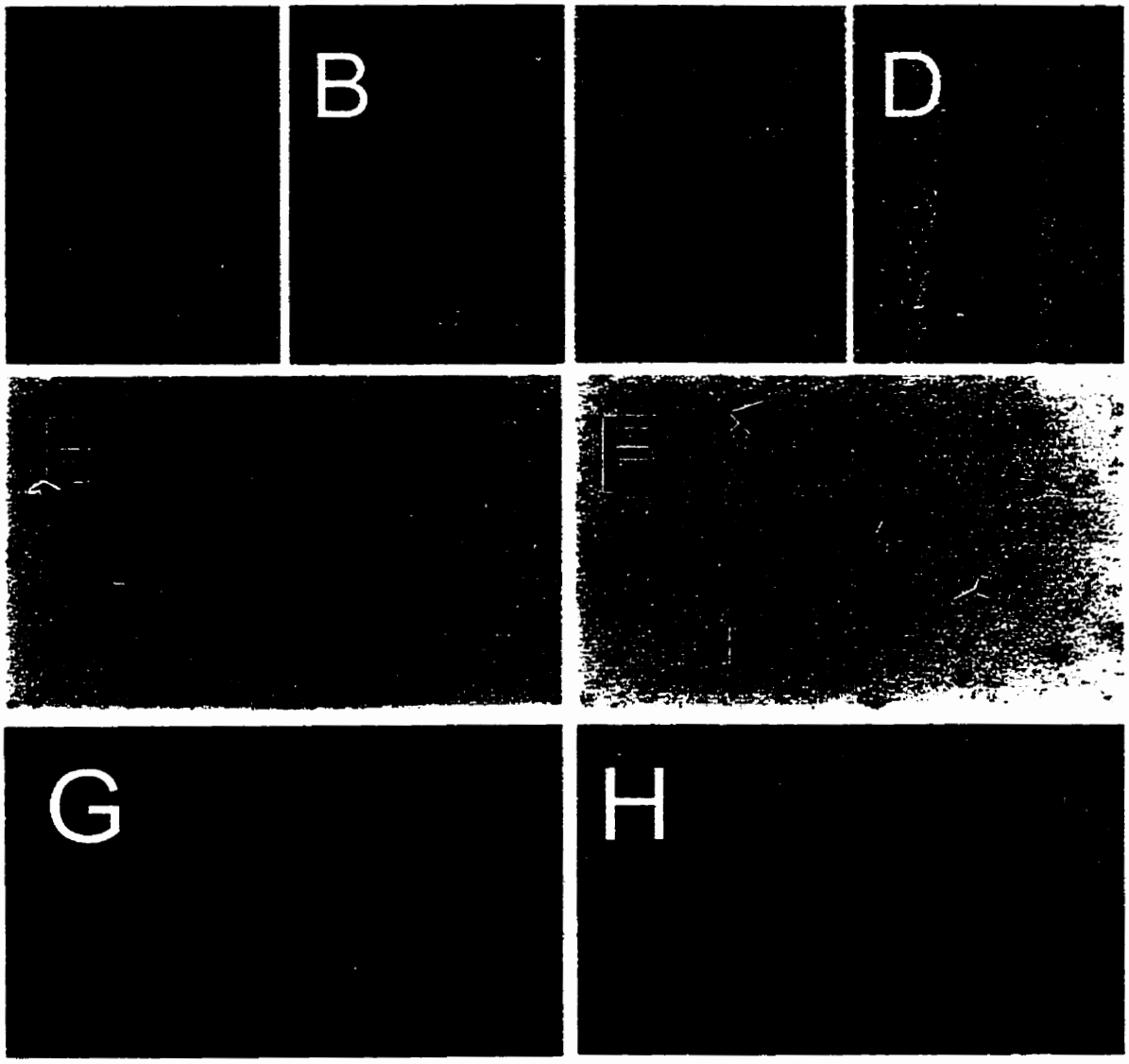

Figure 27: Multi-tissue Western Blot Using Anti-rCNT2 Antibody

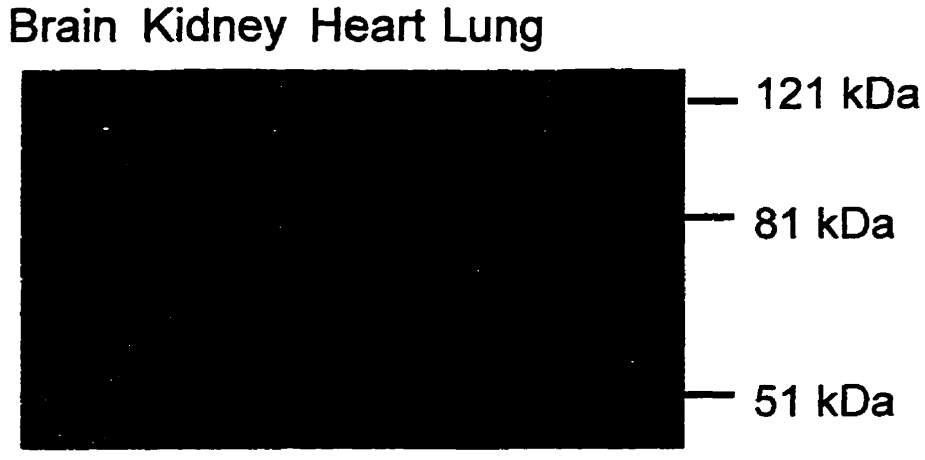

A western blot was treated with rCNT2 antiserum (500x dilution) and subsequently with biotinylated goat anti-rabbit IgG, streptavidin-linked horseradish peroxidase (POD) and diaminobenzidine (DAB) substrate system. A band of 80-90 kDa was detected with high levels in heart and kidney and lower levels in lung and brain.

Sections of rat brain were fixed and treated with antiserum against an rCNT2 peptide. Signal was detected using a secondary biotinylated goat anti-rabbit IgG antibody, streptavidin-linked horseradish peroxidase (POD) and diaminobenzidine (DAB) POD substrate. Results in hippocampus are shown here. *A* shows a grayscale representation of the DAB colour product in dentate gyrus (*DG*) granule cells the CA1 subfield (*CA1*) of the hippocampus (40x magnification). A control section treated with normal rabbit serum is shown in *B* and displays no signal. *C* represents DG granule cells at 400x magnification. Staining occurs on the cell perimeters.

Figure 28: Distribution of rCNT2 Immunoreactivity in Rat Hippocampus

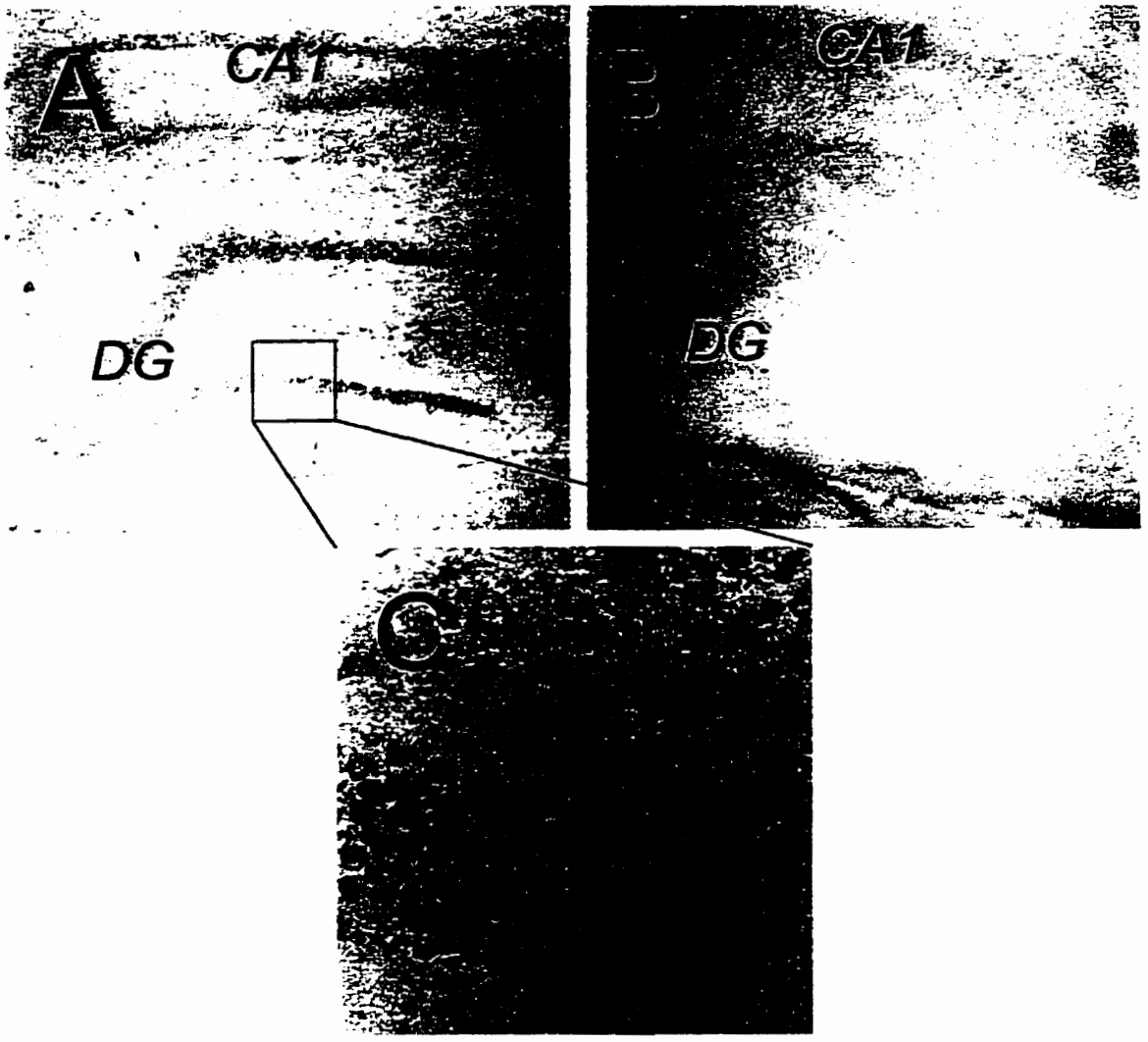

Figure 29: Distribution of rCNT2 Immunoreactivity in Rat Cerebellum

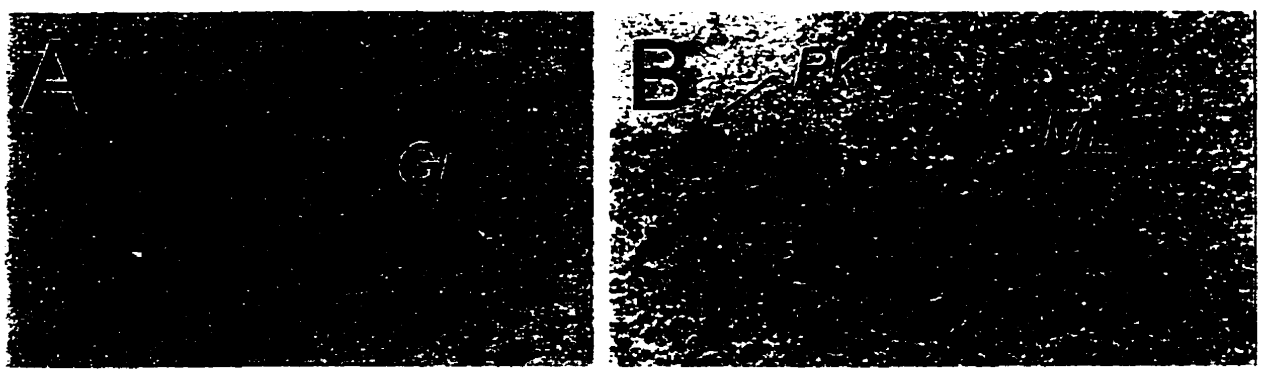

Sections of rat brain were fixed and treated with antiserum against an rCNT2 peptide. Signal was detected using a secondary biotinylated goat anti-rabbit IgG antibody, streptavidin-linked horseradish peroxidase (POD) and diaminobenzidine (DAB) POD substrate. *A* and *B* show a grayscale representation of the DAB colour product in cerebellum at 400x magnification. A control section treated with normal rabbit serum is shown in *A* and displays no signal while *B* shows dense staining in the granule cell layer (*Gr*). Very little staining of Purkinje cells (*Pk*) and cells of the molecular layer (*ML*) was noted.

Sections of rat brain were fixed and treated with antiserum against an rCNT2 peptide. Signal was detected using a secondary biotinylated goat anti-rabbit IgG antibody, streptavidin-linked horseradish peroxidase (POD) and diaminobenzidine (DAB) POD substrate. Results in cerebral cortex and choroid plexus are shown here. Control sections treated with normal rabbit serum are shown in *A* and *C* and display no signal. *B* shows that a proportion of cells are labeled in the cortex (indicated by arrows) (400x magnification). *D* shows heavy staining of layer II of the cerebral cortex on either side of the bisection line of the 2 cerebral hemispheres (100x magnification). *E* clearly shows that cell bodies within the papillae of the choroid plexus are stained by the anti-rCNT2 antibody.

Figure 30: Distribution of rCNT2 Immunoreactivity in Rat Cerebral Cortex and Choroid Plexus

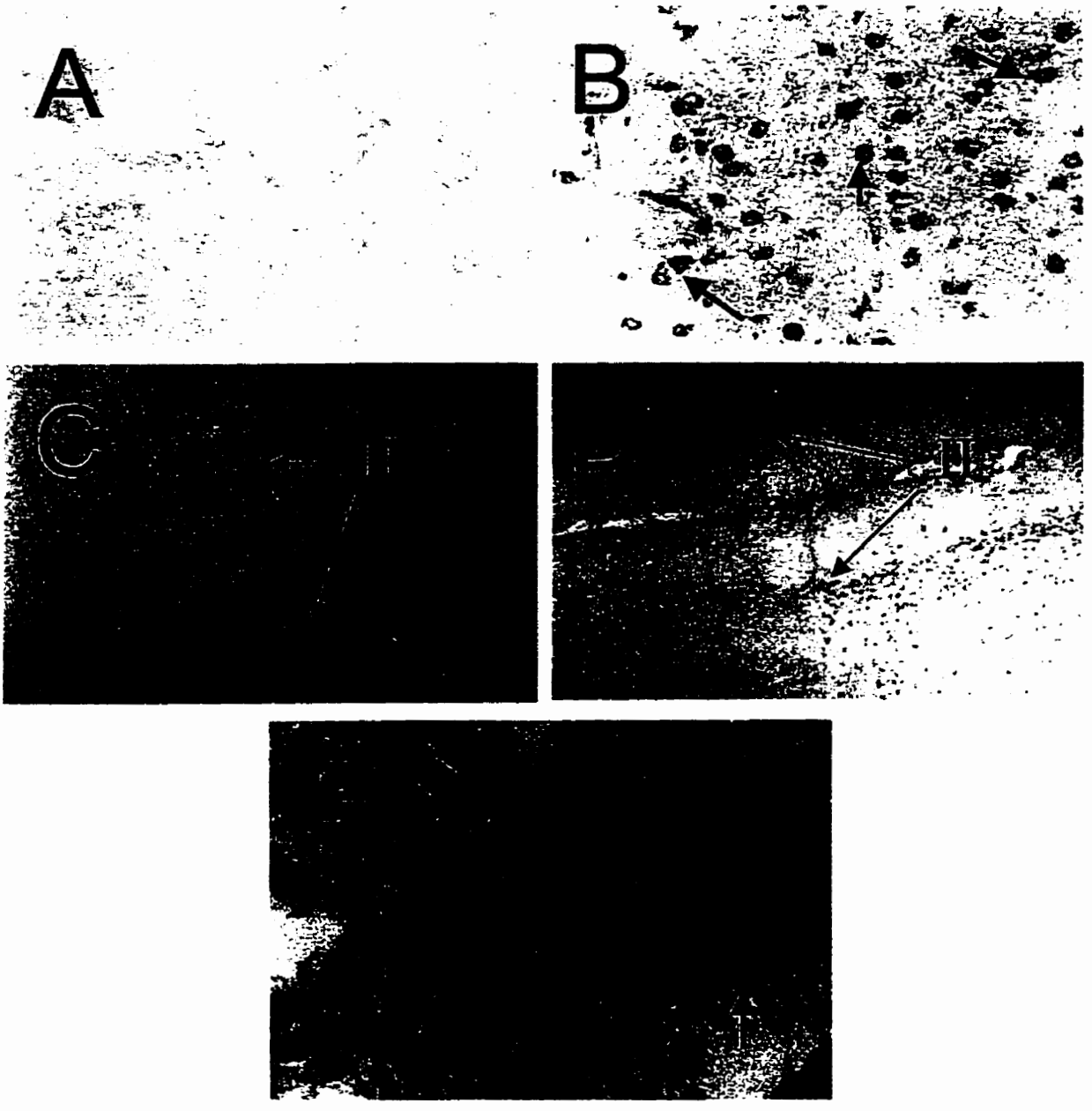

Sense and antisense cRNA probes were transcribed from a 231-bp cDNA fragment of rCNT1 ligated into the PCR-Script Direct vector and were hybridized to 14 μm fresh frozen coronal rat brain sections. *A* and *B* represent results of *in situ* hybridization obtained with the sense cRNA probe for rCNT1 while *C* and *D* are results with the antisense probe (20x magnification). Nuclei were stained with hematoxylin as seen in bright-field images *A* and *C*. *B* and *D* are dark-field images in which silver grains appear white. A consistent low level of antisense hybridization signal was seen for rCNT1 throughout the hippocampus (*D*). Dentate gyrus granule (*DG*) cells and pyramidal neurons in the CA1-CA4 subfields showed a hybridization signal as do the molecular layer (*ML*) and stratum radiatum (*SR*). The sense probe did not produce a hybridization signal (*B*).

Figure 31: Distribution of rCNT1 mRNA in Rat Hippocampus

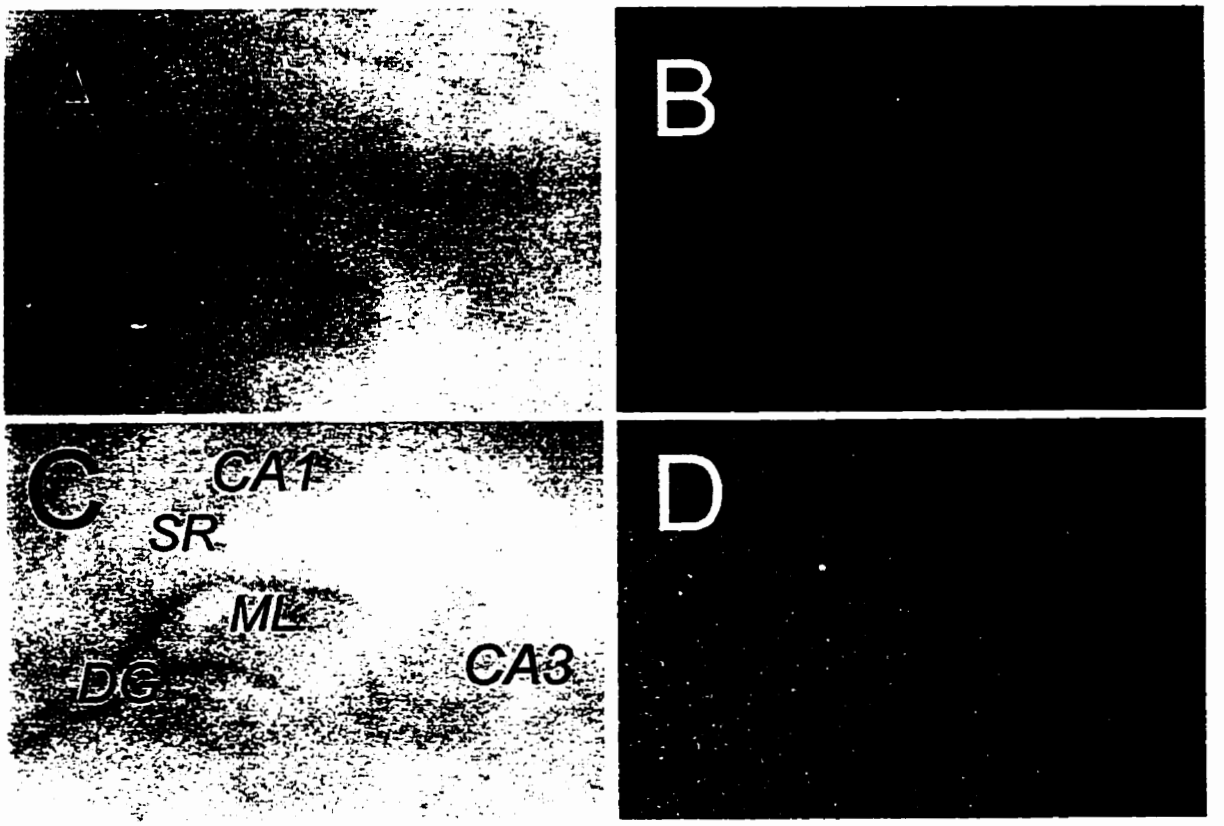

Sense and antisense cRNA probes were transcribed from a 231-bp cDNA fragment of rCNT1 ligated into the PCR-Script Direct vector and were hybridized to 14 μm fresh frozen coronal rat brain sections. *A* and *B* represent results of *in situ* hybridization obtained with the sense cRNA probe for rCNT1 while *C* and *D* are results with the antisense probe (100x magnification). Nuclei were stained with hematoxylin as seen in bright-field images *A* and *C*. *B* and *D* are dark-field images in which silver grains appear white. All cerebellar layers displayed a consistent low level of antisense hybridization signal for rCNT1 (*D*). The sense probe did not produce a hybridization signal (*B*). *Pk*, Purkinje layer; *Gr*, Granule layer; *PL*, Subpial layer of the brain; *ML*, Molecular layer.

Figure 32: Distribution of rCNT1 mRNA in Rat Cerebellum

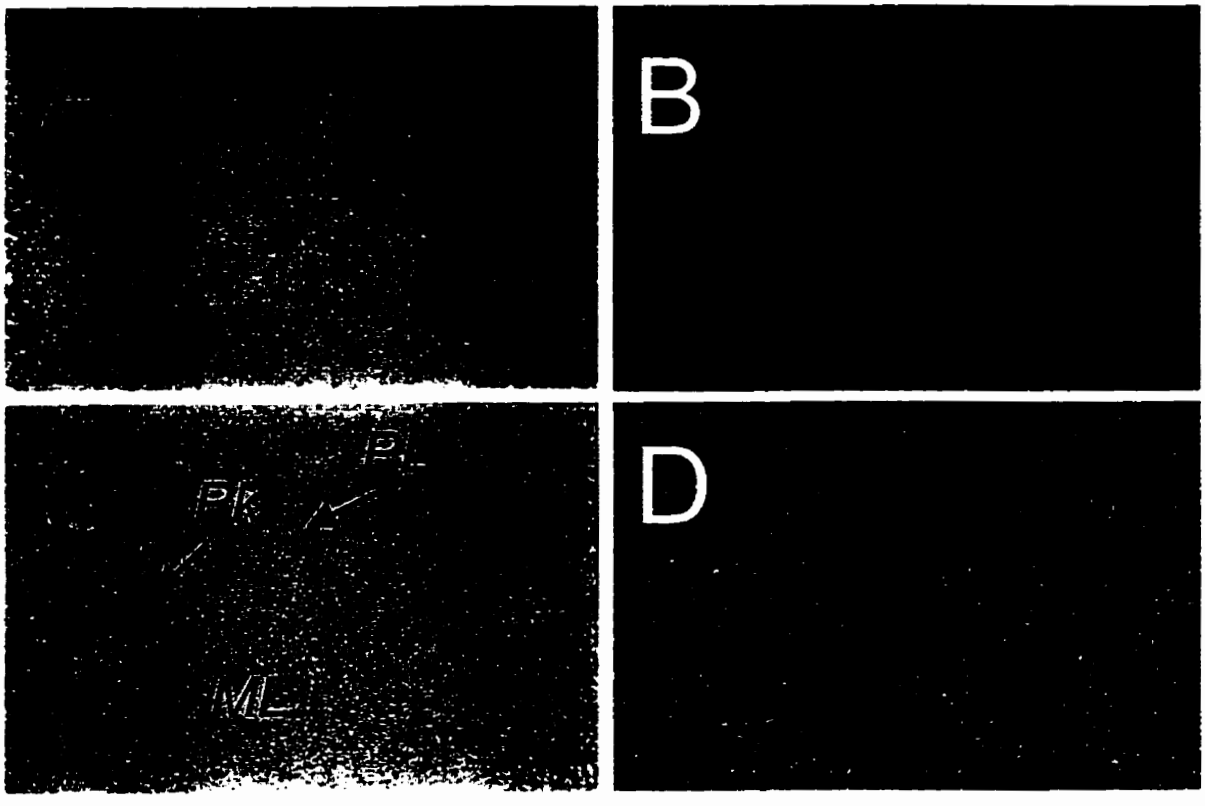

Figure 33: Multi-tissue Western Blot Using Anti-rCNT1 Antibody (AB1)

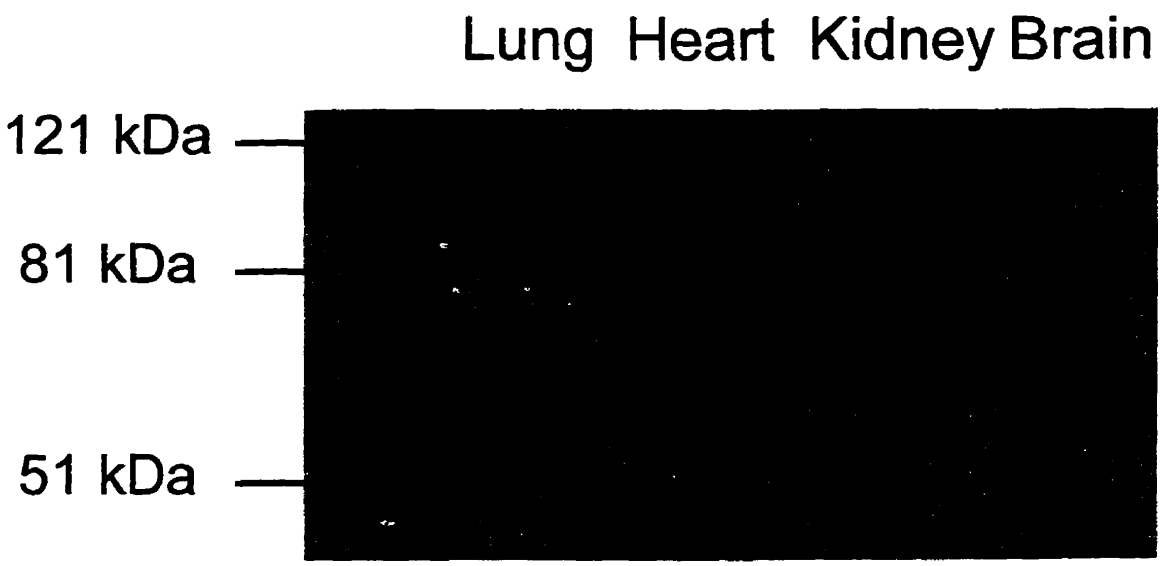

A western blot was treated with rCNT1 antibody AB1 (4000x dilution) and subsequently with biotinylated goat anti-rabbit IgG, streptavidin-linked horseradish peroxidase (POD) and diaminobenzidine (DAB) substrate system. A band of 80-90 kDa was detected with high levels in heart and kidney and lower levels in lung and brain.

Figure 34: Apparent Nuclear Staining with rCNT1 AB2

Sections of rat brain were fixed and treated with the AB2 rCNT1 antibody. Signal was detected using a secondary biotinylated goat anti-rabbit IgG antibody, streptavidin-linked horseradish peroxidase (POD) and diaminobenzidine (DAB) POD substrate. This figure shows that AB2 produced a signal in every discernable cell nucleus in the cerebellum, much the same as a nuclear stain like hematoxylin. Results were the same throughout all brain regions tested.

Figure 35: Distribution of rCNT1 Immunoreactivity in Rat Hippocampus

Sections of rat brain were fixed and treated with the AB1 rCNT1 antibody. Signal was detected using a secondary biotinylated goat anti-rabbit IgG antibody, streptavidin-linked horseradish peroxidase (POD) and diaminobenzidine (DAB) POD substrate. Results in cerebral cortex and choroid plexus are shown here. A control section treated with normal rabbit serum is shown in *A* and displays no signal. *B* shows staining of granule cells of the dentate gyrus (*DG*) and CA1 sublield (*CA1*) (40x magnification). Light staining of the molecular layer and stratum radiatum was noted.

Sections of rat brain were fixed and treated with the AB2 rCNT1 antibody. Signal was detected using a secondary biotinylated goat anti-rabbit IgG antibody, streptavidin-linked horseradish peroxidase (POD) and diaminobenzidine (DAB) POD substrate. Results in cerebral cortex and choroid plexus are shown here. Control sections treated with normal rabbit serum are shown in *A* and *C* and display no signal. *B* shows labeling of multiple layers of the cerebellum. Granule cells (*Gr*) and Purkinje cells (*Pk*) show immunoreactivity for rCNT2. A small number of cells in the molecular layer (*ML*) are also stained (400x magnification). *D* shows that a proportion of cells are labeled in the cortex (indicated by arrows) (400x magnification).

Figure 36: Distribution of rCNT1 Immunoreactivity in Rat Cerebellum and Cerebral Cortex

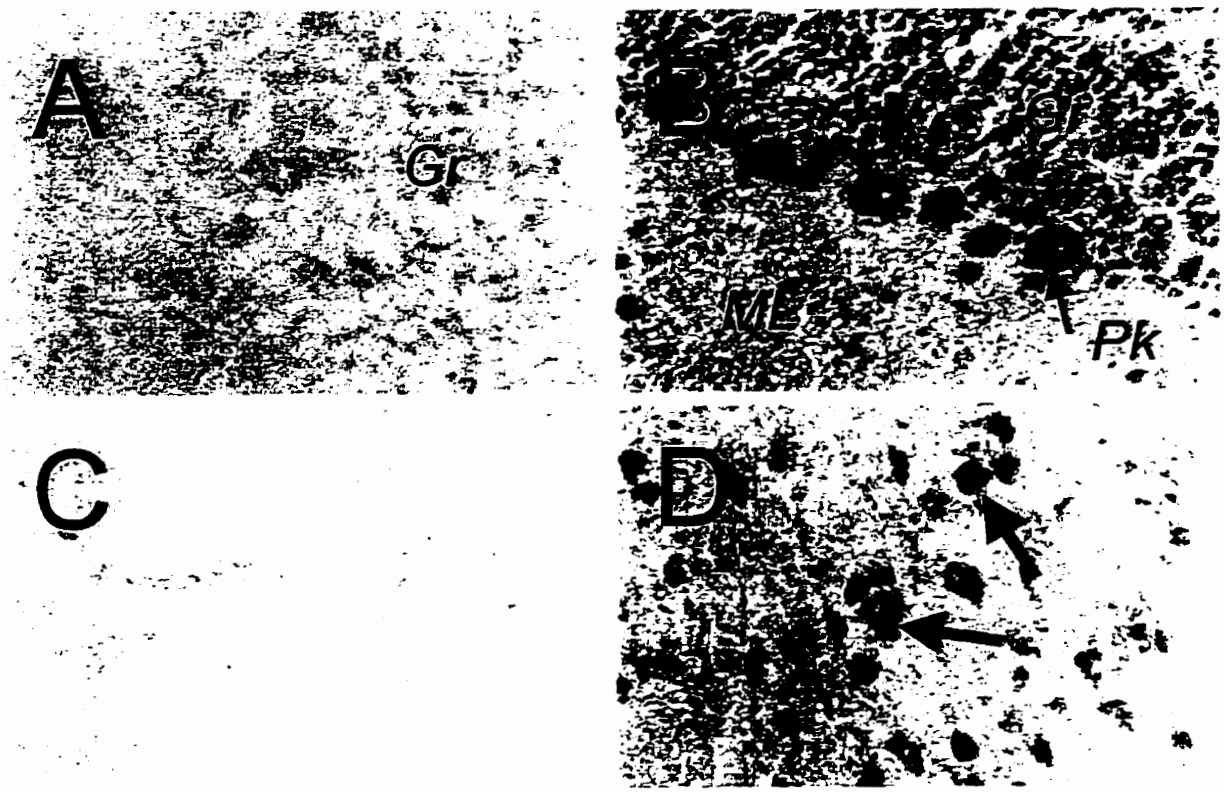

Chapter 7

General Discussion

The results presented in this thesis are the first to report the distribution of specific nucleoside transporter subtypes, other than ENT1, in brain. Probes for both hENT1 and hENT2 detected RNA species in every region tested in northern analysis of human brain total RNA. In general, message for all four cloned nucleoside transporter subtypes, determined by *in situ* hybridization, was seen in rat hippocampus, cerebellum cerebral cortex, striatum and other regions with varying relative abundances among regions for each transporter. rENT1 and rENT2 message was abundant throughout neuronal and non-neuronal cells layers of hippocampus and cerebellum and was detected in 50% and 80-90% of cerebral cortical neurons, respectively; results were similar in striatum and thalamus. rCNT1 expression was consistent throughout the layers of the hippocampus and cerebellum but generally at a low level; only about 10-20% of cells in cortex and striatum were positive. rCNT2 distribution appeared more heterogeneous. About 40-50% of cortical cells were positive. In hippocampus, dentate gyrus granule cells and CA1 pyramidal cells were rich in rCNT2 mRNA. Similarly, cerebellar granule neurons showed a strong hybridization signal. In contrast, predominantly non-neuronal cell layers in hippocampus and cerebellum showed low signal intensity. Binding of [^{3}H]NBMPR to rat brain sections to identify rENT1 transporters supported results from *in situ* hybridization in thalamus, cortex and striatum, however, in contrast to *in situ* hybridization, low signal intensity was seen in hippocampus and cerebellum indicating

low protein expression. Immunocytochemistry using antibodies for rCNT1 and rCNT2 generally confirmed results seen with *in situ* hybridization.

We saw a wide regional and cellular distribution for both equilibrative nucleoside transporters, rENT1 and rENT2, in rat brain. This suggests that the primary function of equilibrative transporters may be common in all cells, such as salvage of nucleosides for nucleotide synthesis. In rat, *ei* (rENT2) appears to be more abundant than rENT1 as 80-90% of cells in the cerebral cortex and other regions studied had rENT2 message while approximately 50-60% contained rENT1 mRNA. This is consistent with functional data in rat cerebral cortical synaptosomes reporting 60% *ei* transport and 40% *es* transport (Lee and Jarvis, 1988a). Many cell types appeared to have mRNA for both equilibrative transporters. The reason why two nucleoside transporter subtypes with nearly identical properties are necessary to a cell is unclear. The ratio of *ei* to *es* transport varies among species (Lee and Jarvis, 1998a,b; Jones and Hammond, 1995). This finding suggests that total equilibrative nucleoside transport capability is important since there is no clear functional outcome of this inter-species variation. The two equilibrative transporter subtypes could be alternatively regulated, providing flexibility in the cell's ability to adjust total equilibrative transport levels. rENT1 has three putative *N*-linked glycosylation sites (Yao *et al.*, 1997) and is known to be glycosylated *in vivo* (Kwong *et al.*, 1993). rENT2 has one conserved and one additional *N*-linked glycosylation site. These differences along with other modifications may lead to differential regulation of rENT1 and rENT2. rENT1 also appears to be regulated by protein kinase C activation (Sen *et al.*, 1998; Lee, 1994; Sinclair and Parkinson, 1998). It is not known if rENT2 is regulated in a similar manner. Similarly, it has not yet been determined whether ENT2 is

sensitive to inhibition by ethanol, as is ENT1. The identity of rENT2 to the full-length rHNP36 product may provide a clue as to the purpose of rENT2. rHNP36 is transcriptionally activated by growth factors indicating a proliferative role (Williams and Lanahan, 1995). It is possible that rENT2 is similarly activated. The truncated hHNP36 protein is nucleolar and has been detected in brain. This likely explains why we saw a band of ~1 kb on human northern blots. The question of interest is: do differences in function and/or regulation of rENT1 and rENT2 exist in cells that express both transporters? Enough evidence exists currently to speculate that this may be the case, however further experiments are required. This is now more feasible with the availability of clones for human and rat ENT2 homologs.

A broad distribution of both concentrative nucleoside transporter subtypes was also seen. Because rCNT1 is selective for pyrimidine nucleosides and rCNT2 is selective for purine nucleosides, this finding is not as surprising as with the equilibrative transporters. Cells making use of concentrative nucleoside transport may need at least two systems to achieve transport of a broad range of nucleoside permeants. Additionally, however, the enriched message for rCNT2 compared to rCNT1 seen in cortex (40-50% *vs* 10-20% of cells, respectively), dentate gyrus, CA1 and cerebellar granule cells indicates that cells in these regions preferentially require a means of transporting purine nucleosides. It is tempting to speculate that the need for regulation of adenosine and its signaling properties in these regions is the reason for this finding.

Both equilibrative and concentrative nucleoside transporters may be involved in the regulation of endogenous adenosine levels in brain. Cloned rENT1 and rENT2 both transported adenosine well (Yao *et al.*, 1997), although kinetic studies have not yet been

published with adenosine. rCNT2 is able to transport adenosine with a K_M of ~6 μM and a V_{max} 35-fold higher than the pyrimidine nucleoside thymidine (Che *et al.*, 1995). rCNT1 has a high affinity for adenosine (~15 μM *vs* ~20 μM for uridine) but a very low V_{max} (V_{max}/K_M = 0.01 *vs* ~0.5 for uridine) (Fang *et al.*, 1996). Adenosine is considered an inhibitor of rCNT1 in view of these data. Regulation of adenosine by rCNT2, rENT1 and rENT2 appears to be important for regulation of adenosine receptor stimulation. We have shown that these three transporter subtypes are present in brain regions rich in adenosine receptors. A_{2A}ARs are abundant in striatum (Parknson and Fredholm, 1990) where we saw varying levels of expression of all four transporter subtypes. A_{2B}ARs are present on glial cells and are nearly ubiquitous in brain; we saw evidence for rENT1, rENT2 and rCNT1 mRNA in glial cells of rat brain. While generally expressed at low levels in brain, A_3ARs are relatively densely localized to the hippocampus and cerebellum in rat brain, two regions where expression of equilibrative and concentrative transporters was evident. Perhaps of greatest interest with respect to cerebral ischemia is the A_1AR. High levels of expression have been reported in cortex, cerebellum, hippocampus and thalamus (Fredholm *et al.*, 1994). Again, these are regions where mRNA and protein for both equilibrative and concentrative nucleoside transporters were detected, suggesting that there may be cellular co-localization and participation by nucleoside transporters in regulation of adenosine receptor activation. Co-localization studies with adenosine receptor probes would be useful to determine which transporter/s is/are co-expressed with ARs on specific cell types.

A case of particular interest to us is regulation of endogenous adenosine levels during cerebral ischemia. Large increases in adenosine levels occur during ischemic

damage because of severely depressed ATP synthesis. As discussed earlier, the effects of adenosine at A_1ARs are neuroprotective. From a therapeutic standpoint, it may be useful to inhibit reuptake of adenosine, thereby enhancing neuroprotective effects of A_1AR stimulation. Theoretically in ischemia, extracellular adenosine levels rise enhancing the concentration gradient driving uptake through equilibrative transporters. In support of this, NBMPR (unpublished data) and propentofylline (Parkinson *et al.*, 1994), inhibitors of adenosine uptake, both protected hippocampal neurons following ischemic injury. Adenosine transport through Na^+-dependent (concentrative) transporters in brain is linked to energy supply in a manner unlike that seen with equilibrative transport. Since adenosine uptake through CNT2 is ATP-dependent, depressed ATP production would be expected to cause inhibition of adenosine uptake and enhancement of extracellular adenosine levels. Some evidence suggests that reversal of CNT2 is possible *in vitro*, allowing adenosine release (Borgland and Parkinson, 1997). There is no supporting evidence for this observation *in vivo*.

It is important to recognize that regulation of endogenous adenosine levels *in vivo* involves multiple processes. Not only adenosine release through transporters must be considered, but also breakdown of extracellular ATP to adenosine, both intra- and extracellular metabolism of adenosine itself, and how different transporter subtypes interact together on different cell types to achieve interstitial adenosine regulation in a localized area. A number of further experiments are required to investigate overall regulation of adenosine. First, it is important to determine the cellular distributions of each cloned transporter subtype. Co-localization studies with GFAP, to determine astrocytic transporter subtypes, and MAP-2, to determine neuronal subtypes in the CA1

subfield of the hippocampus would be useful for our interest in ischemia in the CA1 subfield of the hippocampus. Further studies co-localizing transporter subtypes with ecto-nucleotidases and ecto-adenosine deaminase activity would also help to clarify the processes by which adenosine is regulated. When this information is available, it will be easier to predict trends in adenosine levels in localized regions of brain.

Finally, while determining the distributions of transporter subtypes in relation to adenosine receptors and metabolizing enzymes is an important step, ultimately the goal is to ascertain the function of these nucleoside transporters *in vivo*. Employing conditional knockout or *in vivo* antisense strategies would provide valuable information regarding function by allowing observation of the phenotypic consequences of deleting or decreasing expression of particular transporter subtypes in brain. Two strategies may be of particular use in the current situation. Knockout of one of the equilibrative transporters would be useful to determine if expression of the remaining equilibrative subtype is enhanced in response to maintain overall equilibrative adenosine transport levels. A knockout strategy would also reveal any obvious phenotypic outcomes of deleting one of the equilibrative transporters and both knockout and antisense strategies would allow analysis of differences in the way adenosine levels are regulated in ischemic conditions relative to normal animals. A similar approach would be helpful in understanding the role of CNT2 in regulating adenosine in brain. Few functional studies have been able to detect concentrative nucleoside transport in brain preparations yet we have shown a wide distribution in rat brain. Traditionally, concentrative nucleoside transporters were considered to have a specialized distribution, being localized to tissues important for transporting many compounds (kidney, jejunum, choroid plexus). As a

result, little is known about the purpose of CNT2 in brain. A knockout strategy would assist in revealing the roles of CNT2 in, adenosine or non-adenosine-mediated.

To summarize, the determination of the regional, and to some extent cellular, distributions of specific nucleoside transporter subtypes in rat and human brain is a valuable contribution to understanding how adenosine levels are regulated in brain. Many studies remain, however, in order to decipher how adenosine levels are regulated *in vivo* in specific brain regions, and to elucidate the functions of specific nucleoside transporter subtypes.

REFERENCES

Abbracchio MP, Burnstock G (1994) Purinoceptors: Are there families of P2X and P2Y purinoceptors? Pharmac Ther 64:445-475.

Abbracchio MP, Ceruti S, Brambilla R, Franceschi C, Malorni W, Jacobson KA, von Lubitz DKJE, Cattabeni F (1997) Modulation of apoptosis by adenosine in the central nervous system: a possible role for the A_3 receptor. Ann NY Acad Sci 825:11-22.

Altiok N, Balmforth AJ, Fredholm BB (1992) Adenosine receptor-induced cAMP changes in D384 astrocytoma cells and the effect of bradykinin thereon. Acta Physiol Scand 144:55-63.

Anderson CM, Parkinson FE (1997) Potential signaling roles for UTP and UDP: sources, regulation and release of uracil nucleotides. Trends Pharmacol Sci 18:387-392.

Anderson CM, Sitar DS, Parkinson FE (1996b) Ability of nitrobenzylthioinosine to cross the blood-brain barrier in rats. Neurosci Lett 219:191-194.

Anderson CM, Xiong W, Young JD, Cass CE, Parkinson FE (1996a) Demonstration of the existence of mRNAs encoding N1/*cif* and N2/*cit* sodium/nucleoside cotransporters in rat brain. Mol Brain Res 42:358-361.

Andiné P, Rudolphi KA, Fredholm BB, Hagberg H (1990) Effect of propentofylline (HWA 285) on extracellular purines and excitatory amino acids in CA1 of rat hippocampus during transient ischaemia. Br J Pharmacol 100:814-818.

Arai A, Lynch G (1992) Factors regulating the magnitude of long-term potentiation induced by theta pattern stimulation. Brain Res 598:173-184.

Banay-Schwartz M, de Guzman T, Lajtha A (1980) Nucleoside uptake by slices of mouse brain. J Neurochem 35:544-551.

Barros LF, Yudilevich DL, Jarvis SM, Beaumont N, Young JD, Baldwin SA (1995) Immunolocalisation of nucleoside transporters in human placental trophoblast and endothelial cells: evidence for multiple transporter isoforms. Pflügers Arch 429:394-399.

Battastini AM, da Rocha JB, Barcellos CK, Dias RD, Sarkis JJ (1991) Characterization of an ATP diphosphohydrolase (EC 3.6.1.5) in synaptosomes from cerebral cortex of adult rats. Neurochem Res 16:1303-1310.

Belt JA (1983) Nitrobenzylthioinosine-insensitive uridine transport in human lymphoblastoid and murine leukemia cells. Biochem Biophys Res Commun 110:417-423.

Belt JA, Marina NM, Phelps DA, Crawford CR (1993) Nucleoside transport in normal and neoplastic cells. Adv Enzyme Regul 33:235-252.

Bender AS, Woodbury DM, White HS (1994) Ionic dependence of adenosine uptake into cultured astrocytes. Brain Res 661:1-8.

Bender AS, Wu PH, Phillis JW (1980) The characterization of [^{3}H]adenosine uptake into rat cerebral cortical synaptosomes. J Neurochem 35:629-640.

Bender AS, Wu PH, Phillis JW (1981) The rapid uptake and release of [^{3}H]adenosine by rat cerebral cortical synaptosomes. J Neurochem 36:651-660.

Berne RM (1963) Cardiac nucleotides in hypoxia: possible role in regulation of coronary blood flow. Am J Physiol 204:317-322.

Bhattacharya S, Dewitt DL, Burnatowska Hledin M, Smith WL, Spielman WS (1993) Cloning of an adenosine A1 receptor-encoding gene from rabbit. Gene 128:285-288.

Bhattacharya S, Linden J (1995) The allosteric enhancer, PD 81,723, stabilizes human A_1 adenosine receptor coupling to G proteins. Biochim Biophys Acta 1265:15-21.

Bischofberger N, Jacobson KA, von Lubitz DKJE (1997) Adenosine A_1 receptor agonists as clinically viable agents for treatment of ischemic brain disorders. Ann NY Acad Sci 825:23-29.

Bisserbe JC, Patel J, Marangos PJ (1985) Autoradiographic localization of adenosine uptake sites in rat brain using [^{3}H]nitrobenzylthioinosine. J Neurosci 5:544-550.

Boehm S, Huck S, Illes P (1995) UTP- and ATP-triggered transmitter release from rat sympathetic neurones via separate receptors. Br J Pharmacol 116:2341-2343.

Borgland SL, Parkinson FE (1997) Uptake and release of [^{3}H]formycin B via sodium-dependent nucleoside transporters in mouse leukemic L1210/MA27.1 cells. J Pharmacol Exp Ther 281:347-353.

Boumah CE, Harvey CM, Paterson AR, Baldwin SA, Young JD, Cass CE (1994) Functional expression of the nitrobenzylthioinosine-sensitive nucleoside transporter of human choriocarcinoma (BeWo) cells in isolated oocytes of Xenopus laevis. Biochem J 299:769-773.

Boyer JL, Lazarowski ER, Chen XH, Harden TK (1993) Identification of a P2Y-purinergic receptor that inhibits adenylyl cyclase. J Pharmacol Exp Ther 267:1140-1146.

Braun S, Levitzki A (1979) Adenosine receptor permanently coupled to turkey erythrocyte adenylate cyclase. Biochemistry 18:2134-2138.

Brodie MS, Lee K, Fredholm BB, Stahle L, Dunwiddie TV (1987) Central versus peripheral mediation of responses to adenosine receptor agonists: evidence against a central mode of action. Brain Res 415:323-330.

Brown RD, Manno JE (1978) ESTRIP, a BASIC computer program for obtaining initial polyexponential parameter estimates. J Pharm Sci 67:1687-1691.

Burnstock G (1972) Purinergic nerves. Pharmac Rev 24:509-581.

Burnstock G (1978) A basis for distinguishing two types of purinergic receptor. In: Cell Membrane Receptors for Drugs and Hormones: A Multidisciplinary Approach (Straub RW, Bolis L eds), pp 107-118. New York: Raven Press.

Burnstock G, Brown CM (1981) An introduction to purinergic receptors. In: Purinergic receptors (Burnstock G ed), pp 1-46. London, UK: Chapman and Hall.

Burnstock G, Kennedy C (1985) Is there a basis for distinguishing two types of P_2-purinoceptor? Gen Pharmacol 16:433-440.

Burnstock G, King B (1996) Numbering of cloned P_2 purinoceptors. Drug Devel Res 38:67-71.

Cai J, Lee CW (1996) Tamoxifen inhibits nitrobenzylthioinosine-sensitive equilibrative uridine transport in human MCF-7 breast cancer cells. Biochem J 320:991-995.

Cass CE (1995) Nucleoside transport. In: Drug transport in antimicrobial and anticancer chemotherapy (Georgopapadakou NH ed), pp 403-450. New York: Marcel Dekker.

Cass CE, Gaudette LA, Paterson ARP (1974) Mediated transport of nucleosides in human erythrocytes: specific binding of the inhibitor nitrobenzylthioinosine to nucleoside transport sites in the erythrocytes membrane. Biochim Biophys Acta 345:1-10.

Cass CE, Paterson ARP (1972) Mediated transport of nucleosides in human erythrocytes. Accelerative exchange diffusion of uridine and thymidine and specificity toward pyrimidine nucleosides as permeants. J Biol Chem 247:3314-3320.

Cass CE, Paterson ARP (1973) Mediated transport of nucleosides by human erythrocytes. Specificity toward pyrimidine nucleosides as permeants. Biochim Biophys Acta 291:734-746.

Ceruti S, Barbieri D, Franchesi C, Giammaroli AM, Rainaldi G, Malorni W, Kim HO, von Lubitz DKJE, Jacobson KA, Cattabeni F, Abbracchio MP (1996) Effects of adenosine A_3 receptor agonists on astrocytes: induction of cell protection at low and cell death at high concentrations. Drug Devel Res 3:177

Chang K, Hanaoka K, Kumada M, Takuwa Y (1995) Molecular cloning and functional analysis of a novel P_2 nucleotide receptor. J Biol Chem 270:26152-26158.

Che M, Ortiz DF, Arias IM (1995) Primary structure and functional expression of a cDNA encoding the bile canalicular, purine-specific Na^+-nucleoside cotransporter. J Biol Chem 270:13596-13599.

Chen CC, Akopian AN, Sivilotti L, Colquhoun D, Burnstock G, Wood JN (1995) A P2X purinoceptor expressed by a subset of sensory neurons. Nature 377:428-431.

Cheng Y, Prusoff WH (1973) Relationship between the inhibition constant (K_i) and the concentration of inhibitor which causes 50 per cent inhibition (I_{50}) of an enzymatic reaction. Biochem Pharmacol 22:3099-3108.

Chomczynski P, Sacchi N (1987) Single-step method of RNA isolation by acid guanidinium thiocyanate-phenol-chloroform extraction. Anal Biochem 162:156-159.

Chow SC, Kass GEN, Orrenius S (1997) Purines and their roles in apoptosis. Neuropharmacology 36:1149-1156.

Ciruela F, Saura C, Canela EI, Mallol J, LLuis C, Franco R (1996) Adenosine deaminase affects ligand-induced signaling by interacting with cell surface adenosine receptors. FEBS Lett 380:219-223.

Ciruela F, Saura C, Canela EI, Mallol J, LLuis C, Franco R (1997) Ligand-induced phosphorylation, clustering, and desensitization of A_1 adenosine receptors. Mol Pharmacol 52:788-797.

Clark M, Dar MS (1989) Effect of acute ethanol on uptake of [^{3}H]adenosine by rat cerebellar synaptosomes. Alcohol Clin Exp Res 13:371-377.

Clark M, Dar MS (1989) Effect of acute ethanol on release of endogenous adenosine from rat cerebellar synaptosomes. J Neurochem 52:1859-1865.

Cohen FR, Lazareno S, Birdsall NJ (1996) The affinity of adenosine for the high- and low-affinity states of the human adenosine A_1 receptor. Eur J Pharmacol 309:111-114.

Collo G, Neidhart S, Kawashima E, Kosco-Vilbois M, North RA, Buell G (1997) Tissue distribution of the $P2X_7$ receptor. Neuropharmacology 36:1277-1284.

Communi D, Parmentier M, Boeynaems JM (1996) Cloning, functional expression and tissue distribution of the human $P2Y_6$ receptor. Biochem Biophys Res Commun 222:303-308.

Communi D, Pirotton S, Parmentier M, Boeynaems JM (1995) Cloning and functional expression of a human uridine nucleotide receptor. J Biol Chem 270:30849-30852.

Connolly GP (1994) Evidence from desensitization studies for distinct receptors for ATP and UTP on the rat superior cervical ganglion. Br J Pharmacol 112:357-359.

Crawford CR, Patel DH, Naeve C, Belt JA (1998) Cloning of the human equlibrative, nitrobenzylmercaptopurine riboside (NBMPR)-insensitive nucleoside transporter ei by functional expression in a transport-deficient cell line. J Biol Chem 273:5288-5293.

Crawley JN, Patel J, Marangos PJ (1983) Adenosine uptake inhibitors potentiate the sedative effects of adenosine. Neurosci Lett 36:169-174.

Dar MS (1990) Functional correlation between subclasses of brain adenosine receptor affinities and ethanol-induced motor incoordination in mice. Pharmacol Biochem Behav 37:747-753.

Dar MS (1990) Central adenosinergic system involvement in ethanol-induced motor incoordination in mice. J Pharmacol Exp Ther 255:1202-1209.

Dar MS (1996) Mouse cerebellar $GABA_B$ participation in the expression of acute ethanol-induced ataxia and in its modulation by the cerebellar adenosinergic A_1 system. Brain Res Bull 41:53-59.

Dar MS (1997) Mouse cerebellar adenosinergic modulation of ethanol-induced motor incoordination: Possible involvement of cAMP. Brain Res 749:263-274.

Dar MS, Bowman ER, Li C (1994) Intracerebellar nicotinic-cholinergic participation in the cerebellar adenosinergic modulation of ethanol-induced motor incoordination in mice. Brain Res 644:117-127.

Dawicki DD, Chatterjee D, Wyche J, Rounds S (1997) Extracellular ATP and adenosine cause apoptosis of pulmonary artery endothelial cells. Am J Physiol 273:L485-94.

Dawson JM, Cook ND, Coade SB, Baum H, Peters TJ (1986) Demonstration of plasma-membrane adenosine diphosphatase activity in rat lung. Biochim Biophys Acta 856:566-570.

De Mendonça A, Ribeiro JA (1994) Endogenous adenosine modulates long-term potentiation in the hippocampus. Neuroscience 62:385-390.

De Mendonça A, Ribeiro JA (1997) Adenosine and neuronal plasticity. Life Sci 60:245-251.

Debanne D, Guerineau NC, Gahwiler BH, Thompson SM (1996) Paired-pulse facilitation and depression at unitary synapses in rat hippocampus: quantal fluctuation affects subsequent release. J Physiol Lond 491:163-176.

Deckert J, Bisserbe JC, Klein E, Marangos PJ (1988) Adenosine uptake sites in brain: regional distribution of putative subtypes in relationship to adenosine A_1-receptors. J Neurosci 8:2338-2349.

Deckert J, Bisserbe JC, Marangos PJ (1987) Quantitative [^{3}H]dipyridamole autoradiography: evidence for adenosine transporter heterogeneity in guinea pig brain. Naunyn Schmiedebergs Arch Pharmacol 335:660-666.

Decking UK, Schlieper G, Kroll K, Schrader J (1997) Hypoxia-induced inhibition of adenosine kinase potentiates cardiac adenosine release. Circ Res 81:154-164.

Delaney SM, Geiger JD (1995) Enhancement of NMDA-induced increases in levels of endogenous adenosine by adenosine deaminase and adenosine transport inhibition in rat striatum. Brain Res 702:72-76.

Delaney SM, Geiger JD (1996) Brain regional levels of adenosine and adenosine nucleotides in rats killed by high-energy focused microwave irradiation. J Neurosci Methods 64:151-156.

Delaney SM, Sutherland GR, Peeling J, Geiger JD (1993) Failure of 2'-deoxycoformycin to protect against transient forebrain ischemia in rat. Neurosci Lett 149:31-34.

DeLeo J, Schubert P, Kreutzberg GW (1988) Propentofylline (HWA 285) protects hippocampal neurons of Mongolian gerbils against ischemic damage in the presence of an adenosine antagonist. Neurosci Lett 84:307-311.

Delicado EG, Sen RP, Miras Portugal MT (1991) Effects of phorbol esters and secretagogues on nitrobenzylthioinosine binding to nucleoside transporters and nucleoside uptake in cultured chromaffin cells. Biochem J 279:651-655.

Drury AN, Szent-Györgyi A (1929) The physiological activity of adenine compounds with special reference to their action upon the mammalian heart. J Physiol Lond 68:213-237.

Dunwiddie TV, Diao L, Kim HO, Jiang J, Jacobson KA (1997) Activation of hippocampal adenosine A_3 receptors produces a desensitization of A_1 receptor-mediated responses in rat hippocampus. J Neurosci 17(2):604-614.

Dunwiddie TV, Haas HL (1985) Adenosine increases synaptic facilitation in the in vitro rat hippocampus: evidence for a presynaptic site of action. J Physiol Lond 369:365-377.

Eccles JC (1964) The physiology of synapses. Berlin: Springer-Verlag.

Fallahi N, Broad RM, Jin SY, Fredholm BB (1996) Release of adenosine from rat hippocampal slices by nitric oxide donors. J Neurochem 67:186-193.

Fang X, Parkinson FE, Mowles DA, Young JD, Cass CE (1996) Functional characterization of a recombinant sodium-dependent nucleoside transporter with selectivity for pyrimidine nucleosides ($cNT1_{rat}$) by transient expression in cultured mammalian cells. Biochem J 317:457-465.

Ferré S, Fredholm BB, Morelli M, Popoli P, Fuxe K (1997) Adenosine-dopamine receptor-receptor interactions as an integrative mechanism in the basal ganglia. Trends Neurosci 20:482-487.

Ferré S, Fuxe K (1992) Dopamine denervation leads to an increase in the intramembrane interaction between adenosine A_2 and dopamine D_2 receptors in the neostriatum. Brain Res 594:124-130.

Ferré S, Fuxe K, von Euler G, Johansson B, Fredholm BB (1992) Adenosine-dopamine interactions in the brain. Neuroscience 51:501-512.

Ferré S, O'Connor WT, Fuxe K, Ungerstedt U (1993) The striopallidal neuron: a main locus for adenosine-dopamine interactions in the brain. J Neurosci 13:5402-5406.

Ferré S, O'Connor WT, Snaprud P, Ungerstedt U, Fuxe K (1994) Antagonistic interaction between adenosine A_{2A} receptors and dopamine D_2 receptors in the ventral striopallidal system. Implications for the treatment of schizophrenia. Neuroscience 63:765-773.

Ferré S, von Euler G, Johansson B, Fredholm BB, Fuxe K (1991) Stimulation of high-affinity adenosine A_2 receptors decreases the affinity of dopamine D_2 receptors in rat striatal membranes. Proc Natl Acad Sci USA 88:7238-7241.

Fink JS, Weaver DR, Rivkees SA, Peterfreund RA, Pollack AE, Adler EM, Reppert SM (1992) Molecular cloning of the rat A_2 adenosine receptor: selective co-expression with D_2 dopamine receptors in rat striatum. Brain Res Mol Brain Res 14:186-195.

Fisher MN, Newsholme EA (1984) Properties of rat heart adenosine kinase. Biochem J 221:521-528.

Flanagan SA, Meckling-Gill KA (1997) Characterization of a novel Na^+-dependent, guanosine-specific nitrobenzylthioinosine-sensitive transporter in acute promyelocytic leukemia cells. J Biol Chem 272:18026-18032.

Fredholm BB, Fuxe K, Agnati L (1976) Effect of some phosphodiesterase inhibitors on central dopamine mechanisms. Eur J Pharmacol 38:31-38.

Fredholm BB (1995) Purinoceptors in the nervous system. Pharmacol Toxicol 76:228-239.

Fredholm BB, Abbracchio MP, Burnstock G, Daly JW, Harden TK, Jacobson KA, Leff P, Williams M (1994) VI. Nomenclature and classification of purinoceptors. Pharmacol Rev 46:143-156.

Fredholm BB, Dunwiddie TV (1988) How does adenosine inhibit transmitter release? Trends Pharmacol Sci 9:130-134.

Fredholm BB, Hedqvist P (1980) Modulation of neurotransmission by purine nucleotides and nucleosides. Biochem Pharmacol 29:1635-1643.

Freissmuth M, Schutz W, Linder ME (1991) Interactions of the bovine brain A_1-adenosine receptor with recombinant G protein alpha-subunits. Selectivity for rG_i alpha-3. J Biol Chem 266:17778-17783.

Furlong TJ, Pierce KD, Selbie LA, Shine J (1992) Molecular characterization of a human brain adenosine A_2 receptor. Brain Res Mol Brain Res 15:62-66.

Gati WP, Paterson AR (1997) Measurement of nitrobenzylthioinosine in plasma and erythrocytes: a pharmacokinetic study in mice. Cancer Chemother Pharmacol 40:342-346.

Gebicke-Haerter PJ, Christoffel F, Timmer J, Northoff H, Berger M, van Calker D (1996) Both adenosine A_1- and A_2-receptors are required to stimulate microglial proliferation. Neurochem Int 29:37-42.

Geiger JD, Fyda DM (1991) Adenosine Transport in Nervous System Tissues. In: Adenosine in the Nervous System (Stone TL ed), pp 1-22. San Diego: Academic Press.

Geiger JD, Nagy JI (1984) Heterogeneous distribution of adenosine transport sites labelled by [^{3}H]nitrobenzylthioinosine in rat brain: an autoradiographic and membrane binding study. Brain Res Bull 13:657-666.

Geiger JD, Parkinson FE, Kowaluk EA (1997) Regulators of Endogenous Adenosine Levels as Therapeutic Agents. In: Purinergic Approaches in Experimental Therapeutics (Jacobson KA, Jarvis MF eds), pp 55-75. New York: Wiley-Liss, Inc.

Gerber U, Greene RW, Haas HL, Stevens DR (1989) Characterization of inhibition mediated by adenosine in the hippocampus of the rat in vitro. J Physiol Lond 417:567-578.

Gerwins P, Fredholm BB (1992) ATP and its metabolite adenosine act synergistically to mobilize intracellular calcium via the formation of inositol 1,4,5-trisphosphate in a smooth muscle cell line. J Biol Chem 267:16081-16087.

Gidday JM, Fitzgibbons JC, Shah AR, Kraujalis MJ, Park TS (1995) Reduction in cerebral ischemic injury in the newborn rat by potentiation of endogenous adenosine. Pediatr Res 38:306-311.

Gidday JM, Kim YB, Shah AR, Gonzales ER, Park TS (1996) Adenosine transport inhibition ameliorates postischemic hypoperfusion in pigs. Brain Res 734:261-268.

Glass M, Faull RL, Dragunow M (1996) Localisation of the adenosine uptake site in the human brain: a comparison with the distribution of adenosine A_1 receptors. Brain Res 710:79-91.

Gordon JL (1986) Extracellular ATP: effects, sources and fate. Biochem J 233:309-319.

Griffith DA, Jarvis SM (1996) Nucleoside and nucleobase transport systems of mammalian cells. Biochim Biophys Acta Rev Biomembr 1286:153-181.

Griffiths M, Beaumont N, Yao SYM, Sundaram M, Boumah CE, Davies A, Kwong FYP, Coe I, Cass CE, Young JD, Baldwin SA (1997a) Cloning of a human nucleoside transporter implicated in the cellular uptake of adenosine and chemotherapeutic drugs. Nature Med 3:89-93.

Griffiths M, Yao SYM, Abidi F, Phillips SEV, Cass CE, Young JD, Baldwin SA (1997b) Molecular cloning and characterization of a nitrobenzylthioinosine-insensitive (*ei*) equlibrative nucleoside transporter from human placenta. Biochem J 328:739-743.

Gu JG, Geiger JD (1992) Transport and metabolism of D-[^{3}H]adenosine and L-[^{3}H]adenosine in rat cerebral cortical synaptoneurosomes. J Neurochem 58:1699-1705.

Gu JG, Kala G, Geiger JD (1993) [^{3}H]adenosine transport in synaptoneurosomes of postmortem human brain. J Neurochem 60:2232-2237.

Gu JG, Nath A, Geiger JD (1996) Characterization of inhibitor-sensitive and -resistant adenosine transporters in cultured human fetal astrocytes. J Neurochem 67:972-977.

Gualix J, Abal M, Pintor J, Garcia Carmona F, Miras Portugal MT (1996) Nucleotide vesicular transporter of bovine chromaffin granules. Evidence for a mnemonic regulation. J Biol Chem 271:1957-1965.

Guieu R, Couraud F, Pouget J, Sampieri F, Bechis G, Rochat H (1996) Adenosine and the nervous system. Clin Neuropharmacol 19:459-474.

Gutierrez MM, Brett CM, Ott RJ, Hui AC, Giacomini KM (1992) Nucleoside transport in brush border membrane vesicles from human kidney. Biochim Biophys Acta 1105:1-9.

Haas HL, Greene RW (1988) Endogenous adenosine inhibits hippocampal CA1 neurones: further evidence from extra- and intracellular recording. Naunyn Schmiedebergs Arch Pharmacol 337:561-565.

Hada J, Kaku T, Morimoto K, Hayashi Y, Nagai K (1996) Adenosine transport inhibitors enhance high K(+)-evoked taurine release from rat hippocampus. Eur J Pharmacol 305:101-107.

Hammond JR, Clanachan AS (1985) Species differences in the binding of [^{3}H]nitrobenzylthioinosine to the nucleoside transport system in mammalian central nervous system membranes: evidence for interconvertible conformations of the binding site/transporter complex. J Neurochem 45:527-535.

Harden TK, Boyer JL, Nicholas RA (1995) P2-purinergic receptors: subtype-associated signaling responses and structure. Annu Rev Pharmacol Toxicol 35:541-579.

Harris EW, Cotman CW (1986) Long-term potentiation of guinea pig mossy fiber responses is not blocked by N-methyl D-aspartate antagonists. Neurosci Lett 70:132-137.

Hassessian H, Bodin P, Burnstock G (1993) Blockade by glibenclamide of the flow-evoked endothelial release of ATP that contributes to vasodilatation in the pulmonary vascular bed of the rat. Br J Pharmacol 109:466-472.

Headrick JP, Bendall MR, Faden AI, Vink R (1994) Dissociation of adenosine levels from bioenergetic state in experimental brain trauma: Potential role in secondary injury. J Cereb Blood Flow Metab 14:853-861.

Heese K, Fiebich BL, Bauer J, Otten U (1997) Nerve growth factor (NGF) expression in rat microglia is induced by adenosine A_{2A}-receptors. Neurosci Lett 231:83-86.

Heurteaux C, Lauritzen I, Widmann C, Lazdunski M (1995) Essential role of adenosine, adenosine A_1 receptors, and ATP-sensitive K^+ channels in cerebral ischemic preconditioning. Proc Natl Acad Sci USA 92:4666-4670.

Hindley S, Herman MAR, Rathbone MP (1994) Stimulation of reactive astrogliosis in vivo by extracellular adenosine diphosphate or an adenosine A_2 receptor agonist. J Neurosci Res 38:399-406.

Hoehn K, White TD (1990) N-methyl-D-aspartate, kainate and quisqualate release endogenous adenosine from rat cortical slices. Neuroscience 39:441-450.

Holton FA, Holton P (1954) The capillary dilator substances in dry powders of spinal roots: a possible role of ATP in chemical transmission from nerve endings. J Physiol Lond 126:124-140.

Holton P (1959) the liberation of adenosine triphosphate on antidromic stimulation of sensory nerves. J Physiol Lond 145:494-504.

Hoque AN, Hoque N, Hashizume H, Abiko Y (1995) A study on dilazep: I. Mechanism of anti-ischemic action of dilazep is not coronary vasodilation but decreased cardiac mechanical function in the isolated, working rat heart. Jpn J Pharmacol 67:225-232.

Hosli E, Hosli L (1988) Autoradiographic studies on the uptake of adenosine and on binding of adenosine analogues in neurons and astrocytes of cultured rat cerebellum and spinal cord. Neuroscience 24:621-628.

Huang Q-Q, Yao SYM, Ritzel MWL, Paterson ARP, Cass CE, Young JD (1994) Cloning and functional expression of a complementary DNA encoding a mammalian nucleoside transport protein. J Biol Chem 269:17757-17760.

Huang QQ, Harvey CM, Paterson AR, Cass CE, Young JD (1993) Functional expression of Na^+-dependent nucleoside transport systems of rat intestine in isolated oocytes of Xenopus laevis. Demonstration that rat jejunum expresses the purine-selective system N1 (cif) and a second, novel system N3 having broad specificity for purine and pyrimidine nucleosides. J Biol Chem 268:20613-20619.

Huber M, Kittner B, Hojer C, Fink GR, Neveling M, Heiss WD (1993) Effect of propentofylline on regional cerebral glucose metabolism in acute ischemic stroke. J Cereb Blood Flow Metab 13:526-530.

Huston JP, Haas HL, Boix F, Pfister M, Decking U, Schrader J, Schwarting RK (1996) Extracellular adenosine levels in neostriatum and hippocampus during rest and activity periods of rats. Neuroscience 73:99-107.

Jacobson KA, von Lubitz DK, Daly JW, Fredholm BB (1996) Adenosine receptor ligands: differences with acute versus chronic treatment. Trends Pharmacol Sci 17:108-113.

James S, Richardson PJ (1993) Production of adenosine from extracellular ATP at the striatal cholinergic synapse. J Neurochem 60:219-227.

Jiang N, Kowaluk EA, Lee CH, Mazdiyasni H, Chopp M (1997) Adenosine kinase inhibition protects brain against transient focal ischemia in rats. Eur J Pharmacol 320:131-137.

Johnston ME, Geiger JD (1989) Sodium-dependent uptake of nucleosides by dissociated brain cells from the rat. J Neurochem 52:75-81.

Jones KW, Hammond JR (1995) Characterization of nucleoside transport activity in rabbit cortical synaptosomes. Can J Physiol Pharmacol 73:1733-1741.

Jones ME (1980) Pyrimidine nucleotide biosynthesis in animals: genes, enzymes, and regulation of UMP biosynthesis. Ann Rev Biochem 49:253-279.

Katsuragi T, Matsuo K, Sato C, Honda K, Kamiya H, Furukawa T (1996) Non-neuronal release of ATP and inositol 1,4,5-trisphosphate accumulation evoked by P_2- and M-receptor stimulation in guinea pig ileal segments. J Pharmacol Exp Ther 277:747-752.

Keil GJ, II, DeLander GE (1994) Adenosine kinase and adenosine deaminase inhibition modulate spinal adenosine- and opioid agonist-induced antinociception in mice. Eur J Pharmacol 271:37-46.

Kohno Y, Sei Y, Koshiba M, Kim HO, Jacobson KA (1996) Induction of apoptosis in HL-60 human promyelocytic leukemia cells by adenosine A_3 receptor agonists. Biochem Biophys Res Commun 219:904-910.

Kollias Baker CA, Ruble J, Jacobson M, Harrison JK, Ozeck M, Shryock JC, Belardinelli L (1997) Agonist-independent effect of an allosteric enhancer of the A_1 adenosine receptor in CHO cells stably expressing the recombinant human A_1 receptor. J Pharmacol Exp Ther 281:761-768.

Kwong FY, Davies A, Tse CM, Young JD, Henderson PJ, Baldwin SA (1988) Purification of the human erythrocyte nucleoside transporter by affinity chromatography. Biochem J 255:243-249.

Lai HL, Yang TH, Messing RO, Ching YH, Lin SC, Chern Y (1997) Protein kinase C inhibits adenylyl cyclase type VI activity during desensitization of the A_{2A}-adenosine receptor-mediated cAMP response. J Biol Chem 272:4970-4977.

Lawrence AJ, Castillo Melendez M, Jarrott B (1994) [^{3}H]Adenosine transport in rat dorsal brain stem using a crude synaptosomal preparation. Neurochem Int 25:221-226.

Lazarowski ER, Watt WC, Stutts MJ, Boucher RC, Harden TK (1995) Pharmacological selectivity of the cloned human P2U-purinoceptor: potent activation by diadenosine tetraphosphate. Br J Pharmacol 116:1619-1627.

Ledent C, Vaugeois J, Schiffman SN, Pedrazzini T, El Yacoub M, Vanderhaeghen J, Costentin J, Heath JK, Vassart G, Parmentier M (1997) Aggressiveness, hypoalgesia and high blood pressure in mice lacking the adenosine A_{2A} receptor. Nature 388:674-678.

Lee CW (1994) Decrease in equilibrative uridine transport during monocytic differentiation of HL-60 leukaemia: involvement of protein kinase. Biochem J 300:407-412.

Lee CW, Jarvis SM (1988a) Nucleoside transport in rat cerebral-cortical synaptosomes. Evidence for two types of nucleoside transporters. Biochem J 249:557-564.

Lee CW, Jarvis SM (1988b) Kinetic and inhibitor specificity of adenosine transport in guinea pig cerebral cortical synaptosomes: evidence for two nucleoside transporters. Neurochem Int 12:483-492.

Lewis C, Neidhart S, Holy C, North RA, Buell G, Surprenant A (1995) Coexpression of $P2X_2$ and $P2X_3$ receptor subunits can account for ATP-gated currents in sensory neurons. Nature 377:432-435.

Libert F, Parmentier M, Lefort A, Dinsart C, Van Sande J, Maenhaut C, Simons MJ, Dumont JE, Vassart G (1989) Selective amplification and cloning of four new members of the G protein-coupled receptor family. Science 244:569-572.

Libert F, Schiffmann SN, Lefort A, Parmentier M, Gerard C, Dumont JE, Vanderhaeghen JJ, Vassart G (1991) The orphan receptor cDNA RDC7 encodes an A_1 adenosine receptor. EMBO J 10:1677-1682.

Libert F, Van Sande J, Lefort A, Czernilofsky A, Dumont JE, Vassart G, Ensinger HA, Mendla KD (1992) Cloning and functional characterization of a human A_1 adenosine receptor. Biochem Biophys Res Commun 187:919-926.

Linden J (1993) Purinergic systems. In: Basic Neurochemistry (Siegel JG, Agranoff B, Albers RW, Molinoff PB eds), pp 401-416. New York: Raven Press.

Linden J (1994) Cloned adenosine A_3 receptors: pharmacological properties, species differences and receptor functions. Trends Pharmacol Sci 15:298-306.

Linden J, Taylor HE, Robeva AS, Tucker AL, Stehle JH, Rivkees SA, Fink JS, Reppert SM (1993) Molecular cloning and functional expression of a sheep A_3 adenosine receptor with widespread tissue distribution. Mol Pharmacol 44:524-532.

Londos C, Cooper DMF, Wolff J (1980) Subclasses of external adenosine receptors. Proc Nat Acad Sci USA 77:2551-2554.

Long CJ, Stone TW (1987) Adenosine reduces agonist-induced production of inositol phosphates in rat aorta. J Pharm Pharmacol 39:1010-1014.

Lustig KD, Shiau AK, Brake AJ, Julius D (1993) Expression cloning of an ATP receptor from mouse neuroblastoma cells. Proc Natl Acad Sci USA 90:5113-5117.

Luthje J, Schomburg A, Ogilvie A (1988) Demonstration of a novel ecto-enzyme on human erythrocytes, capable of degrading ADP and of inhibiting ADP-induced platelet aggregation. Eur J Biochem 175:285-289.

Maenhaut C, Van Sande J, Libert F, Abramowicz M, Parmentier M, Vanderhaegen JJ, Dumont JE, Vassart G, Schiffmann S (1990) RDC8 codes for an adenosine A_2 receptor with physiological constitutive activity. Biochem Biophys Res Commun 173:1169-1178.

Mager R, Ferroni S, Schubert P (1990) Adenosine modulates a voltage-dependent chloride conductance in cultured hippocampal neurons. Brain Res 532:58-62.

Magnuson DS, Knudsen BE, Geiger JD, Brownstone RM Nath A (1995) Human immunodeficiency virus type 1 tat activates non-N-methyl-D-aspartate excitatory amino acid receptors and causes neurotoxicity. Ann Neurol 37(3):373-380.

Mahan LC, McVittie LD, Smyk Randall EM, Nakata H, Monsma FJ, Jr., Gerfen CR, Sibley DR (1991) Cloning and expression of an A_1 adenosine receptor from rat brain. Mol Pharmacol 40:1-7.

Mally J, Stone TW (1994) The effect of theophylline on Parkinsonian symptoms. J Pharm Pharmacol 46:515-517.

Meyerhof W, Muller Brechlin R, Richter D (1991) Molecular cloning of a novel putative G-protein coupled receptor expressed during rat spermiogenesis. FEBS Lett 284:155-160.

Miller LP, Hsu C (1992) Therapeutic potential for adenosine receptor activation in ischemic brain injury. J Neurotrauma 9 Suppl 2:S563-S577.

Muller J, Rocha JB, Battastini AM, Sarkis JJ, Dias RD (1993) Postnatal development of ATPase-ADPase activities in synaptosomal fraction from cerebral cortex of rats. Neurochem Int 23:471-477.

Mun EC, Tally KJ, Matthews JB (1998) Characterization and regulation of adenosine transport in T84 intestinal epithelial cells. Am J Physiol 274:G261-G269.

Munshi R, Pang IH, Sternweis PC, Linden J (1991) A_1 adenosine receptors of bovine brain couple to guanine nucleotide-binding proteins G_{i1}, G_{i2}, and G_o. J Biol Chem 266:22285-22289.

Nagy LE, Diamond I, Casso DJ, Franklin C, Gordon AS (1990) Ethanol increases extracellular adenosine by inhibiting adenosine uptake via the nucleoside transporter. J Biol Chem 265:1946-1951.

Nanoff C, Freissmuth M, Tuisl E, Schutz W (1990) P_2-, but not P_1-purinoceptors mediate formation of 1,4,5-inositol trisphosphate and its metabolites via a pertussis toxin-insensitive pathway in the rat renal cortex. Br J Pharmacol 100:63-68.

Nanoff C, Jacobson KA, Stiles GL (1991) The A_2 adenosine receptor: guanine nucleotide modulation of agonist binding is enhanced by proteolysis. Mol Pharmacol 39:130-135.

Neary JT, Rathbone MP, Cattabeni F, Abbracchio MP, Burnstock G (1996) Trophic actions of extracellular nucleotides and nucleosides on glial and neuronal cells. Trends Neurosci 19:13-18.

Nicholas RA, Watt WC, Lazarowski ER, Li Q, Harden K (1996) Uridine nucleotide selectivity of three phospholipase C-activating P_2 receptors: identification of a UDP-selective, a UTP-selective, and an ATP- and UTP-specific receptor. Mol Pharmacol 50:224-229.

Nuttle LC, el Moatassim C, Dubyak GR (1993) Expression of the pore-forming P2Z purinoreceptor in Xenopus oocytes injected with poly(A)$^+$ RNA from murine macrophages. Mol Pharmacol 44:93-101.

O'Connor SD, Stojanovic M, Radulovacki M (1991) The effect of soluflazine on sleep in rats. Neuropharmacology 30:671-674.

O'Regan MH, Simpson RE, Perkins LM, Phillis JW (1992) The selective A_2 adenosine receptor agonist CGS 21680 enhances excitatory transmitter amino acid release from the ischemic rat cerebral cortex. Neurosci Lett 138:169-172.

Ogata T, Schubert P (1996) Programmed cell death in rat microglia is controlled by extracellular adenosine. Neurosci Lett 218:91-94.

Ohkubo T, Mitsumoto Y, Mohri T (1991) Characterization of the uptake of adenosine by cultured rat hippocampal cells and inhibition of the uptake by xanthine derivatives. Neurosci Lett 133:275-278.

Olah ME, Ren H, Ostrowski J, Jacobson KA, Stiles GL (1992) Cloning, expression, and characterization of the unique bovine A_1 adenosine receptor. Studies on the ligand binding site by site-directed mutagenesis. J Biol Chem 267:10764-10770.

Olah ME, Stiles GL (1995) Adenosine receptor subtypes: characterization and therapeutic regulation. Annu Rev Pharmacol Toxicol 35:581-606.

Ongini E, Adami M, Ferri C, Bertorelli R (1997) Adenosine A_{2A} receptors and neuroprotection. Ann NY Acad Sci 825:30-48.

Ongini E, Fredholm BB (1996) Pharmacology of adenosine A_{2A} receptors. Trends Pharmacol Sci 17:364-372.

Pajor AM, Wright EM (1992) Cloning and functional expression of a mammalian Na^+/nucleoside cotransporter. A member of the SGLT family. J Biol Chem 267:3557-3560.

Pak MA, Haas HL, Decking UKM, Schrader J (1994) Inhibition of adenosine kinase increases endogenous adenosine and depresses neuronal activity in hippocampal slices. Neuropharmacology 33:1049-1053.

Palea S, Artibani W, Ostardo E, Trist DG, Pietra C (1993) Evidence for purinergic neurotransmission in human urinary bladder affected by interstitial cystitis. J Urol 150:2007-2012.

Palmer TM, Gettys TW, Jacobson KA, Stiles GL (1994) Desensitization of the canine A2a adenosine receptor: delineation of multiple processes. Mol Pharmacol 45:1082-1094.

Palmer TM, Stiles GL (1995) Adenosine receptors. Neuropharmacology 34:683-694.

Palmer TM, Stiles GL (1997) Identification of an A_{2A} adenosine receptor domain specifically responsible for mediating short-term desensitization. Biochemistry 36:832-838.

Park CK, Rudolphi KA (1994) Antiischemic effects of propentofylline (HWA 285) against focal cerebral infarction in rats. Neurosci Lett 178:235-238.

Parkinson FE, Fredholm BB (1990) Autoradiographic evidence for G-protein coupled A_2-receptors in rat neostriatum using [^{3}H]-CGS 21680 as a ligand. Naunyn Schmiedebergs Arch Pharmacol 342:85-89.

Parkinson FE, Paterson AR, Young JD, Cass CE (1993) Inhibitory effects of propentofylline on [^{3}H]adenosine influx. A study of three nucleoside transport systems. Biochem Pharmacol 46:891-896.

Parkinson FE, Rudolphi KA, Fredholm BB (1994) Propentofylline: a nucleoside transport inhibitor with neuroprotective effects in cerebral ischemia. Gen Pharmacol 25:1053-1058.

Pazzagli M, Corsi C, Fratti S, Pedata F, Pepeu G (1995) Regulation of extracellular adenosine levels in the striatum of aging rats. Brain Res 684:103-106.

Pearson JD, Carleton JS, Gordon JL (1980) Metabolism of adenine nucleotides by ectoenzymes of vascular endothelial and smooth-muscle cells in culture. Biochem J 190:421-429.

Phillis JW (1989) Adenosine in the control of cerebral circulation. Cerebrovasc Brain Metab Rev 1(1):27-54.

Phillis JW, Clough-Helfman C (1990) Oxypurinol, but not deoxycoformycin, administered post-ischemia, protects against CA1 hippocampal damage in the gerbil. Int J Pur Pyr Res 1:31-35.

Phillis JW, O'Regan MH (1989) Deoxycoformycin antagonizes ischemia-induced neuronal degeneration. Brain Res Bull 22:537-540.

Phillis JW, O'Regan MH (1996) Effects of an inhibitor of adenosine deaminase, deoxycoformycin, and of nucleoside transport, propentofylline, on post-ischemic recovery of adenine nucleotides in rat brain. Neurochem Res 21:347-353.

Phillis JW, O'Regan MH, Walter GA (1988) Effects of deoxycoformycin on adenosine, inosine, hypoxanthine, xanthine, and uric acid release from the hypoxemic rat cerebral cortex. J Cereb Blood Flow Metab 8:733-741.

Phillis JW, Smith Barbour M (1993) The adenosine kinase inhibitor, 5-iodotubercidin, is not protective against cerebral ischemic injury in the gerbil. Life Sci 53:497-502.

Pierce KD, Furlong TJ, Selbie LA, Shine J (1992) Molecular cloning and expression of an adenosine A_{2B} receptor from human brain. Biochem Biophys Res Commun 187:86-93.

Plesner L (1995) Ecto-ATPases: Identities and Functions. Int Rev Cytol 158:141-199.

Popoli P, Gimenez Llort L, Pezzola A, Reggio R, Martinez E, Fuxe K, Ferre S (1996) Adenosine A_1 receptor blockade selectively potentiates the motor effects induced by dopamine D_1 receptor stimulation in rodents. Neurosci Lett 218:209-213.

Porkka-Heiskanen T, Strecker RE, Thakkar M, Bjorkum AA, Greene RW, McCarley RW (1997) Adenosine: a mediator of the sleep-inducing effects of prolonged wakefulness. Science 276:1265-1268.

Proctor WR, Dunwiddie TV (1984) Behavioral sensitivity to purinergic drugs parallels ethanol sensitivity in selectively bred mice. Science 224:519-521.

Rainnie DG, Grunze HC, McCarley RW, Greene RW (1994) Adenosine inhibition of mesopontine cholinergic neurons: implications for EEG arousal. Science 263:689-692.

Ramkumar V, Olah ME, Jacobson KA, Stiles GL (1991) Distinct pathways of desensitization of A_1- and A_2-adenosine receptors in DDT1 MF-2 cells. Mol Pharmacol 40:639-647.

Rathbone MP, Middlemiss PJ, Kim JK, Gysbers JW, DeForge SP, Smith RW, Hughes DW (1992) Adenosine and its nucleotides stimulate proliferation of chick astrocytes and human astrocytoma cells. Neurosci Res 13:1-17.

Reppert SM, Weaver DR, Stehle JH, Rivkees SA (1991) Molecular cloning and characterization of a rat A_1-adenosine receptor that is widely expressed in brain and spinal cord. Mol Endocrinol 5:1037-1048.

Revan S, Montesinos MC, Naime D, Landau S, Cronstein BN (1996) Adenosine A_2 receptor occupancy regulates stimulated neutrophil function via activation of a serine/threonine protein phosphatase. J Biol Chem 271:17114-17118.

Ritzel MW, Yao SY, Huang MY, Elliott JF, Cass CE, Young JD (1997) Molecular cloning and functional expression of cDNAs encoding a human Na^+-nucleoside cotransporter (hCNT1). Am J Physiol 272:C707-14.

Rubio R, Berne RM, Bockman EL, Curnish RR (1975) Relationship between adenosine concentration and oxygen supply in rat brain. Am J Physiol 228(6):1896-1902.

Rudolphi KA, Schubert P, Parkinson FE, Fredholm BB (1992) Neuroprotective role of adenosine in cerebral ischaemia. Trends Pharmacol Sci 13:439-445.

Sajjadi FG, Takabayashi K, Foster AC, Domingo RC, Firestein GS (1996) Inhibition of TNF-alpha expression by adenosine: role of A_3 adenosine receptors. J Immunol 156:3435-3442.

Salvatore CA, Jacobson MA, Taylor HE, Linden J, Johnson RG (1993) Molecular cloning and characterization of the human A_3 adenosine receptor. Proc Natl Acad Sci USA 90:10365-10369.

Samii A, Bickel U, Stroth U, Pardridge WM (1994) Blood-brain barrier transport of neuropeptides: analysis with a metabolically stable dermorphin analogue. Am J Physiol 267:E124-31.

Satoh S, Matsumura H, Suzuki F, Hayaishi O (1996) Promotion of sleep mediated by the A_{2A}-adenosine receptor and possible involvement of this receptor in the sleep induced by prostaglandin D_2 in rats. Proc Natl Acad Sci USA 93:5980-5984.

Sattin A, Rall TW (1970) The effect of adenosine and adenine nucleotides on the cyclic adenosine 3'-5'-phosphate content of guinea pig cerebral cortex slices. Mol Pharmacol 6:13-23.

Schubert P, Ogata T, Marchini C, Ferroni S, Rudolphi K (1997) Protective mechanisms of adenosine in neurons and glial cells. Ann NY Acad Sci 825:1-10.

Schwaninger M, Neher M, Viegas E, Schneider A, Spranger M (1997) Stimulation of interleukin-6 secretion and gene transcription in primary astrocytes by adenosine. J Neurochem 69:1145-1150.

Sebastião AM, Ribeiro JA (1996) Adenosine A_2 receptor-mediated excitatory actions on the nervous system. Prog Neurobiol 48:167-189.

Seifert R, Schultz G (1989) Involvement of pyrimidinoceptors in the regulation of cell functions by uridine and by uracil nucleotides. Trends Pharmacol Sci 10:365-369.

Sen RP, Delicado EG, Alvarez H, Brocklebank AM, Wiley JS, Miras-Portugal MT (1998) Flow cytometric studies of nucleoside transport regulation in single chromaffin cells. FEBS Lett 422:368-372.

Sexl V, Mancusi G, Holler C, Gloria Maercker E, Schutz W, Freissmuth M (1997) Stimulation of the mitogen-activated protein kinase via the A_{2A}-adenosine receptor in primary human endothelial cells. J Biol Chem 272:5792-5799.

Siesjo BK, Bengtsson F (1989) Calcium fluxes, calcium antagonists, and calcium-related pathology in brain ischemia, hypoglycemia, and spreading depression: a unifying hypothesis. J Cereb Blood Flow Metab 9:127-140.

Sinclair CJD, Parkinson FE (1998) Stimulation of nucleoside efflux and inhibition of adenosine kinase by A_1 adenosine receptor activation. J Pharmacol Exp Ther submitted:

Sjolund KF, Sollevi A, Segerdahl M, Lundeberg T (1997) Intrathecal adenosine analog administration reduces substance P in cerebrospinal fluid along with behavioral effects that suggest antinociception in rats. Anesth Analg 85:627-632.

Snyder SH (1985) Adenosine as a neuromodulator. Annu Rev Neurosci 8:103-124.

Sollevi A (1997) Adenosine for pain control. Acta Anaesthesiol Scand Suppl 110:135-136.

Spector R, Huntoon S (1984) Specificity and sodium dependence of the active nucleoside transport system in choroid plexus. J Neurochem 42:1048-1052.

Stehle JH, Rivkees SA, Lee JJ, Weaver DR, Deeds JD, Reppert SM (1992) Molecular cloning and expression of the cDNA for a novel A_2-adenosine receptor subtype. Mol Endocrinol 6:384-393.

Surprenant A, Rassendren F, Kawashima E, North RA, Buell G (1996) The cytolytic P2Z receptor for extracellular ATP identified as a P2X receptor ($P2X_7$). Science 272:735-738.

Sweeney MI (1996) Adenosine release and uptake in cerebellar granule neurons both occur via an equilibrative nucleoside carrier that is modulated by G proteins. J Neurochem 67:81-88.

Sweeney MI, White TD, Sawynok J (1987) Involvement of adenosine in the spinal antinociceptive effects of morphine and noradrenaline. J Pharmacol Exp Ther 243:657-665.

Szondy Z (1994) Adenosine stimulates DNA fragmentation in human thymocytes by Ca^{2+}-mediated mechanisms. Biochem J 304:877-885.

Takagi H, King GL, Robinson GS, Ferrara N, Aiello LP (1996) Adenosine mediates hypoxic induction of vascular endothelial growth factor in retinal pericytes and endothelial cells. Invest Ophthalmol Vis Sci 37:2165-2176.

Thorn JA, Jarvis SM (1996) Adenosine transporters. Gen Pharmacol 27:613-620.

Todorov LD, Mihaylova Todorova S, Westfall TD, Sneddon P, Kennedy C, Bjur RA, Westfall DP (1997) Neuronal release of soluble nucleotidases and their role in neurotransmitter inactivation. Nature 387:76-79.

Townsend Nicholson A, Shine J (1992) Molecular cloning and characterisation of a human brain A_1 adenosine receptor cDNA. Brain Res Mol Brain Res 16:365-370.

Tso JY, Sun XH, Kao TH, Reece KS, Wu R (1985) Isolation and characterization of rat and human glyceraldehyde-3-phosphate dehydrogenase cDNAs: genomic complexity and molecular evolution of the gene. Nucleic Acids Res 13:2485-2502.

Valera S, Hussy N, Evans RJ, Adami N, North RA, Surprenant A, Buell G (1994) A new class of ligand-gated ion channel defined by P2X receptor for extracellular ATP. Nature 371:516-519.

van Calker D, Muller M, Hamprecht B (1979) Adenosine regulated via two different types of receptors, the accumulation of cyclic AMP in cultured brain cells. J Neurochem 33:999-1005.

Vijayalakshmi D, Belt JA (1988) Sodium-dependent nucleoside transport in mouse intestinal epithelial cells. Two transport systems with differing substrate specificities. J Biol Chem 263:19419-19423.

von Lubitz DKJE (1997) Adenosine A_3 receptor and brain. A culprit, a hero, or merely yet another receptor? Ann NY Acad Sci 825:49-67.

von Lubitz DKJE, Carter MF, Beenhakker R, Lin C-S, Jacobson KA (1997) Adenosine: a prototherapeutic concept in neurodegeneration. Ann N Y Acad Sci 825:163-178.

von Lubitz DKJE, Carter MF, Deutsch SI, Lin RC-S, Mastropaolo J, Meshulam Y, Jacobson KA (1995) The effects of adenosine A_3 receptor stimulation on seizures in mice. Eur J Pharmacol 275:23-29.

von Lubitz DKJE, Lin RC-S, Melman N, Ji X, Carter MF, Jacobson KA (1994) Chronic administration of selective adenosine A_1 receptor agonist or antagonist in cerebral ischemia. Eur J Pharmacol 256:161-167.

von Lubitz DKJE, Lin RCS, Paul IA, Beenhakker M, Boyd M, Bischofberger N, Jacobson KA (1996) Postischemic administration of adenosine amine congener (ADAC): Analysis of recovery in gerbils. Eur J Pharmacol 316:171-179.

von Lubitz DKJE, Paul IA, Ji XD, Carter M, Jacobson KA (1994) Chronic adenosine A_1 receptor agonist and antagonist: effect on receptor density and N-methyl-D-aspartate induced seizures in mice. Eur J Pharmacol 253:95-99.

Walker BA, Rocchini C, Boone RH, Ip S, Jacobson MA (1997) Adenosine A_{2A} receptor activation delays apoptosis in human neutrophils. J Immunol 158:2926-2931.

Walter GA, Phillis JW, O'Reagan MH (1988) Determination of rat cerebrospinal fluid concentrations of adenosine, inosine, hypoxanthine, xanthine and uric acid by high performance liquid chromatography. J Pharm Pharmacol 40:140-142.

Wang TF, Guidotti G (1996) CD39 is an ecto-(Ca^{2+},Mg^{2+})-apyrase. J Biol Chem 271:9898-9901.

Webb TE, Simon J, Krishek BJ, Bateson AN, Smart TG, King BF, Burnstock G, Barnard EA (1993) Cloning and functional expression of a brain G-protein-coupled ATP receptor. FEBS Lett 324:219-225.

Williams JB, Lanahan AA (1995) A mammalian delayed-early response gene encodes HNP36, a novel, conserved nucleolar protein. Biochem Biophys Res Commun 213:325-333.

Winn HR, Rubio R, Berne RM (1979a) Brain adenosine production in the rat during 60 seconds of ischemia. Circ Res 45(4):486-492.

Winn HR, Rubio R, Berne RM (1981a) Brain adenosine concentrations during hypoxia in rat. Am J Physiol 241(2):H235-H242.

Winn HR, Rubio R, Berne RM (1981b) The role of adenosine in the regulation of cerebral blood flow. J Cereb Blood Flow Metab 1(3):239-244.

Winn HR, Welsh JE, Berne RM, Rubio R (1979b) Changes in brain adenosine during bicuculline-induced seizures: effect of altered arterial oxygen tensions. Trans Am Neurol Assoc 104:239-241.

Wright KP, Jr., Badia P, Myers BL, Plenzler SC, Hakel M (1997) Caffeine and light effects on nighttime melatonin and temperature levels in sleep-deprived humans. Brain Res 747:78-84.

Wu X, Yuan G, Brett CM, Hui AC, Giacomini KM (1992) Sodium-dependent nucleoside transport in choroid plexus from rabbit. Evidence for a single transporter for purine and pyrimidine nucleosides. J Biol Chem 267:8813-8818.

Yakel JL, Warren RA, Reppert SM, North RA (1993) Functional expression of adenosine A_{2B} receptor in Xenopus oocytes. Mol Pharmacol 43:277-280.

Yao SYM, Ng AML, Muzyka WR, Griffiths M, Cass CE, Baldwin SA, Young JD (1997) Molecular cloning and functional characterization of nitrobenzylthioinosine (NBMPR)-sensitive (*es*) and NBMPR-insensitive (*ei*) equilibrative nucleoside transporter proteins (rENT1 and rENT2) from rat tissues. J Biol Chem 272:28423-28430.

Yao SYM, Ng AML, Ritzel MWL, Gati WP, Cass CE, Young JD (1996) Transport of adenosine by recombinant purine- and pyrimidine-selective sodium/nucleoside cotransporters from rat jejunum expressed in *Xenopus laevis* oocytes. Mol Pharmacol 50:1529-1535.

Yoshikawa T, Pardridge WM (1992) Biotin delivery to brain with a covalent conjugate of avidin and a monoclonal antibody to the transferrin receptor. J Pharmacol Exp Ther 263:897-903.

Young D, Dragunow M (1994) Status epilepticus may be caused by loss of adenosine anticonvulsant mechanisms. Neuroscience 58:245-261.

Zhang G, Franklin PH, Murray TF (1993) Manipulation of endogenous adenosine in the rat prepiriform cortex modulates seizure susceptibility. J Pharmacol Exp Ther 264:1415-1424.

Zhou QY, Li C, Olah ME, Johnson RA, Stiles GL, Civelli O (1992) Molecular cloning and characterization of an adenosine receptor: the A_3 adenosine receptor. Proc Natl Acad Sci USA 89:7432-7436.

Zimmermann H (1992) 5'-Nucleotidase: molecular structure and functional aspects. Biochem J 285:345-365.

Zimmermann H (1994) Signaling via ATP in the nervous system. Trends Neurosci 17:420-426.

IMAGE EVALUATION TEST TARGET (QA-3)

150mm

6"

APPLIED IMAGE . Inc
1653 East Main Street
Rochester, NY 14609 USA
Phone: 716/482-0300
Fax: 716/288-5989